MECHANISTIC INSIGHTS INTO THE ACTION OF THE ACTIVATOR PROTEIN-1 MEMBER C-JUN AT BOTH THE MOLECULAR AND PHYSIOLOGICAL LEVELS

XIE MIN

NATIONAL UNIVERSITY OF SINGAPORE

2015

MECHANISTIC INSIGHTS INTO THE ACTION

OF THE ACTIVATOR PROTEIN-1 MEMBER

C-JUN AT BOTH THE MOLECULAR AND

PHYSIOLOGICAL LEVELS

XIE MIN
(B.Sc., NUS)

A THESIS SUBMITTED

FOR THE DEGREE OF DOCTOR OF PHILOSOPHY

DEPARTMENT OF BIOCHEMISTRY

YONG LOO LIN SCHOOL OF MEDICINE

NATIONAL UNIVERSITY OF SINGAPORE

2015

Declaration

I hereby declare that this thesis is my original work and it has been written by me in its entirety. I have duly acknowledged all the sources of information which have been used in this thesis.

This thesis has not been submitted for any degree in any university previously.

_____

XIE MIN

2015

Acknowledgements

This study would not have been possible without the help and support of many people. First and foremost, I would like to thank my supervisor Professor Kanaga Sabapathy, for providing me the opportunity to work in this lab and for his patience and invaluable guidance throughout these years. This experience has undoubtedly enhanced my scientific knowledge and techniques, improved my critical think and skills in writing and presentations; allowing me to build confidence in my ability for pursuing future career.

I would like to thank the members of my Thesis Advisory Committee, Professor David M Virshup, Assistant Professor Koji Itahana and Dr Yeong Foong May for agreeing to be in my committee and have provided useful suggestions, inspiring discussions and encouragements throughout this study.

I would like to thank the collaborator, Professor Anna M Diehl, Chief, Division of Gastroenterology, Department of Medicine, Duke University Medical Center, Durham, North Carolina, USA for providing help in investigating Hedgehog signaling pathway.

In addition, I would like to thank all the past and present members (specially Dr Kenneth Lee and Derrick Chia) of the Laboratory of Molecular Carcinogenesis as well as other colleagues at National Cancer Centre Singapore for their help.

Last but not least, I would like to thank my friends and family members for their support and understanding over these years.

Table of Contents

Summary

c-JUN is a major component of the activator protein-1 transcription factor complex and its activation depends mainly on phosphorylation by the c-JUN amino-terminal kinases. c-JUN has been implicated in a wide range of physiological and pathological processes including development, regeneration and tumorigenesis. However the direct gene targets that mediate these specific processes remain to be investigated.

To identify novel c-JUN targets, we performed whole genome expression array analyses from (1) viable embryos and (2) UV or cisplatin-treated primary mouse embryonic fibroblasts (MEFs) of mice carrying wild type *c-Jun* (*c-Jun$^{+/+}$*), knockout *c-Jun* (*c-Jun$^{-/-}$*) or an amino-terminal nonphosphorylatable mutant form of *c-Jun* (*c-Jun$^{AA/AA}$*). We identified a large number of differentially expressed genes by comparing the gene expression profiles between *c-Jun$^{+/+}$* and *c-Jun$^{-/-}$* samples. In contrast, we observed only a small number of differently expressed genes between *c-Jun$^{AA/AA}$* and *c-Jun$^{+/+}$* samples. These differentially expressed genes were then categorized as c-JUN amino-terminal phosphorylation (JNP)-dependent or -independent targets. Our data demonstrated that JNP is required only for a small subset of c-JUN target gene transcription. Furthermore, the differentially expressed genes were also classified into stress-dependent or -independent target groups, which revealed the presence of c-JUN-dependent genes that are regulated by stress factors, as well as a significant group that are regulated in a stress-independent manner.

To explore novel c-JUN regulated biological processes, we analyzed the differentially expressed genes via Ingenuity Pathway Analysis, and the

Hepatic fibrosis/Hepatic stellate cell (HSC) activation was predicted to be the topmost affected pathway. Therefore, we assessed the activated HSC status in the embryos and detected dramatically high levels of activated HSCs in $c\text{-}Jun^{-/-}$ embryos as compared to $c\text{-}Jun^{+/+}$ embryos. This result again suggested an important role of c-JUN in hepatic fibrosis. To elucidate the role of c-JUN in hepatic fibrosis, we utilized the $c\text{-}Jun$ conditional knockout mice to inactivate $c\text{-}Jun$ in adult liver HSCs (1) and both hepatocytes and hematopoietic cells (2), by using Col-CreER and Mx-Cre transgenic mice respectively. Fibrosis was induced by chronic injections of carbon tetrachloride over time to adult mice and livers were harvested and analyzed for degree of fibrosis and HSC activation. Surprisingly, we observed that deletion of $c\text{-}Jun$ in HSCs resulted in significantly more activated HSCs and more fibrosis whereas deletion of $c\text{-}Jun$ in hepatocytes and hematopoietic cells resulted in significantly less activated HSCs and less fibrosis. These results revealed that c-JUN acts as a dual regulator in hepatic fibrosis, highlighting the importance of understanding how c-JUN functions in different liver cell types. Interestingly, hedgehog (Hh)-regulated transcription factor $Gli2$ expression was markedly increased in $c\text{-}Jun^{-/-}$ MEFs as compared to $c\text{-}Jun^{+/+}$ MEFs. This correlates with previous studies showing a crucial role for Hh signaling in HSC activation and promotion of hepatic fibrosis. We therefore examined the Hh pathway activation in embryos and detected profoundly elevated Hh signaling in $c\text{-}Jun^{-/-}$ embryos compared to $c\text{-}Jun^{+/+}$ embryos. Taken together, these data strongly suggest that the crosstalk between c-JUN and the Hh signaling pathway could be a possible mechanism of how c-JUN regulates hepatic fibrosis.

List of Tables

List of Figures

List of Abbreviations

αSMA – α smooth muscle actin

ANOVA – analysis of variance

Alfp – albumin promoter and alpha feto-protein

AP-1 – activator protein-1

APC – Adenomatous polyposis coli

ASV 17 – avian sarcoma virus 17

ATF – activating transcription factor

BCP – 1-Bromo-3-chloropropane

BDL – bile duct ligation

BrdU – Bromodeoxyuridine

BSA – Albumin, Bovine

bZIP – basic region-leucine zipper

CBP – CREB binding protein

CCl_4 – carbon tetrachloride

CDDP – cisplatin

CDK – cyclin-dependent kinase

CGN – cerebellar granule neuron

CkII – casein kinase II

Con A – Concanavalin A

CRE – cyclic AMP responsive element

C-terminal – carboxyl-terminal

DDC – 3,5-diethoxycarbonyl-1,4-dihydrocollidine

DEN – Diethylnitrosamine

Dhh – Desert hedgehog

DMEM – Dulbecco's modified Eagle's medium

dpc – day post coitum

ECM – extracellular matrix

EGF – epidermal growth factor

EGFR – EGF receptor

ER – estrogen receptor

ERK – extracellular signal-regulated kinase

ES – embryonic stem

FC – fold change

FDR – false discovery rate

gbw – gram body weight

GFAP – glial fibrillary acidic protein

Gli – Glioblastoma

GR – glucocorticoid receptor

Gsk – glycogen synthase kinase

H&E – Hematoxylin-Eosin

HCC – hepatocellular carcinoma

Hh – Hedgehog

Hhip – Hh-interacting protein

HSC – hepatic stellate cell

i.p. – intraperitoneal

IHC – immunohistochemistry

Ihh – Indian hedgehog

IL – interleukin

IPA – Ingenuity Pathway Analysis

IR – ionizing radiation

IVT – in vitro transcription

Jab1 – Jun activation domain-binding protein 1

JNK – c-JUN amino-terminal kinase

JNP – c-JUN amino-terminal phosphorylation

LPS – lipopolysaccharide

MAF – musculoaponeurotic fibrosarcoma

MAPK – mitogen activated protein kinase

MAPKK, MEK,MKK – MAPK kinase

MAPKKK, MEKK – MAPK kinase kinase

MCDE – methionine choline-deficient, ethionine-supplemented diet

MEF – mouse embryonic fibroblast

MMP – matrix metalloproteinase

NAFLD – nonalcoholic fatty liver disease

NASH – nonalcoholic steatohepatitis

NGF – nerve growth factor

nos2 – inducible nitric oxide synthase

N-terminal – amino-terminal

NuRD – nucleosome remodeling and histone deacetylation

PB – Phenobarbital

PBS – phosphate buffered saline

PCA – principal component analysis

PCR – polymerase chain reaction

PDGF – platelet-derived growth factor

PH – partial hepatectomy

PI – propidium iodide

Poly I/C – Polyinosinic-polycytidylic acid sodium

PPAR – Peroxisome Proliferator-Activated Receptor

Ptc – Patched

qRT-PCR – quantitative real-time PCR

RAR – retinoic-acid receptor

ROS – reactive oxygen species

RSK2 – ribosomal S6 kinase 2

SD – standard deviation

Shh – Sonic hedgehog

Smo – Smoothened

SOS – Son of Sevenless

SRF – serum response factor

TBS – Tris Buffered Saline

TCF – ternary complex factor

TGF – transforming growth factor

TIMP – tissue inhibitor of metalloproteinase

TNF – tumor necrosis factor

TPA – 12-*O*-tetradecanoylphorbol-13-acetate

TRE – TPA response element

UV – ultraviolet light

Chapter 1

Introduction

1.1 General introduction to eukaryotic gene expression regulation

Eukaryotic organisms are constantly and simultaneously exposed to various kinds of physiological and environmental stimuli, such as nutrients, heat, radiation and mechanical stresses. These signals from outside the cells need to be transmitted all the way to the nucleus to cause gene expression changes to modify their behaviors accordingly (Figure 1) (Lodish, 2004 Chapter 15, Krauss, 2014 Chapter 1). This is a decision making process and therefore, is critical for normal life. Hence gene expression needs to be tightly regulated both temporally and spatially to ensure that the organisms can mount appropriate responses to specific stimuli. Deregulated gene expression can result in diseases and disorders (Lodish, 2004).

Cells regulate gene expression (induce or inhibit specific gene product) in a complex way. Simplistically, it can be regulated at any step from chromatin level to transcription, to RNA transport or degradation, to translation or post-translation (Krauss, 2014 Chapter 4). Transcriptional regulation controls the level and duration of mRNA synthesis and is usually influenced by regulatory DNA sequences (named promoters, enhancers and silencers) and sequence-specific DNA-binding proteins (generally termed as transcription factors). There are additional proteins such as coactivators/repressors, chromatin remodeling factors etc., that also play crucial roles in transcriptional regulation. All these factors interplay and form a complex regulatory network to help or hinder the recruitment of RNA polymerase to the promoter, thus mediating the selective control of transcriptional activities (Johnson *et al*., 1989).
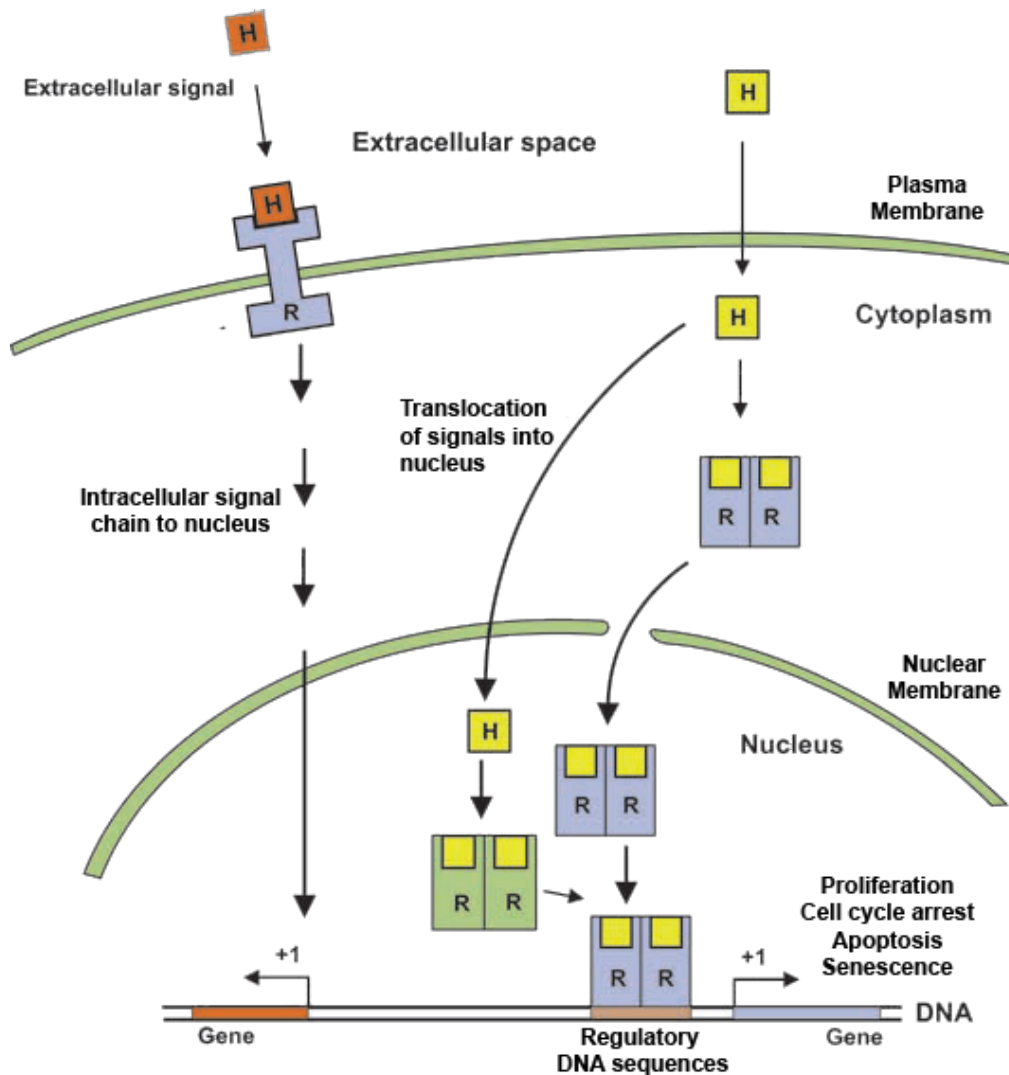
Figure 1. Integrating signals with gene expression
Signals from outside the cells can be transmitted into the nucleus via (1) plasma membrane receptors via intracellular signaling molecules and/or (2) cytosolic nuclear receptors that move into the nucleus directly upon binding ligands. The signals converge to activate trancriptional regulatory proteins that eventually cause gene expression changes and cell fate decision. Figure adapted from Krauss, 2014 Figure 1.8.

Transcription factors can trans-activate (upregulate) or trans-repress (downregulate) gene expression in a context-dependent manner. Important transcription factors like p53 can control the expression of key proteins (e.g. p21, Puma and Noxa) to determine cell fate (e.g. cell cycle arrest, apoptosis and senescence) (Levine, 1997, Zuckerman *et al*., 2009). Therefore it is of

particular importance to understand how transcription factors and their responsive target genes work in facilitating the cells/organisms to accommodate to the environmental changes.

1.2 AP-1 family of transcription factors

Activator protein-1 (AP-1) is one of the earliest identified mammalian transcription factors. AP-1 was first identified as a 12-*O*-tetradecanoyl-phorbol-13-acetate (TPA)-inducible transcription factor that could bind to the promoter/enhancer elements of several genes such as human metallothionein IIA, simian virus 40, collagenase and stromelysin to potentiate their transcription (Angel *et al*., 1991). In addition to TPA, AP-1 can be induced by a wide diversity of physiological and pathological signals including growth factors, neurotransmitters, genotoxic stresses, oncogenic proteins, inflammatory cytokines and chemokines, as well as bacterial and viral infections; and functions in almost all areas of eukaryotic cellular behavior, including cell proliferation and apoptosis, tissue development and regeneration, tumor initiation and progression (Shaulian *et al*., 2002, Eferl *et al*., 2003b, Zenz *et al*., 2006).

1.2.1 AP-1 family components

AP-1 is not a single protein, but consists of a dimeric complex of members from the Jun, Fos, ATF (activating transcription factor) and MAF (musculoaponeurotic fibrosarcoma) subfamily of proteins (Figure 2). Protein members from each subfamily are listed in Table 1 and among all the AP-1

members, Jun and Fos proteins are the prototypic components of the AP-1 complex (Shaulian *et al.*, 2002, Eferl *et al.*, 2003b).
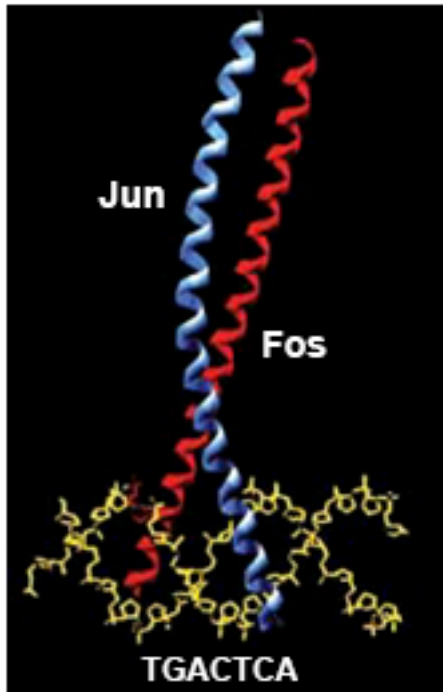
Figure 2. The AP-1 transcription factor
The AP-1 transcription factor is a dimer composed of members from the Jun, Fos, ATF and MAF subfamilies. Jun and Fos proteins are the prototypic components of the AP-1 complex (based on Protein Data Bank entry 1fos). AP-1 components dimerize through their leucine zipper domains and are able to recognize diverse DNA-binding sequences. The figure depicts crystal structure from c-JUN and c-FOS (62 amino acids each). Figure adapted from Eferl & Wagner, 2003 Figure 1a.

Table 1. List of all the AP-1 family members

AP-1 Subfamily	Jun	Fos	ATF	MAF
Member	c-JUN	c-FOS	ATF2	c-MAF
	JUNB	FOSB	LRF1/ATF3	MAFA
	JUND	FRA1	B-ATF	MAFB
		FRA2	JDP1	MAFG/F/K
			JDP2	NRL

Proteins constituting the AP-1 complex dimerize through their leucine zipper domains (Figure 2). Jun proteins can homo- and heterodimerize, whereas Fos proteins can only heterodimerize with other AP-1 proteins. AP-1 proteins, having the capabilities to form multiple combinations of homo- and heterodimers, are able to recognize diverse DNA-binding sequences which in turn regulate a broad spectrum of target gene expression (Karin *et al*., 1997, Shaulian *et al*., 2002, Eferl *et al*., 2003b).

1.2.2 AP-1 dimer composition

Is there any specific function of these different AP-1 dimers? Or do Jun-Jun, Jun-Fos and Jun-ATF classes of AP-1 dimers function redundantly? Many studies have suggested that different AP-1 dimers are regulated by different signaling pathways, interacting with different proteins and displaying different stabilities, DNA-binding specificities and trans-activating capacities (Hai *et al*., 1991, Chinenov *et al*., 2001, van Dam *et al*., 2001, Bakiri *et al*., 2002, Wisniewska *et al*., 2007, Walters *et al*., 2014).

Firstly, different classes of AP-1 dimers can be activated by different specific stimulus. For example, growth factors or phorbol esters primarily stimulate the *de novo* synthesis of Jun-Fos by activating extracellular signal-regulated kinases (ERKs); while stresses like ultraviolet light (UV) predominantly enhance the activity of Jun-ATF via phosphorylation of e.g. c-JUN at serines 63/73 and ATF2 at threonines 69/71 by Jun amino-terminal kinases (JNKs) (van Dam *et al*., 2001).

In addition, Jun-Jun and Jun-Fos dimers bind to the heptameric sequence 5'-TGA(C/G)TCA-3', known as TPA-response element (TRE) with high affinity; whereas Jun-ATF dimers bind preferentially to the octameric cyclic AMP-responsive element (CRE) 5'-TGACGTCA-3' (Figure 3) (Karin *et al.*, 1997, van Dam *et al.*, 2001, Eferl *et al.*, 2003b).

Figure 3. Examples of AP-1 dimer composition
Jun-Fos and Jun-ATF are different AP-1 dimers that bind preferentially with different consensus sequences and regulate different sets of target genes. Figure adapted from van Dam & Castellazzi, 2001 Figure 1.

Within Jun-Fos dimers, despite that all the Fos family proteins can form stable heterodimers with c-JUN, different dimers confer different transcriptional activity. Transcriptional activity of c-JUN on certain target genes was stimulated when heterodimerized with c-FOS but, on the contrary, it was suppressed when bound to FRA2 (Suzuki *et al.*, 1991).

In accordance, tethered AP-1 dimers have been generated by using a specially designed flexible polypeptide to join specific AP-1 components (e.g. c-JUN~c-FOS, JUNB~c-FOS, JunD~c-FOS and c-JUN~FRA2) in order to study the function of individual AP-1 dimers (Bakiri *et al.*, 2002). In addition, transgenic mice expressing individual forced AP-1 dimers have also been

generated for *in vivo* studies (Hasenfuss *et al*., 2014b). Interestingly, when expression of these forced AP-1 dimers was restricted to the liver parenchyme, all forced Jun~c-FOS dimers (c-JUN~c-FOS, JunB~c-FOS and JunD~c-FOS) strongly stimulated liver Peroxisome Proliferator-Activated Receptor γ (PPARγ) signaling (while c-JUN~c-Fos exhibited the strongest induction) and caused a lethal liver dysplasia phenotype. In contrast, forced c-JUN~FRA2 dimer suppressed PPARγ signaling and could therefore protect the mice from high fat diet-induced nonalcoholic fatty liver disease (NAFLD) (Hasenfuss *et al*., 2014b). These data further provided *in vivo* evidence that different composition of the AP-1 dimers can lead to completely opposite physiological outcome.

Hence, understanding AP-1 function and regulation requires careful investigation due to the broad combinatorial possibilities of AP-1 dimers.

1.2.3 AP-1 abundance and activity

The AP-1 abundance and activity can be regulated at multiple levels, including transcriptional, post-translational modification and interaction with ancillary proteins. The specific regulation at each level is delineated below.

Firstly, AP-1 components are regulated at the transcriptional level. As AP-1 controls both basal and inducible transcriptional activity, some AP-1 components (often JUND, FRA1 and FRA2) are abundant under unstimulated condition for its basal activity, whereas the transcription of other AP-1 components (like c-JUN and c-FOS) needs to be potentiated by stimuli. Hence the subunit composition of the AP-1 complexes would change with regard to

the relative proportions of different components present in the cells at a given time, which would in turn modulate AP-1 DNA-binding as well as target gene transcription (Wisdom, 1999).

Secondly, AP-1 components are regulated at the protein level. In the case of c-JUN, its amino-terminal (N-terminal) phosphorylation reduces its ubiquitin-dependent degradation therefore increases its stability to a certain extent (Musti *et al*., 1997). However, carboxyl-terminal (C-terminal) region of c-FOS is important for its degradation by c-JUN and multiple protein kinases (Tsurumi *et al*., 1995).

Thirdly, both pre-existing and newly synthesized AP-1 components are modified at the post-translational level. Phosphorylation by protein kinases from the mitogen activated protein kinase (MAPK) family in modulating AP-1 activities has been studied most extensively. Further details of this family of kinases are discussed in the next part. Additionally, other kinases such as casein kinase II (CkII), glycogen synthase kinase 3β (Gsk-3β) and ribosomal S6 kinase 2 (RSK2) have also been reported to phosphorylate Jun and Fos proteins thereby regulating their DNA-binding and transactivation potential (Eferl *et al*., 2003b).

Lastly, other transcriptional regulators synergize or interfere with AP-1 proteins and thereby regulate their activity. The DNA-binding potential of AP-1 can be influenced by cofactors like Jun activation domain-binding protein 1 (Jab1) (Zenz *et al*., 2006). Transactivation activity of AP-1 can be enhanced by interaction with transcriptional coactivators such as members of the CREB binding protein (CBP)/p300 family (Karin *et al*., 1997). In contrast,

glucocorticoid receptor (GR) and retinoic-acid receptor (RAR) are examples of ancillary proteins that can inhibit AP-1 activity (Angel *et al.*, 1991, Eferl *et al.*, 2003b).

1.3 MAPK family of protein kinases

The MAPKs are a group of evolutionarily conserved proline-directed serine/threonine protein kinases that are activated by dual phosphorylation on threonine and tyrosine residues in response to a wide range of extracellular stumuli. The MAPK pathway is a very important intracellular signaling pathway that serves to receive, amplify and integrate signals from extracellular environment to the transcriptional machinery in the nucleus, which ultimately results in a diverse array of cellular and physiological responses such as proliferation, apoptosis, differentiation and inflammation (Whitmarsh *et al.*, 1996, Karin, 1998, Chang *et al.*, 2001).

1.3.1 MAPK signaling cascade

The canonical MAPK signaling (Figure 4) is organized in a phosphorelay system composed of three sequentially activated protein kinases: MAPK, MAPK kinase (MAPKK, MEK or MKK) and MAPK kinase kinase (MAPKKK or MEKK). Specific signals trigger the activation of MAPKKKs, which in turn phosphorylate and activate MAPKKs; MAPKKs thereafter phosphorylate and activate MAPKs which then translocate into cell nucleus and phosphorylate a variety of transcription factors on specific sites to regulate their transcriptional activity (Karin, 1998, Chang *et al.*, 2001, Cargnello *et al.*, 2011)
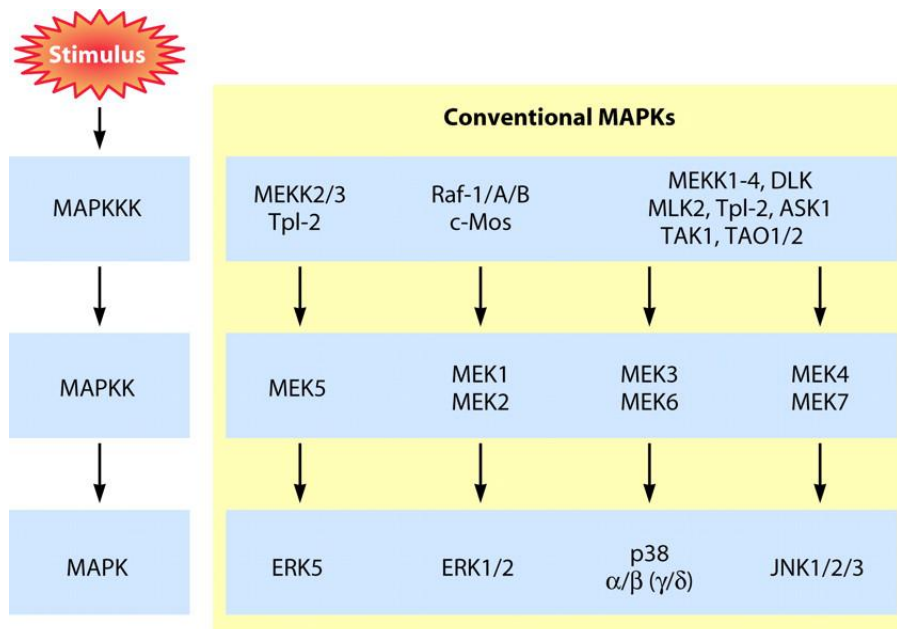
Figure 4. Canonical MAPK signaling cascade
MAPK signaling is activated by a wide range of extracellular stimuli and organized in a phosphorelay system. Conventionally, there are three major groups of MAPKs: ERKs (ERK1/2), JNKs (JNK1/2/3) and p38 proteins (p38α/β/γ/δ). Figures adapted from Cargnello & Roux, 2011 Figure 2.

In mammals, there are three major groups of MAPKs that have been identified: the ERKs (ERK1/2), JNKs (JNK1/2/3) and p38 proteins (p38α/β/γ/δ) (Figure 4) (Karin, 1998, Chang *et al*., 2001, Cargnello *et al*., 2011). Individual MAPKs can be activated and signal independently from each other. The ERKs are more efficiently activated by signals like growth factors and phorbol esters, which transmit through receptors containing intrinsic tyrosine kinase domains or receptors that interact with cytoplasmic tyrosine kinases, thus preferentially regulate cellular growth, differentiation and transformation (Boulton *et al*., 1990). The JNKs and p38 MAPKs are more potently activated by environmental stresses and proinflammatory cytokines and function mainly in inflammation and apoptosis (Bogoyevitch *et al*., 2010, Cuadrado *et al*., 2010).

11

1.3.2 The regulation of AP-1 by MAPKs

One important nuclear target of these MAPKs is AP-1. MAPKs regulate AP-1 activity by both increasing the abundance of AP-1 components through upregulation of transcription and enhancing the AP-1 activity via phosphorylation (Karin, 1995, Whitmarsh *et al*., 1996, Karin *et al*., 1997).

ERKs, JNKs and p38 MAPKs all have been demonstrated to increase *c-Fos* transcription through phosphorylation and activation of members from ternary complex factor (TCF) DNA-binding proteins. TCF together with a dimeric serum response factor (SRF) form a ternary complex that can bind to *c-Fos* promoter and activate its transcription upon various stimuli (Whitmarsh *et al*., 1996, Shaulian *et al*., 2002). Moreover, JNKs have been shown to increase *c-Jun* transcription through phosphorylation and activation of c-JUN and ATF2. Since *c-Jun* promoter is constitutively occupied by c-JUN-ATF2 heterodimer, phosphorylation of c-JUN and ATF2 by JNKs increases their transcriptional activity, thereby leading to an increase in *c-Jun* transcription (Whitmarsh *et al*., 1996, Mechta-Grigoriou *et al*., 2001).

Phosphorylation of AP-1 components by MAPKs has been extensively documented. ERKs have been reported to directly phosphorylate FRA1 and FRA2; JNKs can phosphorylate c-JUN and ATF2; p38 kinases can also phosphorylate ATF2, all of which contributes to enhanced AP-1 activity (Whitmarsh *et al*., 1996, Karin *et al*., 1997, Shaulian *et al*., 2002).

1.3.3 The JNK/Jun signal transduction pathway

The JNK protein kinases were first identified through their ability to
phosphorylate c-JUN on its N-terminal stimulatory sites. The JNKs are
encoded by three genes: *jnk1*, *jnk2* and *jnk3* (Figure 5). The *jnk1* and *jnk2*
genes are ubiquitously expressed whereas the *jnk3* expression is limited to
brain, heart and testis. These three genes are alternatively spliced to generate
ten JNK isoforms (Davis, 2000, Manning *et al*., 2003).
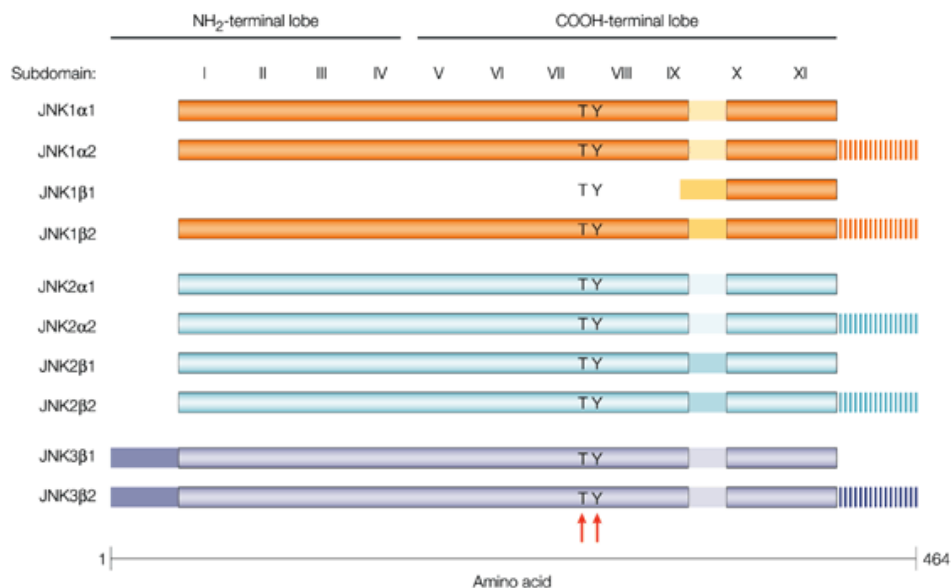
Figure 5. JNK isoforms
The JNKs are encoded by three genes (*jnk1*, *jnk2* and *jnk3*) that are alternatively
spliced to generate ten JNK isoforms. Figure adapted from Manning & Davis, 2003
Figure 1.

JNKs can be activated by diverse stimuli, such as cytokines (tumor necrosis
factor [TNF], interleukin [IL]-1, transforming growth factor [TGF]-β, platelet-
derived growth factor [PDGF], epidermal growth factor [EGF]), pathogens
(lipopolysaccharide [LPS]), reactive oxygen species (ROS), stresses (UV,

13

ionizing radiation [IR], hypoxia, endoplasmic reticulum stress), etc. (Seki *et al*., 2012). Most of the above mentioned stimuli activate JNKs which in turn activate c-JUN. c-JUN then dimerizes with other AP-1 members and regulates downstream gene expression.

JNKs can phosphorylate c-JUN and ATF2 (Shaulian *et al*., 2002). c-JUN is expressed at a relatively low level under normal unstimulated condition. JNKs phosphorylate c-JUN efficiently to thereby enhance its transcriptional activity. Phosphorylation can occur at serines 63/73 and/or threonines 91/93 (Vinciguerra *et al*., 2008, Reddy *et al*., 2013). Unlike c-JUN, ATF2 is constitutively expressed. ATF2 is also rapidly phosphorylated by JNKs following stimulation and can dimerize with c-JUN to regulate certain AP-1 target genes (Gupta *et al*., 1995).

Interestingly, JNKs can also phosphorylate JunD by a slightly different process. JNK requires a docking site in its substrate to tether and phosphorylate it (Karin *et al*., 1997). JunD lacks the JNK docking site but contains JNK phosphoacceptor sites. JUNB, on the other hand, possesses the JNK docking site but does not have proper JNK phosphoacceptor sites. As a result, JUNB is not phosphorylated by JNKs whereas JunD can be phosphorylated by JNKs only when it forms heterodimers with c-JUN or JUNB which have the effective JNK docking sites.

1.4 Basic Introduction to c-JUN

The mouse and human *c-Jun* share high degree of identity. Human c-*jun* gene is located on chromosome 1 and murine c-*jun* gene is on chromosome 4.

Cloning of the *c-Jun* gene revealed that it has no introns (Vogt, 2001), thus, c-Jun has no isoforms and no post-transcriptional regulation.

1.4.1 The discovery of c-JUN

c-Jun was originally discovered as a cellular counterpart of *v-jun*, an oncogene isolated from the genome of the avian sarcoma virus 17 (ASV 17) (Maki *et al*., 1987). Two seminal findings placed c-JUN as the core component of the AP-1 complex. (1) Structural analysis revealed a homology between the C-terminal region of c-JUN and the DNA-binding domain of a yeast transcription factor GCN4. As GCN4 was already known to bind to AP-1 site, this led to the discovery that c-JUN is part of the AP-1 complex (Bohmann *et al*., 1987, Vogt *et al*., 1987, Angel *et al*., 1988a). (2) c-JUN was also recognized as a Fos-associated protein that could cooperate with Fos to stimulate gene expression. With more identity and functional tests, c-JUN was quickly determined as the major component of the AP-1 complex (Rauscher *et al*., 1988, Sassone-Corsi *et al*., 1988).

1.4.2 The structure of c-JUN

The simplified structure of c-JUN is illustrated in Figure 6. c-JUN protein, like all other AP-1 family members, belongs to the basic region-leucine zipper (bZIP) group of DNA-binding transcription factors (Shaulian *et al*., 2002, Eferl *et al*., 2003b).

15

Figure 6. The basic structure of the murine c-JUN
c-JUN possesses a transactivation domain that covers the majority of its N-terminus however lacking defining structural borders. c-JUN also contains a DNA-binding domain (yellow) and a dimerization domain (blue) at its C-terminus. A delta domain (pink) locates near its N-terminus, functions as the JNK docking site. JNKs bind and phosphorylate c-JUN at mainly serines 63 and 73; this phosphorylation event is named as c-JUN amino-terminal phosphorylation (JNP).

c-JUN can form homo- or heterodimers with various bZIP proteins through its C-terminal dimerization domain. This dimerization domain contains five heptad repeats of the leucine residues forming an amphipathic helix that is referred as the leucine zipper motif and is responsible for protein-protein interaction (Vogt, 2001).

A highly charged basic region located immediately N-terminal to the leucine zipper motif is the DNA-binding domain of c-JUN, which makes direct contact with DNA. Importantly, dimerizations between the AP-1 components is a prerequisite for their DNA-binding (Vogt, 2001).

There is a region of 27 amino acids, termed the delta domain, near the N-terminus of c-JUN that is not present in v-Jun. This domain was found to be required for c-JUN poly-ubiquitination and subsequent proteolysis and is hence involved in regulating c-JUN turnover. v-Jun therefore could escape poly-ubiquitination and is more stable than c-JUN (Treier *et al.*, 1994). Moreover, as mentioned before, the delta domain also serves as the docking

16

site for JNKs to phosphorylate c-JUN. The integrity of this docking site is essential for c-JUN phosphorylation by JNKs. v-Jun therefore is not phosphorylated by JNKs (Adler *et al.*, 1992, Hibi *et al.*, 1993).

The transactivation domain of c-JUN lacks defining structural features. Numerous independent studies on various c-JUN deletion mutants have revealed that the majority of its N-terminal region constitutes its transactivation domain (Vogt, 2001). The transactivation domain has been shown to be important in most c-JUN functions such as transcriptional activation, cell proliferation, cell death and transformation (Shaulian *et al.*, 2001, Shaulian *et al.*, 2002, Eferl *et al.*, 2003b).

1.4.3 The regulation of c-JUN

The regulation of c-JUN generally occurs at transcriptional and post-translational levels.

The *c-Jun* gene is transcribed at low levels prior to stimulation. Nevertheless it is an immediate early gene whose transcription is rapidly induced following stimulation (Karin *et al.*, 1997). The *c-Jun* promoter region is highly conserved between mouse, rat and human (Mechta-Grigoriou *et al.*, 2001). c-JUN can positively autoregulate its own transcription through the interaction with two TRE-like sequences present within its promoter (Angel *et al.*, 1988b).

The activity of c-JUN is primarily regulated by phosphorylation. Structural analysis revealed that c-JUN has many potential phosphorylation sites, such as serines 63, 73, 243, threonines 91, 93, 239 and tyrosine 170. Most of these

residues and the associated kinases have been examined (Barila *et al*., 2000, Morton *et al*., 2003, Gao *et al*., 2006, Zhu *et al*., 2006, Vinciguerra *et al*., 2008, Xie *et al*., 2010, Reddy *et al*., 2013). Among all the phosphorylation sites, serines 63 and 73 have been studied most intensively as they are recognized as the most crucial sites in regulating c-JUN stability and activity (Shaulian *et al*., 2002, Eferl *et al*., 2003b). Moreover, phosphorylation of c-JUN at a cluster of sites located just upstream of its basic region (DNA-binding domain) was found to inhibit c-JUN binding to DNA. Dephosphorylation at one or more of these sites could therefore increase c-JUN DNA-binding and transactivation activity (Boyle *et al*., 1991).

Poly-ubiquitination is another post-translational modification that regulates c-JUN protein turnover. Several E3 ubiquitin ligases have been identified to target c-JUN for proteasomal degradation, such as Itch and COP1 (Gao *et al*., 2004, Wertz *et al*., 2004). Phosphorylation of c-JUN at multiple sites within its transactivation domain by MAPKs generally reduces its poly-ubiquitination and stabilizes c-JUN (Musti *et al*., 1997). Interestingly, Fbw7, the substrate recognition component of an SCF-type E3 ubiquitin ligase that is highly expressed in the nervous system, specifically targets the N-terminal phosphorylated c-JUN and facilitates its degradation, thus antagonizing excessive c-JUN activity in neurons (Nateri *et al*., 2004).

1.4.4 c-JUN amino-terminal phosphorylation (JNP)

To date, JNK is still considered as the primary regulator of c-JUN and its phosphorylation on serines 63/73 within c-JUN transactivation domain is believed to be the most crucial event in regulating c-JUN activity. This

phosphorylation event is thus termed as c-JUN amino-terminal phosphorylation (JNP) (Figure 6) (Behrens *et al.*, 1999).

Collectively, JNP is found to (1) regulate the ubiquitin-mediated degradation of c-JUN to thus increase c-JUN abundance; (2) increase c-JUN DNA binding; (3) increase the ability of c-JUN to interact with coactivators like CBP/p300 thus enhance c-JUN transactivation potential (Karin *et al.*, 1997, Mechta-Grigoriou *et al.*, 2001).

1.5 c-JUN and JNP in cell life and death

Initial studies using cells and mice deficient for c-JUN or JNP have provided substantial functional insights in their functions in regulating cell proliferation, oncogenic transformation and apoptosis.

<u>1.5.1 Cell cycle progression and proliferation</u>

c-JUN is a positive regulator of cell proliferation supported by multiple lines of evidence and will be briefly described. (1) c-JUN depletion using antisense RNA in erythroleukemia cells inhibited cell proliferation (Smith *et al.*, 1992). (2) c-JUN-deficient primary mouse embryonic fibroblasts (MEFs) exhibited severe proliferation defects with almost no growth rate in culture and quickly entered premature senescence (Johnson *et al.*, 1993, Schreiber *et al.*, 1999). (3) Similar phenotype was also observed in immortalized *c-Jun*$^{-/-}$ MEFs and re-introduction of c-JUN could rescue this phenotype and increase proliferation (Schreiber *et al.*, 1999). (4) c-JUN-deficient primary keratinocytes (Li *et al.*, 2003, Zenz *et al.*, 2003) and fetal hepatoblasts (Eferl *et al.*, 1999) also displayed markedly reduced proliferation *in vitro*. (5)

Moreover, loss of c-JUN significantly impaired postnatal hepatocyte proliferation *in vivo* as assessed by Bromodeoxyuridine (BrdU) labeling (Behrens *et al*., 2002). c-JUN could, in addition, affect cell cycle re-entry. (6) Microinjection of c-JUN antibody into quiescent mouse fibroblasts greatly inhibited DNA synthesis and prevented cell cycle re-entry following serum stimulation (Kovary *et al*., 1991). (7) While wild type fibroblasts underwent a transient cell cycle arrest after exposure to UV, *c-Jun*$^{-/-}$ cells exhibited prolonged growth arrest and failed to resume proliferation (Shaulian *et al*., 2000). (8) Quiescent adult hepatocytes lacking c-JUN also failed to re-enter cell cycle after partial hepatectomy (PH) thus resulting in impaired liver regeneration (Behrens *et al*., 2002).

Genetic and biochemical analysis have revealed that the regulation of cell cycle progression and cell proliferation by c-JUN is through its ability to downregulate p53. c-JUN has been shown to bind and suppress *p53* transcription, thereby indirectly downregulating the p53 target gene *p21*, an inhibitor of cyclin-dependent kinase (CDK). Hence absence of c-JUN results in elevated levels of both p53 and p21, subsequently low CDK activity and therefore retards cell cycle progression. Importantly, deletion of p53 could completely rescue the proliferation defect of *c-Jun*$^{-/-}$ cells (Schreiber *et al*., 1999). Similarly, c-JUN can also repress UV-induced p53-mediated p21 induction. Thus absence of c-JUN leads to prolonged activation of p53 and p21 following UV stimulation, leading to inefficient cell cycle re-entry (Shaulian *et al*., 2000). Furthermore, c-JUN has also been proposed to control cell cycle progression by directly regulating cyclin D1 expression (Bakiri *et*

al., 2000), suggesting that c-JUN can regulate multiple cell proliferation pathways.

On the other hand, JNP has been shown to affect cell proliferation only partially. Cells harboring mutant *c-Jun* alleles, where the JNK phosphoacceptor sites serines 63 and 73 were mutated to alanines (*c-Jun$^{AA/AA}$*), exhibited a partial proliferation defect. Proliferation analysis by counting the cumulative cell numbers demonstrated that the proliferation rate of primary *c-Jun$^{AA/AA}$* MEFs and keratinocytes were intermediate between *c-Jun$^{+/+}$* and *c-Jun$^{-/-}$* cells (Behrens *et al*., 1999, Li *et al*., 2003).

1.5.2 Cellular oncogenic transformation

Since discovery, *c-Jun* has been recognized as the cellular homologue of a retroviral oncogene that can transform chicken cells (Maki *et al*., 1987). Moreover, c-JUN activity can be augmented by various tumor promoters and activated oncoproteins (Vogt, 2001, Eferl *et al*., 2003b). Detailed investigations have then established its role in oncogenic transformation.

Overexpression of *c-Jun* alone could transform immortalized rodent fibroblasts and the transformed cells could form tumors in nude mice, emphasizing its ability in malignant transformation (Schutte *et al*., 1989). However, overexpression of *c-Jun* alone was not sufficient to transform primary rodent embryo cells. Transformation of primary cells, instead required *c-Jun* in combination with other activated oncogene such as *H-ras* that could then give rise to tumors in nude mice (Schutte *et al*., 1989, Vandel *et al*., 1996). Importantly, c-JUN is required for Ras-mediated oncogenesis, as

c-Jun^{-/-} cells were refractory to Ras-induced transformation and were unable to form tumors in nude mice (Johnson *et al*., 1996a). In addition, c-JUN also efficiently cooperates with c-FOS to enhance osteosarcoma formation caused by *c-Fos* overexpression (Wang *et al*., 1995).

JNP has been demonstrated to contribute partially to c-JUN's ability to cooperate with other oncoproteins. Although immortalized *c-Jun*^{+/+} and *c-Jun*[AA/AA] fibroblasts exhibited morphologically indistinguishable oncoprotein-induced *in vitro* transformation, the ability of the transformed cells to form tumors in nude mice varied dramatically. Absence of JNP considerably reduced v-Ras-induced tumor volume and significantly delayed v-Fos-induced tumor initiation (Behrens *et al*., 2000).

1.5.3 Programmed cell death

The role of c-JUN in apoptosis is cell type dependent. Several cell types have been examined to evaluate the effect of c-JUN on apoptosis, including lymphoid cells, neuronal cells, fibroblasts and hepatocytes. c-JUN was observed to promote apoptosis in some cell types and prevent apoptosis in others (Mechta-Grigoriou *et al*., 2001, Shaulian *et al*., 2001, Shaulian *et al*., 2002).

(1) Inhibition of c-JUN by antisense oligonucleotides protected growth factor deprivation-induced apoptosis in IL-6 and IL-2 dependent cell lines (Colotta *et al*., 1992). (2) Inhibition of c-JUN by a neutralizing antibody or targeted deletion of c-JUN by Cre recombinase reduced apoptosis of primary sympathetic neuron cultures from nerve growth factor (NGF) withdrawal

(Estus *et al*., 1994, Palmada *et al*., 2002). (3) c-JUN-deficient fibroblasts were resistant to apoptosis triggered by genotoxic stresses such as UV (Shaulian *et al*., 2000) and alkylating agents (Kolbus *et al*., 2000). (4) Moreover, overexpression of c-JUN alone was sufficient to trigger apoptosis in sympathetic neurons (Ham *et al*., 1995) and fibroblasts (Bossy-Wetzel *et al*., 1997). All these data demonstrate the pro-apoptotic effect of c-JUN.

In contrast to the pro-apoptotic function during survival factor withdrawal or genotoxic stresses as mentioned above, c-JUN also exerts a protective role particularly in liver cells during embryonic development. c-JUN-deficient embryo livers exhibited massive apoptosis in hepatoblasts and hematopoietic cells (Hilberg *et al*., 1993, Eferl *et al*., 1999).

JNP is important for c-JUN-induced apoptosis. The involvement of JNP in apoptosis has been demonstrated in fibroblasts, lymphocytes and neuronal cells. N-terminal truncated (dominant negative) c-JUN mutants which are disabled for JNP but still possess the dimerization and DNA-binding ability have been utilized to assess the effect of JNP on apoptosis. (1) Expression of dominant negative c-JUN mutant greatly inhibited apoptosis in human monoblastic leukemia cells upon various stresses including IR, hydrogen peroxide, UV, heat shock and TNF-α (Verheij *et al*., 1996). (2) Expression of different forms of dominant negative c-JUN mutants significantly reduced apoptosis induced by NGF withdrawal in both sympathetic neurons and PC12 cells respectively (Ham *et al*., 1995, Xia *et al*., 1995). (3) The N-terminal pseudo-phosphorylated c-JUN mutant induced cerebellar granule neuron (CGN) cell death and the N-terminal nonphosphorylatable c-JUN mutant

blocked CGN cell death (Watson *et al.*, 1998). (4) Primary sympathetic neurons isolated from *c-Jun*^{AA/AA} mice significantly delayed trophic factor deprivation-induced apoptosis (Besirli *et al.*, 2005). (5) *c-Jun*^{AA/AA} mice-derived primary cortical/hippocampal neurons were resistant to kainic acid-induced cytotoxicity and therefore the mice were also protected from kainic acid-induced epileptic seizures (Behrens *et al.*, 1999).

1.6 c-JUN and JNP in development

The emergence of genetic modification techniques allows distinct genes to be inactivated, mutated or ectopically expressed in mice in order to study their physiological functions. Mice harboring various types of genetically modified *c-Jun* have revealed many physiological and pathological functions of c-JUN and JNP.

c-JUN is expressed almost ubiquitously during and is essential for embryonic development. Homozygous *c-Jun* knockout mice (*c-Jun*^{-/-}) are embryonically lethal and die at mid-gestation between embryonic day E12.5 and E14.5 days (Hilberg *et al.*, 1993, Johnson *et al.*, 1993). The major organs affected by genetic *c-Jun* ablation are the liver and the heart (Hilberg *et al.*, 1993, Eferl *et al.*, 1999).

Surprisingly, JNP is dispensable for embryonic development. Homozygous *c-Jun* knock-in mice carrying mutant alleles of *c-Jun*, where the two most important phosphoacceptor sites serines 63 and 73 mutated to alanines (*c-Jun*^{AA/AA}) to prevent the their phosphorylation by JNKs, are viable and fertile with no major defects (Behrens *et al.*, 1999).

c-JUN conditional knockout (*c-Jun* gene flanked by two *loxP* sites, *c-Jun^{f/f}*) mice (Behrens *et al*., 2002) were generated to bypass the embryonic lethality caused by absence of *c-Jun*. Based on the Cre-loxP recombination system (Orban *et al*., 1992), c-JUN can be somatically removed at various stage of life and/or in different cell types/organs thus enabling further investigation on loss-of-function phenotypes.

1.6.1 Liver development

One of the most important organs affected by c-JUN deletion during embryonic development is the liver. Detailed histological analyses revealed that the morphological abnormalities of *c-Jun^{-/-}* livers emerged from E13.0; characterized by increased number of apoptotic and necrotic hepatoblasts and hematopoietic cells. Although the exact cause of the lethality of *c-Jun* null fetuses has not been determined yet, their liver defect was suggested to be the main reason (Hilberg *et al*., 1993, Eferl *et al*., 1999).

Another key evidence delineating the significance of c-JUN in liver development is from the analysis of the chimeric mice generated from *c-Jun^{-/-}* embryonic stem (ES) cells. Although *c-Jun^{-/-}* ES cells were able to differentiate into all organs (including liver), *c-Jun^{-/-}* ES cell derivatives were progressively lost in chimeric mouse livers after birth, presumably by imbalanced *c-Jun^{+/+}* and *c-Jun^{-/-}* hepatic cell turnover in the adult chimeric mice (Hilberg *et al*., 1993, Eferl *et al*., 1999).

Rodent liver continues to develop postnatally characterized by rapid hepatocyte proliferation and several fold increase of liver mass within the first

few weeks after birth (Behrens *et al.*, 2002). Function of c-JUN in postnatal liver development has also been analyzed using mice with perinatal (around E17.5) hepatocyte-specific inactivation of *c-Jun* (*c-Jun$^{f/f}$;Alfp-Cre*; Alfp: albumin promoter and alpha feto-protein enhancers). These mice are viable with reduced liver and body weight compare to wild type mice and do not display any overt impaired liver functions. However the postnatal hepatocyte proliferation was significantly reduced as assessed by BrdU incorporation of S-phase hepatocytes, indicating that c-JUN is required for early postnatal hepatocyte proliferation (Behrens *et al.*, 2002).

1.6.2 Heart development

Besides the liver defect, all c-JUN null fetuses analyzed also showed defect in heart development. Histological analysis of E12.5 embryos revealed a malformation of the heart outflow tract in all *c-Jun$^{-/-}$* fetuses, which resemble the congenital human disease of a persistent truncus arteriosus, indicating a role of c-JUN in embryonic heart development (Eferl *et al.*, 1999).

1.6.3 Skin development

The mammalian skin consists of two primary layers, the epidermis and the dermis, which are separated by the basal lamina. From embryonic development till birth, c-JUN expression was found to be restricted to the epidermis layer in mice (Angel *et al.*, 2001). Normal development of epidermis requires proper keratinocytes proliferation, differentiation and migration. Two separate studies using Cre recombinase driven by different keratinocyte-specific promoters (Keratin 5 [K5] and Keratin 14 [K14]) to

conditionally ablate c-JUN in epidermis both revealed interesting functions of c-JUN in skin development (Li *et al*., 2003, Zenz *et al*., 2003).

Mice with epidermis-specific inactivation of c-JUN (*c-Jun^{f/f};K5-Cre* and *c-Jun^{f/f};K14-Cre*) developed normal skin but both showed distinctively impaired eyelid development. The eyelids of wild type mice remain fused until approximately 10 days after birth. However, the mutant mice are born with open eyes and this phenotype is readily detectable before birth. The eyelids of these mutant mice fail to fuse during ontogenesis most likely due to insufficient EGF receptor (EGFR) expression in the keratinocytes at the leading edges of the developing eyelids, which results in defective eyelid epithelial cell migration. In addition, keratinocytes lacking c-JUN also exhibited defect in actin microfilaments distribution and organization. This cytoskeletal defect may be involved in the failure of mutant epidermis to spread forward over the developing cornea (Li *et al*., 2003, Zenz *et al*., 2003).

1.7 c-JUN and JNP in tumorigenesis

c-JUN and JNK activation have been associated in many human cancers (Wang *et al*., 2000, Liu *et al*., 2002, Papachristou *et al*., 2003). Manipulation of c-JUN and JNP in various mouse cancer models have provided some molecular explanations of how c-JUN and JNP contribute to tumorigenesis.

1.7.1 Skin cancer

The skin tumor prone K5-SOS-F transgenic mice, which express a dominant form of the guanine nucleotide exchange factor Son of Sevenless (SOS) in the basal keratinocytes develop skin papillomas with 100% penetrance (Sibilia *et*

al., 2000) and were used to investigate the role of c-JUN in skin carcinogenesis.

K5-SOS-F mice with conditional *c-Jun* deletion in keratinocytes exhibited significantly confined and reduced number of proliferating keratinocytes and approximately 50% decreased tumor volume compared to the control mice, albeit their tumor numbers, apoptotic index, histological appearance and cellular composition were comparable to the control mice. Moreover, c-JUN was found to transcriptionally regulate EGFR expression. Thus the reduced expression of EGFR observed in tumors lacking c-JUN has been attributed as the main reason of reduced tumor growth. Hence, c-JUN was suggested to regulate skin tumor development through its modulation of EGFR signaling (Zenz *et al.*, 2003).

K5-SOS-F mice harboring the *c-Jun*$^{AA/AA}$ mutant (to prevent JNP) also exhibited significantly reduced tumor sizes compared to the control mice at early stage of papilloma progression. However this protection was gradually lost with increasing age. Therefore, inactivating JNP resulted in delayed skin tumor formation induced by the hSOS-F transgene instead of abolishing it (Behrens *et al.*, 2000).

1.7.2 Intestinal cancer

Adenomatous polyposis coli (APC) is a tumor suppressor and a key regulator of intestinal neoplasia. Humans carrying germline mutations in the *Apc* gene are at risk of developing multiple intestinal adenomas that can progress to cancer (Moser *et al.*, 1993). Mice heterozygous for a nonsense mutation at

codon 850 of the *Apc* gene (*Apc^{Min/+}*) (Moser *et al.*, 1993) were used to investigate the involvement of c-JUN in intestinal cancer development.

Genetic abrogation of JNP in the *Apc^{Min/+}* mice (*Apc^{Min/+};c-Jun^{AA/AA}*) significantly reduced their tumor numbers and sizes and prolonged their lifespan. The average lifespan of *Apc^{Min/+};c-Jun^{+/+}* and *Apc^{Min/+};c-Jun^{AA/AA}* mice were 15.7 versus 23.1 weeks respectively. Moreover, genetic abrogation of c-JUN showed a more pronounced effect. *Apc^{Min/+}* mice with conditional *c-Jun* deletion in gut did not display any clinical sign of cancer development even at the age of 9 months. Collectively, these indicate that inactivation of JNP delays but inactivation of c-JUN protects *Apc^{Min/+}* mice from intestinal cancer development (Nateri *et al.*, 2005).

The mechanism of which c-JUN promotes intestinal tumorigenesis is through its JNP-dependent interactions with TCF4 and β-catenin, forming a ternary complex to regulate certain target gene transcription such as *c-Jun* and *Cd44* (Nateri *et al.*, 2005).

1.7.3 Liver cancer

This will be discussed in section 1.8.4.

1.8 c-JUN and JNP in liver pathology

While c-JUN is essential in the fetal liver development, it appears to be dispensable for basic liver functions in the adult mice. *In vivo* studies comparing mice with c-JUN deletion in the adult livers to wild type mice revealed no overt differences at the morphological level as well as at the

biochemical (serum lipids and enzymes) level (Behrens *et al*., 2002). Nevertheless, JNK/c-JUN signaling is active and is a major player in many liver pathogenesis of various etiologies such as TNF-α, ischemia/reperfusion, acetaminophen and high fat diet (Seki *et al*., 2012). Studies analyzing mice with targeted disruption of c-JUN in the adult livers under various kinds of liver pathological conditions have uncovered many crucial roles of c-JUN in liver pathology and will be further discussed.

1.8.1 Liver as an organ

Liver is a vital organ and its functions include storing glycogen, vitamins and iron etc. to provide energy to the body, removal of toxic waste and drugs from the blood, helping to digest food and absorb nutrients and much more (Kuntz *et al*., 2008). Due to the fact that it is playing such an important role, strong emphasis has been placed on it and studied extensively.
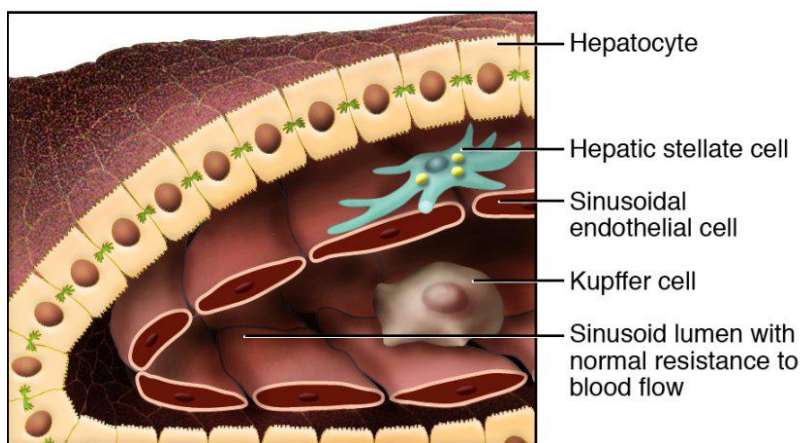
Figure 7. Hepatic cell types and sinusoid
Liver contains many different cell types, including hepatocyte (epithelial parenchymal cell), sinusoidal endothelial cell, Kupffer cell (resident macrophage) and hepatic stellate cell (HSC). Hepatic sinusoid is a type of capillary blood vessel lined with fenestrated sinusoidal endothelial cells and serves as the location for microcirculation. Figure adapted from Bataller & Brenner, 2005 Figure 1.

Liver is made up of a plethora of different cell types including hepatocyte, sinusoidal endothelial cell, Kupffer cell and hepatic stellate cell (HSC) (Figure 7). Hepatocytes are the main parenchymal cells, making up 70-85% of the liver mass, separated from the liver sinusoids by the perisinusoidal space (Berry *et al.*, 2000). They are cuboidal in shape and have distinctly round nuclei (Coleman *et al.*, 2009). Sinusoidal endothelial cells are a type of non-parenchymal cells that line to form sinusoid, which is the liver capillary. While they separate hepatocytes from sinusoidal blood, one of its role is hepatic microcirculation (Hernandez-Gea *et al.*, 2011). Kupffer cells are the largest population of macrophages that are reside within the liver sinusoid (Klein *et al.*, 2007). HSCs are vitamin A-storing cells residing in the perisinusoidal space, between the hepatocytes and the sinusoidal endothelial cells (Bataller *et al.*, 2005).

1.8.2 Liver regeneration

Adult liver has a unique regenerative capability to reconstitute functional liver parenchyma within a short period of time after a substantial loss of liver mass. This regenerative process is mainly achieved by the rapid replication of the remaining hepatocytes. Adult hepatocytes, albeit quiescent and highly differentiated, have the ability to re-enter the cell cycle to grow, divide and ultimately restore the original liver mass within a few days (Fausto, 2000, Behrens *et al.*, 2002).

The impact of c-JUN on liver regeneration has been examined by 70% PH in adult mice with conditional inactivation of c-JUN in (1) hepatocytes (*c-Jun^{f/f};Alfp-Cre^{tg}*) and (2) hepatocytes and hematopoietic cells (*c-Jun^{f/f};Mx-*

Cre^{*tg*}). Both mutant mice exhibited severely impaired liver regeneration and approximately 50% mortality within 3 days after surgery, whereas wild type mice showed normal regeneration with 100% survival. The proliferating hepatocytes were severely reduced in mutant livers, indicating that c-JUN is required for mature hepatocytes to re-enter cell cycle and proliferate to reconstitute liver parenchyma after PH surgery (Behrens *et al*., 2002, Stepniak *et al*., 2006). Interestingly, this liver regeneration defect of the c-JUN mutant mice can be completely rescued in a p53 or p21-negative genetic background; hepatocyte proliferation after PH was fully restored in the double mutant mice (Stepniak *et al*., 2006).

Although both c-JUN and JNP were strongly induced by PH in wild type mice, *c-Jun*^{*AA/AA*} mice, nevertheless, exhibited normal liver regeneration and no mortality after PH, indicating that JNP is not required for c-JUN function in hepatocyte proliferation (Behrens *et al*., 2002).

1.8.3 Inflammatory liver diseases

Inflammatory liver diseases are usually caused by hepatoviral infection and/or unhealthy diet. NAFLD is a common type of inflammatory liver disease and manifests as a metabolic syndrome as it is commonly associated with insulin resistance and obesity (Loomba *et al*., 2013). NAFLD ranges from simple steatosis to steatohepatitis. It is characterized by excessive lipid accumulation in hepatocytes as well as increased circulating free fatty acids which promote the production of proinflammatory cytokines such as TNF-α and endoplasmic reticulum stress. These in turn lead to hepatocellular injury and thus may

progress to more severe liver diseases such as cirrhosis and hepatocellular carcinoma (HCC) (Asrih *et al*., 2015).

c-JUN has been found to be strongly expressed in the livers of patients with acute hepatitis (Hasselblatt *et al*., 2007) as well as with various degrees of NAFLD (Dorn *et al*., 2014). Detailed mouse model and biochemical studies have revealed a significant protective role of activated c-JUN in several types of liver injury and inflammation.

In a hepatitis model, Concanavalin A (Con A) was used to induce liver injury through T cell activation, as well as expressing and releasing of TNF-α, thereby promoting hepatocyte death. With c-JUN deletion in (1) hepatocytes (*c-Jun^{f/f};Alfp-Cre^{tg}*) and (2) hepatocytes and hematopoietic cells (*c-Jun^{f/f};Mx-Cre^{tg}*), Con A injection led to markedly increased mortality in both mutant mice as compared to wild type mice. The protection of hepatocyte death by c-JUN was found to depend on its positive regulation of inducible nitric oxide synthase (*nos2*) gene and subsequent production of hepatoprotective nitric oxide (Hasselblatt *et al*., 2007). In a endoplasmic reticulum stress model, thapsigargin and tunicamycin were used to induce endoplasmic reticulum stress followed by activation of the unfolded protein response. This can trigger cell death if the endoplasmic reticulum stress is not resolved. Hepatocytes lacking c-JUN (*c-Jun^{f/f};Alfp-Cre^{tg}*) exhibited exacerbated and sustained endoplasmic reticulum stress characterized by massive cytoplasmic vacuolization and profound endoplasmic reticulum distension, therefore increased ballooning (death) compared to wild type hepatocytes. Interestingly, c-JUN-promoted hepatocyte survival during endoplasmic reticulum stress is

33

probably linked with autophagy as $c\text{-}Jun^{-/-}$ hepatocytes showed defects in autophagosome formation upon thapsigargin treatment (Fuest *et al*., 2012).

1.8.4 Liver carcinogenesis

HCC is the most common type of primary liver cancer and the third leading cause of cancer-related death in the world. The main risk factors for HCC include hepatitis viral infection, aflatoxin B-contaminated diet, alcohol abuse, obesity-related fatty liver disease and cirrhosis (Nordenstedt *et al*., 2010). Numerous genetically engineered mouse models have been generated mimicking the hot spot mutations frequently found in patients. Moreover, chemical induced cancer mouse models have been established to examine the mechanism of tumor initiation and promotion as well as anti-cancer therapies (Heindryckx *et al*., 2009, Bakiri *et al*., 2013). Diethylnitrosamine (DEN) is the most widely used chemical to induce liver cancer in mice, as the course of cancer development is similar to human HCC. DEN is a potent carcinogen that can induce hepatocyte DNA damage. When injected into very young mice (with actively proliferating hepatocytes), even a single low dose of DEN is able to initiate and cause HCC. However, when administrated to adult mice, a much higher dose of DEN and assistance from tumor promoters such as phenobarbital (PB) or carbon tetrachloride (CCl_4) are required to induce HCC (Heindryckx *et al*., 2009, Bakiri *et al*., 2013).

DEN/PB protocol was used to investigate the function of c-JUN in liver cancer development. Mice with hepatocyte-specific c-JUN deletion (*c-Jun^{f/f};Alfp-Cre^{tg}*) as well as mice with hepatocyte and hematopoietic cell-specific c-JUN deletion (*c-Jun^{f/f};Mx-Cre^{tg}*), both showed dramatically reduced

tumor numbers and sizes (Eferl *et al*., 2003a, Min *et al*., 2012). Same protocol was used to induce liver cancer in *c-Jun*$^{AA/AA}$ mice, whereas no differences in terms of tumor formation as well as tumor cell apoptosis were observed (Eferl *et al*., 2003a). These data demonstrated that c-JUN is required, but JNP is not required for liver tumor development.

The mechanism underlining c-JUN promoting liver tumor progression is via protection of tumor cells from apoptosis. In fact, c-JUN-deficient liver tumors exhibit markedly increased tumor cell death rather than reduced proliferation. Two pathways have been proposed to contribute to this situation. First, c-JUN can antagonize p53 and its pro-apoptotic target gene *Noxa* thereby suppressing the tumor cell death (Eferl *et al*., 2003a). On the other hand, c-JUN can also suppress c-FOS and its target gene *SIRT6*, a deacetylase that limits *survivin* promoter acetylation and transcriptional activation. Hence, c-Jun induces the expression of the anti-apoptotic survivin thereby promoting hepatocyte survival and tumor initiation (Min *et al*., 2012).

Taken together, c-JUN appears to be a positive regulator in several kinds of liver pathogenesis. Liver fibrosis is a typical response to hepatic injury (e.g. hepatocellular death) and occurs in almost all types of liver diseases (Seki *et al*., 2015). Therefore, it is conceivable that c-JUN may play a role in regulating hepatic fibrosis.

1.9 Hepatic fibrosis

1.9.1 Introduction to hepatic fibrosis

a Normal liver

Portal triad
Bile duct
Hepatocytes
HSC
Sinusoidal space of Disse
Portal vein
Sinusoidal endothelial cells
KC
Terminal hepatic vein
Hepatic arteriole

b Fibrotic liver

HSC activation and proliferation
Loss of hepatocyte microvilli
Loss of endothelial fenestrations
Distortion of veins
Increase in fibril-forming collagen in space of Disse

Fibril-forming collagens (Types I, III, V)
Basement membrane collagens (Types IV, VI)
Glycoconjugates (laminin, fibronectin, glycosaminoglycans, tenascin)

Hernandez-Gea V, Friedman SL. 2011.
Annu. Rev. Pathol. Mech. Dis. 6:425–56

Figure 8. Alterations of hepatic architecture
(**a**) In normal liver, HSCs are quiescent vitamin A-storage cells. The perisinusoidal space contains low density basement membrane-like matrix; (**b**) In fibrotic liver, HSCs activate, lose their vitamin A droplets, proliferate and migrate, secreting large amounts of fibrillar ECM proteins into the perisinusoidal space. Figure adapted from Hernandez-Gea & Friedman, 2011 Figure 2.

Hepatic fibrosis is a common public health problem that affects hundreds of millions of patients worldwide. Main risk factors like hepatitis viral infection, alcohol abuse and nonalcoholic steatohepatitis (NASH) can cause hepatic fibrosis. Advanced hepatic fibrosis can lead to cirrhosis, HCC or other liver-related morbidity and mortality (Bataller *et al.*, 2005, Schuppan *et al.*, 2013).

Hepatic fibrosis is defined as the excessive accumulation of fibrillar proteins in the perisinusoidal space. It is a dynamic process of imbalanced synthesis and degradation of the extracellular matrix (ECM) components. The synthesis of the ECM is characterized by both quantitative increase as well as qualitative alteration (from the low density basement membrane-like matrix shift to the interstitial fibrillar collagens) of the ECM components (Figure 8). The degradation of the ECM components is through a family of enzymes called matrix metalloproteinases (MMPs). One mode of regulation of MMPs is through tissue inhibitor of metalloproteinases (TIMPs), a family of proteinases that function to antagonize specific MMPs thus preventing the ECM degradation. Therefore MMPs and TIMPs work synergistically to regulate the turnover and remodeling of ECM. During fibrosis progression, the increased stiffness of ECM forms fibrous scars that progressively substitute the functional liver parenchyma, resulting in distorted liver architecture, altered liver function and portal hypertension, ultimately leading to pathological changes to the organ such as liver cancer (Bataller *et al.*, 2005, Friedman, 2008b, Hernandez-Gea *et al.*, 2011).

Hepatic fibrosis usually results from chronic liver damage and is classified as a wound healing response that engages a range of cell types. During liver

injury, hepatocytes are the main targets for most hepatotoxic agents and can regenerate to replace the dead cells. Damaged hepatocytes release signals like ROS, thereby stimulating the accumulation of inflammatory cells as well as activation of fibrogenic cells. Acute liver injury activates a transient wound healing response and causes limited fibrosis. The fibrotic components will be degraded after successful repair of the liver. In contrast, chronic liver injury activates a persistent wound healing response with repeated injury and healing, thus resulting in excessive accumulation of ECM and fibrosis (Bataller *et al*., 2005, Friedman, 2008b, Hernandez-Gea *et al*., 2011).

1.9.2 Hepatic stellate cell is the main fibrogenic cell type

The fibrogenic cells during liver injury and repair are derived from multiple sources including activated HSCs, periportal fibroblasts, bone marrow-derived mesenchymal cells and fibrocytes. Activated HSCs have been identified as the most dominant source (Friedman, 2008a, Forbes *et al*., 2011, Hernandez-Gea *et al*., 2011).

HSCs are a heterogeneous group of cells with similar functions. HSCs are formerly described as "lipocytes" based on their features of fat (vitamin A) uptake and storage. The name "hepatic stellate cell" has been standardized to reflect its resting morphology of a star-like shape found in normal liver (Bataller *et al*., 2005, Friedman, 2008a).

HSCs are well-known for their role in hepatic injury and repair. Upon liver injury, the structure and function of HSCs change dramatically, lose their characteristic vitamin A droplets and evolve into contractile myofibroblasts-

38

like cells. These activated HSCs proliferate and migrate to the sites of injury, producing and secreting large amounts of fibrous proteins to the ECM. Hence HSC activation and transdifferentiation are at the center of hepatic fibrosis progression (Bataller *et al*., 2005, Friedman, 2008a, Friedman, 2008b, Hernandez-Gea *et al*., 2011).

Conceptually, HSC activation consists of two major phases: initiation and perpetuation. Initiation results mostly from paracrine stimulation due to changes in the surrounding environment such as signals released from damaged/dead hepatocytes and activated inflammatory cells. Perpetuation involves both paracrine and autocrine loops to maintain and amplify the activated phenotypes including loss of vitamin A-storing capacity, proliferation, contractility and most importantly fibrogenesis (Friedman, 2000, Friedman, 2008a, Friedman, 2008b).

In order for activated HSC to be detected correctly, various markers such as α-smooth muscle actin (αSMA), desmin and vimentin have been determined and are considered as classical activated HSC markers. Promoters of these cytoskeletal proteins, as well as type I collagen and glial fibrillary acidic protein (GFAP) have been extensively used by numerous studies to specifically drive transgene expression in HSCs (Friedman, 2008a).

1.9.3 AP-1 and hepatic fibrosis

Several genes (e.g. TIMP-1, IL-6, Osteopontin etc.) involved in HSC activation and hepatic fibrosis are known AP-1 target genes. Specifically, JUND knockout mice (*Jund*$^{-/-}$) are significantly protected from CCl$_4$-induced

hepatic fibrosis and this has been attributed to impaired transcriptional activation of TIMP-1 due to the loss of JUND (Smart *et al*., 2006). Additionally, mice with ectopic induction of FRA1 (tetracycline-responsive element controlling FRA1) expression develop periportal hepatic fibrosis spontaneously. However, absence of FRA1 does not protect fibrosis development induced by three independent experimental fibrotic models (BDL [bile duct ligation], CCl_4 and DDC [3,5-diethoxycarbonyl-1,4-dihydrocollidine]) (Hasenfuss *et al*., 2014a).

Surprisingly, c-JUN's role in hepatic fibrosis has not been delineated albeit being a central molecule of the AP-1 family and an essential factor involved in multiple aspects of liver physiology.

1.9.4 Current treatment for hepatic fibrosis

Till date, despite clinical documentations about the reversal of liver fibrosis or even cirrhosis, there is no curative treatment for liver fibrosis. Currently, the most efficient way for fibrosis reversal is by removal of the causal agents such as denying alcohol intake or antiviral treatments. Moreover, there is evidence that once the damage persists for long period, even at a very low level, there is a steep decrease in the healing potential. For more serious conditions such as cirrhosis with clinical complications, the only approach currently is to undergo liver transplantation (Bataller *et al*., 2005, Schuppan *et al*., 2013). Hence development of effective antifibrotic therapies, including slowing or halting the progression of fibrosis or even promoting the regression of fibrosis, are required and might be possible in future.

1.10 Hedgehog signaling and liver repair

1.10.1 Canonical Hedgehog (Hh) signaling
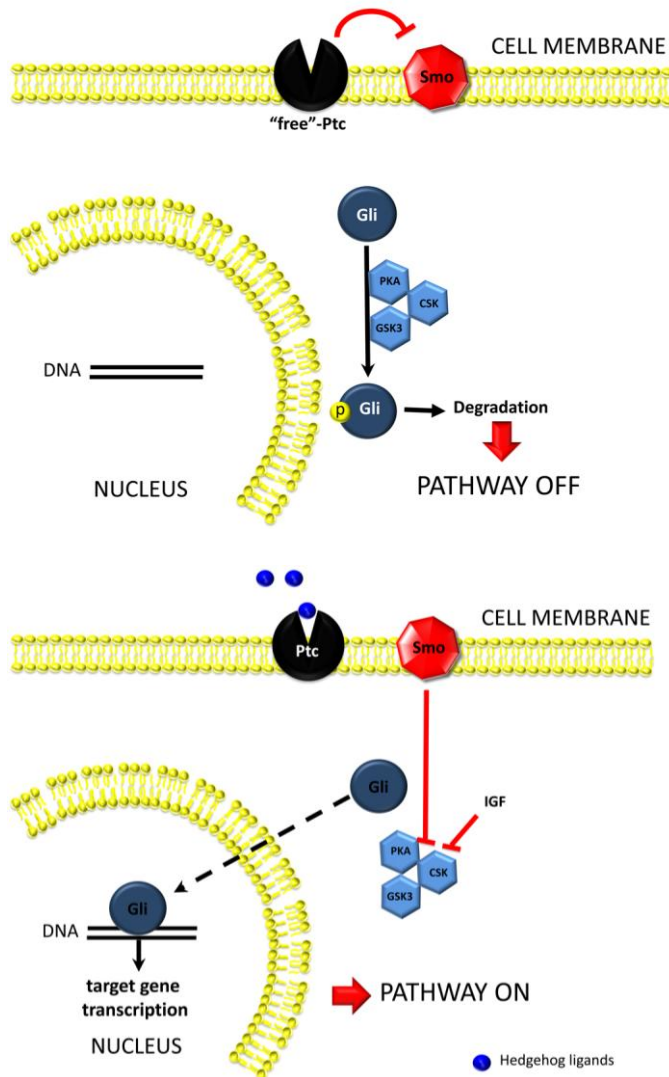
Figure 9. Canonical Hedgehog (Hh) signaling
Canonical Hh signaling pathway and components. Figure adapted from
Omenetti *et al*., 2011 Figure 1.

The Hh pathway is a highly conserved signaling pathway involved in

embryogenesis, development and tissue remodeling. The Hh proteins are

soluble ligands that include Sonic hedgehog (Shh), Indian hedgehog (Ihh) and

Desert hedgehog (Dhh). The canonical Hh pathway is illustrated in Figure 9.

Patched (Ptc) is a transmembrane receptor that physically interacts with the Hh ligands. In the absence of Hh ligands, Ptc represses the activation of Smoothened (Smo), thereby preventing Smo from interacting with the Glioblastoma (Gli) family of transcription factors (Gli1, Gli2 and Gli3), leading to their phosphorylation and subsequent degradation. Upon Hh ligand binding, Ptc liberates Smo. The activated Smo in turn permits the stabilization and nuclear translocation of the Gli transcription factors. Nuclear accumulations of the Gli transcription factors thus regulate the expression of Hh-target genes, which include several Hh pathway components such as Ptc, Gli1 and Gli2. Gli1 and Gli2 generally function to amplify the Hh signaling, whereas Gli3 primarily acts as the signaling repressor. Moreover, Hh-interacting protein (Hhip) is another transmembrane protein that competes with Ptc for binding with Hh ligands and therefore antagonizes Hh signaling (Omenetti *et al.*, 2008, Choi *et al.*, 2011, Omenetti *et al.*, 2011).

1.10.2 Hh-producing cells and Hh-responsive cells

Hh-producing cells are cells that can synthesize and release soluble Hh ligands to the extracellular space. Hh-responsive cells are cells that express the Hh receptor Ptc thus are able to interact with the Hh ligands and trigger intracellular signaling cascades. Hh pathway activation typically enhances the growth and viability of the Hh-responsive cells (Choi *et al.*, 2011, Omenetti *et al.*, 2011).

Hh-producing cells may or may not be Hh-responsive cells themselves. Studies have identified that many types of organ stromal cells and progenitor cells are Hh-responsive cells whereas the mature epithelial cells are generally

42

not (Omenetti *et al*., 2008). In the liver, mature hepatocytes are Hh-producing cell but not Hh-responsive cell, whereas HSCs are both Hh-producing cell and Hh-responsive cell. Therefore Hh-dependent paracrine and autocrine signaling can regulate HSC cell fate (Sicklick *et al*., 2005, Yang *et al*., 2008, Jung *et al*., 2010).

1.10.3 Hh signaling in adult liver repair

Adult liver repair requires regeneration of the liver parenchyma to replace damaged epithelial cells. Cell lineage tracing has revealed that new hepatocytes can be derived from both proliferation of undamaged hepatocytes and differentiation of the liver progenitor cells. Liver progenitor cell populations are heterogeneous, including Lgr5 positive cells, Sox9 positive cells and Keratin 19 (K19) positive cells. Interestingly, quiescent HSCs express high levels of Lgr5 and could differentiate into hepatocytes during liver repair, hence HSC also functions as a source of liver progenitor cells (Swiderska-Syn *et al*., 2014).

Healthy adult livers do not exhibit active Hh signaling. Activation of Hh signaling occurs rapidly following liver injury. Damaged epithelial cells produce Hh ligands; these ligands diffuse away and enter the bile canaliculi and liver sinusoids and activate Hh signaling in Hh-responsive cells such as HSCs and other liver progenitor cells (Omenetti *et al*., 2011). The role of active Hh signaling in adult liver repair has been investigated in various models including methionine choline-deficient, ethionine-supplemented diet (MCDE), BDL and PH. Inhibition of Hh signaling by targeted disruption of Smo in HSCs in all models significantly reduced HSC activation and

attenuated hepatic fibrosis. However, absence of Hh signaling also impaired liver repair due to abrogated accumulations of various liver progenitor populations (Michelotti *et al.*, 2013, Swiderska-Syn *et al.*, 2014).

1.11 Aims

c-JUN was first discovered as a cellular homologue of the retroviral oncoprotein v-Jun and as a central molecule of the AP-1 transcription factor complex. Since then on, accumulating evidence have surfaced to emphasize on c-JUN/AP-1 functions in transcriptional regulation of multiple biological processes such as embryonic and tumor development (Mechta-Grigoriou *et al.*, 2001, Vogt, 2001). The activity of c-JUN/AP-1 was thought to be regulated mainly by N-terminal phosphorylation at serines 63/73 through JNKs, which respond to a wide range of stress stimuli in regulating various aspects of cellular physiologies including inflammation (Karin, 1995, Karin *et al.*, 1997). Till date, deregulated c-JUN expression has been detected in a spectrum of diseases and disorders with particular attention in the liver, neurons and skin (Shaulian *et al.*, 2002, Eferl *et al.*, 2003b).

The cellular functions (such as cell proliferation, apoptosis and transformation) and the physiological functions (such as development, regeneration and tumorigenesis) of c-JUN and its related target genes in certain cell/tissue types have been discovered and studied in great detail. However, despite the increasing knowledge of c-JUN, its role in several other physiological conditions (such as fibrosis) and other cell/tissue types (such as adipose tissue) is still not clear and remains to be elucidated. The aim of my study is thus to identify and characterize novel c-JUN target genes and

biological processes on a global scale, and focus on characterizing in detail a top pathway identified with specific emphasis on certain tissue/cell types.

Chapter 2

Materials and Methods

2.1 Materials

2.1.1 Mice

Table 2. Genetically modified mice used in this study

Mouse Strain (Background)	Genotype	Description	Source
c-JUN knockout (C57BL/6 × 129)	$c\text{-}Jun^{+/-}$	Mouse harboring a frameshift mutant $c\text{-}Jun$ allele (Johnson $et\ al.$, 1993).	The Jackson Laboratory
c-JUN knock-in (C57BL/6 × 129)	$c\text{-}Jun^{AA/+}$	Mouse harboring a mutant $c\text{-}Jun$ allele with serines 63 and 73 mutated to alanines (Behrens $et\ al.$, 1999).	Dr Axel Behrens
c-JUN conditional knockout (C57BL/6)	$c\text{-}Jun^{f/f}$	Mouse carrying floxed $c\text{-}Jun$ alleles which the $c\text{-}Jun$ gene is flanked by two $loxP$ sites (Behrens $et\ al.$, 2002).	Dr Erwin Wagner
Mx-Cre transgenic (C57BL/6 × 129)	$Mx\text{-}Cre^{tg}$	Mouse carrying Cre transgenes whose expression are controlled by an interferon-inducible $Mx1$ promoter (Kuhn $et\ al.$, 1995).	Dr Zhao Qi Wang
Col-CreER transgenic (C57BL/6)	$Col\text{-}CreER^{tg}$	Mouse carrying $CreER$ transgenes which are directed by $Col1a2$ promoter. The CreER recombinase needs to be activated by tamoxifen (Zheng $et\ al.$, 2002).	The Jackson Laboratory

2.1.2 Cells

Freshly isolated primary MEFs were used in this study.

2.1.3 Drugs and treatments

Table 3. Drugs and treatments used in this study

Name	Source	Catalog No.
Carbon tetrachloride (CCl_4)	Sigma	319961
cis-Diammineplatinum (II) dichloride (Cisplatin, CDDP)	Sigma	P4394
Olive oil	Sigma	O1514
Polyinosinic-polycytidylic acid sodium salt (Poly I/C)	Sigma	P0913
Tamoxifen	Sigma	T5648
UV Stratalinker® 2400	Stratagene	-

2.1.4 Chemicals and Reagents

Table 4. Chemicals and Reagents used in this study

Chemicals and Reagents	Source	Catalog No.
1-Bromo-3-chloropropane (BCP)	Sigma	B9673
Albumin, Bovine (BSA)	Amresco	0332
cOmplete ULTRA Tablets, Mini, EDTA-free (protease inhibitor cocktail)	Roche	05892791001
Direct Red 80 (Sirius Red)	Sigma	365548
Eosin Y solution, aqueous	Sigma	HT110232
Formaldehyde solution min. 37%	Merck	-
Hematoxylin Solution, Mayer's	Sigma	MHS16
Hematoxylin solution A according to Weigert	Sigma	03973

Hydrochloric acid 37%	Sigma	258148
Phosphatase Inhibitor Cocktail 2	Sigma	P5726
Picric acid solution	Sigma	P6744
Propidium iodide (PI)	Sigma	P4170
Protein Block Serum-Free	Dako	X0909
Proteinase K	Amresco	0706
QuantiFast SYBR Green PCR Kit	Qiagen	204057
SuperScript® II Reverse Transcriptase	Invitrogen	18064-014
Trisodium citrate dihydrate	Sigma	S1804
TRIzol® Reagent	Invitrogen	15596018
Tween 20	Sigma	274348
Xylene	Fisher Scientific	-

2.1.5 Antibodies

Table 5. Antibodies used in this study

Primary Antibodies	Usage	Source	Catalog No
Annexin V-FITC	flow cytometry	BD Biosciences	556419
Anti-Actin	immunoblot	Sigma	A2066
c-JUN (60A8)	immunoblot	Cell Signaling	9165
c-JUN (H-79)	immunoblot	Santa Cruz Biotechnology	sc-1694
JNK1/JNK2	immunoblot	BD Biosciences	554285
Phospho-c-JUN (Ser 63) II	immunoblot	Cell Signaling	9261
Phospho-SAPK/JNK (Thr183/Tyr185) (G9)	immunoblot	Cell Signaling	9255

αSMA	immunostaining	Abcam	AB-32575
Desmin	immunostaining	Abcam	AB6322
Ihh	immunostaining	Abcam	Ab39634
Gli2	immunostaining	GenWay Biotech	GWB-B3B44

Secondary Antibodies	Usage	Source	Catalog No
Anti-rabbit IgG, HRP-linked	immunoblot	Cell Signaling	7074
Anti-mouse IgG, HRP-linked	immunoblot	Cell Signaling	7076
Anti-rabbit IgG	immunoblot	Sigma	A9169
Anti-mouse IgG	immunoblot	Sigma	A2304
Anti-rabbit, HRP-labelled polymer	immunostaining	Dako	K4003
Anti-mouse, HRP-labelled polymer	immunostaining	Dako	K4001

2.1.6 Homemade solution

Table 6. Components of homemade solutions used in this study

Experiment	Solution name	Components
Mouse genotyping	Tail lysis buffer	1% SDS, 50 mM Tris pH 8.0, 10 mM NaCl, 10 mM EDTA
	TE buffer	10 mM Tris pH 8.0, 1 mM EDTA
Immunoblot	Protein lysis buffer	1% Nonidet P40, 50 mM Tris pH 7.6, 150 mM NaCl, 5 mM EDTA, 50 mM NaF, 1 mM Na_3VO_4

	Sample loading buffer (6X)	0.375M Tris pH 6.8, 12% SDS, 60% (v/v) glycerol, 0.6M DTT, 0.06% bromophenol blue
	Running buffer (10X)	0.25 M Tris, 1.92 M Glycine, 1% SDS
	Transfer buffer	25 mM Tris, 192 mM Glycine, 20% (v/v) methanol
	Tris Buffered Saline (TBS 20X)	0.4 M Tris, 2.74 M NaCl, pH 7.6
	Membrane Blocking buffer	5% (w/v) non-fat milk powder in 1XTBS with 0.1% (v/v) Tween-20
	Primary antibody dilution buffer	5% (w/v) BSA in 1XTBS with 0.1% (v/v) Tween-20
	Secondary antibody dilution buffer	1% (w/v) BSA in 1XTBS with 0.1% (v/v) Tween-20
	Washing buffer	1XTBS with 0.1% (v/v) Tween-20
immunostaining	Sodium Citrate Buffer	10 mM Trisodium citrate dihydrate, pH 6.0
	Washing buffer	1XTBS with 0.01% (v/v) Tween-20

2.1.7 Primers

Table 7. Genotyping primers used in this study

Strain	Primer	Sequence 5'-3'	Target
c-JUN knockout	neo_for	TTCGGCTATGACTGGGCACAACAG	mutant
	endo_for	CTGAGTGTGGCAGAGACAGC	wild type
	endo_rev	GCTAGCACACTCACGTTGGTAGG	

c-JUN knock-in & conditional knockout	Lox5	CTCATACCAGTTCGCACAGGC	-
	Lox6	CGCTAGCACTCACGTTGGTAG	-
Mx-Cre & Col-CreER	12249	TCCAATTTACTGACCGTACACCAA	Cre transgene
	12250	CCTGATCCTGGCAATTTCGGCTA	
	oIMR7338	CTAGGCCACAGAATTGAAAGATCT	internal control
	oIMR7339	GTAGGTGGAAATTCTAGCATCATCC	

Table 8. qRT-PCR primers used in this study

Gene Symbol	Primer Sequence 5' - 3'	
9830001H06RIK	forward	CTCCCAGAGCTACTGAGAG
	reverse	GAAATGCACAACCCATAC
1500004F05Rik	forward	TGCCGAATTCTCTGATGC
	reverse	AAGTCCAGAAGCCAGCCT
2610528A11Rik	forward	AGATGAAGCGTTGATGCC
	reverse	CTGAGCCTGGACCTTAGTGA
Ablim1	forward	GCTTCTTCCCATGTTCTC
	reverse	GTATGCTGCCAGGGTAAC
Agtr1b	forward	CAAGGAAGCAACACATCA
	reverse	GGGAGAGAATCACAGCAG
Ambra1	forward	CACATGCCTTCTCTAATTC
	reverse	AAGCAATACTCCACTCCTC
Ampd1	forward	GTCACCGCTGAGTAACAA
	reverse	CTTGGTGAAGTGGAACTG
Angptl2	forward	AGAAGTCGCTGCCAATAG
	reverse	CAAGACTCAGGAAGCCAC

Arhgap5	forward	CAGTCAATGCTGTAGCTGG
	reverse	CGCTCTGTTTTATCTGGGA
Arid5b	forward	GGGCTCAACTTCAAAGACG
	reverse	AGGGCTAATGCGAACTGG
Arl13b	forward	TGCTAAGACACCCGAGGA
	reverse	CACTTGTGCTCGTTGACCA
BC023969	forward	AGGGACACAAGGGTACAAGG
	reverse	GTCATAGGTTGGCACTGTAGG
C1qa	forward	TCCATACCAGAACCACAC
	reverse	CCTGCTAACACCTGAAAG
C1qb	forward	TGCCTGGCCTCTACTACT
	reverse	TCAAGACTACCCCACCTG
C1qc	forward	ACTACACATCGCATACGG
	reverse	GAGAAGACGCTGTTGGAG
C3ar1	forward	ATGGCTGAATAACACTGC
	reverse	TTAGGCATTGGTTGGTAG
Cd14	forward	CCAGTCAGCTAAACTCGC
	reverse	TCCTATCCAGCCTGTTGT
Chd7	forward	TGAAGCTGTGTTGAAAGGC
	reverse	GGCAAAGCTCCTCTTCTG
Cp	forward	ACACCAAGGAGTATGAGGGAG
	reverse	TGGTAAATCCTGGTCACACAA
Cpeb4	forward	CACTTGACCCACGGAAAAC
	reverse	GCGACTCTTCCAGCTCCTT
Ctrl	forward	TGAATCAGTGTCGGCAGTA
	reverse	CTTGCTGACCCGAGTGTA

Cyp1b1	forward	CCTGCCACTATTACGGACATC
	reverse	AGCTGGAGAATCGCATTGA
Dcn	forward	ACACCAACATAACTGCGA
	reverse	CATTCTCCATAACGGTGA
Depdc1a	forward	GGACTTTGGTTTATTGGG
	reverse	AAGAGAATAAGGCAGGAGG
Dock11	forward	TGGGTGTTCAGCGTTCAA
	reverse	ATTCACGGCGTTTCTCATAA
Dyrk1a	forward	GGAGTTAGAAGAGCCCAC
	reverse	AACCAAGAAGGGAGTCAG
E030042N06Rik	forward	AGCCTGGGTCAGTTTACAAG
	reverse	GAAGACAAACGGAACCCTAC
Elavl1	forward	TTCCAAAGCTCTTCAAAGTC
	reverse	ACAGAATTGCAGTCAGTGGT
Elk3	forward	CCTGGGATGCTGAGTAGTAG
	reverse	GTTTCTGTTGACGAGTGCC
Emilin2	forward	CCTATAAGCCAGCTCTGC
	reverse	AGGCCACATAAGCACTTC
Eml4	forward	GAGGAAAGGACTGTAGAGCGA
	reverse	CGGCTATCTGTCCAGTTGC
Enpp1	forward	GAGTGTCCAGCAGAGTTTGA
	reverse	GCTTGCTAATGACAGGAAGA
Erc2	forward	GTGTTTATGATGAGCCCT
	reverse	CACTATCAAACAAGGGTCT
Erlin1	forward	GTTGGCTCCTTATGCAGTGT
	reverse	CAGCCTGGATAGTGAGACCT

Fam174b	forward	GTTCTGACTGGGGTTGTG
	reverse	CCAAGGCTGAGAGGATGT
Fermt3	forward	GAAGAGCTGGATGAGGAT
	reverse	CCTGGTGACAACAAGTGA
Fgf1	forward	CAGTACTTGGCCATGGAC
	reverse	CTCCGTGTAACAAGCCTT
Flt4	forward	GAACCGCATGTATGACTG
	reverse	TCCTAGTGGTGAGCTTGA
Gabpb2	forward	CTCTTGACTCCTCGACCCAG
	reverse	TGACCAGCAGGCACAGTTAG
Gdf9	forward	AATGCTGTGGGCCTTAGA
	reverse	GCCCTTTACACCTACGGAC
Glt25d1	forward	GAACTCAGATGTGCTCCA
	reverse	GCTCTCTGTTGTCTGCCT
Gm5544	forward	GAATTGGCCTGGTCTAGC
	reverse	GTTTCACTACCCGAGGGA
Gpr1	forward	GGTGGCCGTTCTGATACT
	reverse	AGAACCCAGCCTGATACT
Gsto2	forward	AAGCTGTTTCCGTATGACC
	reverse	TACAGTCTCTTCCGCATCTC
Gtf3c1	forward	CGGACTACAGTCATTCAGG
	reverse	CTGTGCTTGAGTTGGAGA
Hipk2	forward	CCGTCTACACTGGATACC
	reverse	GCAGTAGAAAATCCCAGC
Hjurp	forward	AGGTGATTCAGAGAGCAGC
	reverse	CAGTTTCCAAGGTGTTTCC

Hoxa5	forward	CGCAAGCTGCACATTAGTCA
	reverse	TCAGGTAGCGGTTGAAGTGG
Ica1	forward	GGACAGAATACAGAGGAGCG
	reverse	CCACCTTTTGACACACATCC
Igf2	forward	CAGTGCCCTCTCCTTATC
	reverse	GCTTGTGCCAATTAAGTTC
Il1rl1	forward	GCTTTCTCCCATTTCTAC
	reverse	ACAGAGATGGCTACAAGAG
Il4ra	forward	AGCTGGGCCTAGAAACTC
	reverse	CAGTGACTTTGGGCAATC
Itsn1	forward	GTGAGTGTGACATGGCGT
	reverse	CTGAAGCCCAAGTAGACAAG
Kif13b	forward	TGAGAGCCTTGGCATATC
	reverse	GCGTGTGCTCCTTTAAGT
Laptm5	forward	TTAGCCTGGCAGATTTAG
	reverse	CTCTTCACACCCCATAGG
Mapk8	forward	CCTGTCAGCCTTATCCCTC
	reverse	TTGCCTACTGCTCATCCTATC
Nasp	forward	AAGCAGTAGCACAGTTTGGC
	reverse	GCTGAGATTCCTTTGCGTC
Nefl	forward	GCCTTGGACATCGAGATTG
	reverse	CTCTGAGAGTAGCCGCTGGT
Nfia	forward	TGGATGGCATGAAGTAGA
	reverse	ACTCTTTCAGCGTCTCCT
Nppb	forward	CTGCTGGAGCTGATAAGA
	reverse	CAAAGCAGCTTGAGATATG

Ola1	forward	GGAAGATTTGGAACCTCACTG
	reverse	TCTGCTGAAGCCTGACTATTG
Pcmtd2	forward	GTCACTGAGTACGCGAAGCA
	reverse	CCAGGCAATTTCCAGTTACAA
Pdgfra	forward	CCACTGTCTCTGTACCCC
	reverse	GAAAGCAGGAAAGATTGG
Pik3r1	forward	CCCATTCTAGAGACAGCC
	reverse	CAGGGCTGTGAAGTTGTC
Plscr2	forward	TGAAGGCTGTGAGTAGGA
	reverse	CCCAGGTCTCTCAATCAT
Pogk	forward	ATCGGTTGGAAAGGGACG
	reverse	TGAGGAAAATGGGAGGTGG
Prnd	forward	CCACAGTAGCAGAGAACCGAG
	reverse	TTATGCCCCTTGCCTTGAC
Prrc1	forward	GGAACCACATCAGCCATTAC
	reverse	ATCCAGGACAGATTTCACCA
Ptger1	forward	CATCCTGAGCAGCACTGG
	reverse	CAGATGTATTGGGGAGCCT
Pus3	forward	AGAAAGCAGACAGACATCCAA
	reverse	TGGAAACTGAGAACGTAGGTC
Rad21	forward	AAGCCCATGTATTTGAGTGC
	reverse	CATTACAGTCTGCGAGGAGG
Rcan1	forward	GATAAACTTCAGCAACCC
	reverse	GGTGGCATCTTCTACTTG
Scd2	forward	AACACGCAGGCTATGATT
	reverse	TCAGTTGCCACCTACTAAGA

Sdcbp	forward	CAGGCGTTTGGAGAGAAG
	reverse	GTTCTGTCCGTTGATCTCAC
Sema7a	forward	GGGCCATCAGCAACTCAA
	reverse	GAACAGGGAAGGACGCAAAG
Sh3rf1	forward	GCCTTTCTTCCACCCTTG
	reverse	ATGCAGGATCTGGGAACC
Shd	forward	GAAGCAGCCGTGGTTTCA
	reverse	GGGTCCTTGCGAATTTCAG
Slc7a2	forward	AGAGGAGGAGTTGGATGA
	reverse	TTAGTGCTGCTTGTATGTG
Sparcl1	forward	CTTTGAGGAGTGTGACCC
	reverse	GTTAAAGCAGGTGAGGTG
Tacc3	forward	GACCAATAAGCGTGAGGC
	reverse	AGATTCCCTCCTGTAACTCG
Tbl1xr1	forward	AACATGGAGAGATAAGGG
	reverse	CAGTTCTCTCTTTCCACC
Tigd3	forward	CCCGTCACTCTCTGGTTCT
	reverse	GTTCAGCTCCATGACTCCC
Tm9sf2	forward	CAACGAGTGCAAGGCTGATA
	reverse	CCCCGAATAATACCTGACCA
Tnfrsf11b	forward	ACAGAGAAGCCACGCAAAAGT
	reverse	AGCTGTGTCTCCGTTTTATCCT
Vwce	forward	CGGGACATGCCAGATAGAG
	reverse	CAGGGGCCAAACAGAAAC
Wrn	forward	GGAACATCTAAGTGACCCAA
	reverse	TGTGTATCTGAAGGGACGG

Ywhaz	forward	TCGCAACCAGAAAGCAAAG
	reverse	CTTCTTGGTATGCTTGCTGTG
Acta2 (αSMA)	forward	GAGGCACCACTGAACCCTAA
	reverse	GTTGTACGTCCAGAGGCATAGA
Des (Desmin)	forward	TACACCTGCGAGATTGATGC
	reverse	ACATCCAAGGCCATCTTCAC
Vim (Vimentin)	forward	TCTCTGGCACGTCTTGACC
	reverse	GCCACGCTTTCATACTGCT
Col1a1	forward	CTGGCGGTTCAGGTCCAAT
	reverse	TGTTCCAGGCAATCCACGAG
Col1a2	forward	AGGCCCAACCTGTAAACACC
	reverse	GAGGACACCCCTTCTACGTT
Tgfb1	forward	CCATTGCTGTCCCGTGCAGA
	reverse	TTGGTTCAGCCACTGCCGTA

2.2 Methods

2.2.1 Mouse breeding

Mice (above six weeks age) of *c-Jun*$^{+/-}$, *c-Jun*$^{AA/+}$, *c-Jun*$^{f/f}$, *Col-CreER*^{tg} and *Mx-Cre*^{tg} genotypes were used for breeding in order to generate required specific genotypes for experiments. Detailed genotypes of the breeders and offspring are shown in the results section.

2.2.2 Mouse treatment

Six-week-old mice were treated twice a week with olive oil or CCl_4 (1 μl per gram body weight [gbw], diluted in olive oil) by intraperitoneal (i.p.) injection for 4, 6 and 8 weeks to induce fibrosis. For $c\text{-}Jun^{f/f};Col\text{-}CreER^{tg}$ and $c\text{-}Jun^{f/f};Col\text{-}CreER^{ntg}$ mice, additional treatment with tamoxifen (1 mg per mouse) was administrated by gavage to activate the Cre recombinase. For $c\text{-}Jun^{f/f};Mx\text{-}Cre^{tg}$ and $c\text{-}Jun^{f/f};Mx\text{-}Cre^{ntg}$ mice, additional dosage of Poly I/C (13 μg/gbw) were administrated by i.p. injection to induce the expression of the *Cre* transgenes. All mice were sacrificed 48-72 hour after the last injection and their livers were excised, frozen or formalin fixed for further analysis. Detailed injection and harvesting schemes are shown in the results section. All animal experiments were approved by and performed in accordance with the guidelines of the SingHealth's Animal Care and Use Committee.

2.2.3 Mouse genotyping

Around 5 mm tail tip of every three-week-old mouse or yolk sacs of individual embryos were collected to confirm the mice genotypes. Samples were digested overnight in tail lysis buffer with 0.4 mg/ml Proteinase K at 55 °C. The genomic DNA was precipitated by adding 0.25 volume of saturated NaCl and one volume of 2-Propanol. The precipitated genomic DNAs were then washed once in 70% ethanol, air dried and resuspended in appropriate amount of TE buffer. These purified genomic DNAs were used as templates to amplify by polymerase chain reaction (PCR) in order to determine genotypes. The genotyping primers are listed in Table 7.

2.2.4 Mouse embryo isolation

Heterozygous $c\text{-}Jun^{+/-}$ male and female mice or $c\text{-}Jun^{AA/+}$ male and female mice were mated and the appearance of the vaginal sperm plug was taken as 0.5 day post coitum (dpc). Pregnant females were sacrificed at 11.5 or 13.5 dpc and the embryos were isolated, frozen or formalin fixed, or immediately used to prepare MEFs for culture.

2.2.5 Primary MEF culture and treatment

MEFs were prepared from embryonic day 11.5 dpc embryos. Briefly, embryo yolk sac and head were removed; the rest of the embryo body was disaggregated by a 1 ml insulin syringe plunger and filtered with a cell strainer. Filtered cells were plated onto one well of a six-well plate in Dulbecco's modified Eagle's medium (DMEM) supplemented with 10% serum, 100 units / ml penicillin and streptomycin, 0.1 mM non-essential amino acids, 2 mM glutamine, 1 mM sodium pyruvate. MEFs were cultured at $37^{o}C$, 5% CO_2 and 3% O_2 condition.

Trypsin-EDTA (0.05%) was used to subculture primary MEFs. Briefly, when cells reach 90% confluency, culture media was discarded and the cells were washed gently with 1X phosphate buffered saline (PBS). The cells were then incubated with appropriate amount of 0.05% Trypsin-EDTA until they completely detached from each other as well as the culture plates. The detached cells were then resuspended in fresh media and divided accordingly.

Early-passaged MEFs were seeded onto appropriate areas of culture plates the day before treatment. On the treatment day, culture media were discarded and

the cells were washed once with 1X PBS; the washed cells were either irradiated with various doses of UV (Stratagene UV Stratalinker 2400) followed by addition of fresh culture media or replaced with fresh media containing various concentrations of CDDP. The treated cells were further incubated and harvested at indicated time points for immunoblot, apoptosis, transcriptome and target gene expression analysis.

2.2.6 Proliferation assay

At least 4 individual MEF clones were used per genotype to generate the growth curve. 1×10^5 number of MEFs were plated onto six-well plates and were counted daily. Independent experiments were performed in duplicates and data collected were represented as mean + standard deviation (SD).

2.2.7 Apoptosis assay

 MEFs were treated with 40 J/m^2 or 80 J/m^2 of UV radiation, 15 μM or 30 μM of CDDP respectively for 24h prior to harvesting. Both live and dead cells were collected, washed once in PBS and incubated with Annexin V-FITC and 0.5 μg/ml of PI in binding buffer (10 mM HEPES pH 7.4, 0.14 M NaCl, 2.5 mM CaCl$_2$) for 15 to 30 minutes in the dark at room temperature. Cells were analyzed by flow cytometry (Becton Dickinson FACSCalibur) immediately after incubation.

2.2.8 Immunoblot assay

Cells were harvested, washed once with PBS and lysed for 30 minutes in lysis buffer with protease inhibitor cocktail and phosphatase inhibitor cocktail on

ice. The suspensions were then spun for 15 minutes at 14000 rpm in refrigerated centrifuge and the supernatant was transferred to new tubes for further experiments or kept in -80 $^{\circ}$C for long term storage.

50 μg whole cell extracts were separated by 10% SDS-PAGE and transferred to PVDF membrane (Millipore). Immunoblotting was performed with the following antibodies: Phospho-c-JUN (Ser 63) II Antibody, c-JUN (60A8) Rabbit mAb, Phospho-SAPK/JNK (Thr183/Tyr185) (G9) Mouse mAb, JNK1/JNK2 and anti-Actin antibody. Blots were incubated with ECL western blotting detection reagent (Amersham) and chemiluminescence was detected with Biomax MR X-ray film (Kodak). Detailed information of all the antibodies were listed in Table 5.

2.2.9 RNA extraction

TRIzol reagent was added to whole mouse embryos, cell pellets, small fractions of mouse livers individually and was lyzed by homogenizer, vortexing or TissueLyser II (Qiagen) respectively. 0.1 volume of BCP were added to separate the lysate into an organic layer and aqueous layer. The aqueous layer was pipetted into a new tube along with 2-Propanol, causing RNA to be precipitated. The precipitated RNAs were then washed in 75% ethanol (prepared in nuclease-free water) to remove impurities, air dried and then resuspended in nuclease-free water.

2.2.10 Transcriptome analysis

Transcriptome of tissues/cells were analyzed by whole genome expression microarrays. In brief, total RNAs were extracted as mentioned above; RNAs

were labeled and hybridized on GeneChip® Mouse Genome 430 2.0 Arrays (Affymetrix); the hybridized arrays were then washed and scanned to generate raw data. All the procedures were performed according to the manufacturer's instructions.

Raw data were processed using Partek Genomic Suite software, normalized by GC-RMA method to convert into a $\log_2$ scale. Differentially expressed genes were identified using Analysis of variance (ANOVA) test and filtered with the statistical cutoff set at false discovery rate (FDR) <0.05 and fold change (FC) >2.0. The Ingenuity Pathway Analysis (IPA) software (www.ingenuity.com) was used to analyze the gene ontology and canonical pathways that are differentially enriched in the various gene sets.

2.2.11 Quantitative gene expression assay

Total RNA was prepared as mentioned above. RNA Concentration was determined by NanoDrop and 1-3 μg of total RNA was used to synthesize cDNA using SuperScript II reverse transcriptase.

Quantitative real-time PCR (qRT-PCR) was performed using gene-specific primers and QuantiFast SYBR Green PCR Kit in Rotor-Gene Q real-time PCR machine (Qiagen) according to manufacturer's instructions.

Relative gene expression was normalized with *gapdh* expression and fold induction was calculated with reference to wild type samples.

2.2.12 Histological analysis

Both the mouse embryo and liver tissue were fixed in 10% formalin for about 16 hours. The embryo was then cut at the sagittal plane through its midline whereas for the liver, each of the four liver lobes were cut and the largest piece of each lobes was taken. They are then dehydrated and embedded in paraffin blocks. Thereafter, tissue was sectioned at a thickness of 5 μm, placed on glass slides and baked in 55°C oven for a few hours. Once the sections were ready to be stained, they were deparaffinized in xylene and rehydrated gradually by a series of decreasing concentrations of ethanol all the way to water.

For Sirius Red staining, sections were stained with hematoxylin (Weigert's) for 8 minutes, washed with running tap water for 10 minutes, followed by incubation with 0.1% (w/v) Sirius Red diluted in picric acid solution for 1 hour. The slides were then rinsed in two quick changes of 0.5% (v/v) acetic acid to remove unbound dye.

For Hematoxylin-Eosin (H&E) staining, sections were first incubated in Hematoxylin (Mayer's) for 15 mins, then rinsed in water followed by a rapid dunk into 1% (v/v) HCl diluted in ethanol and back into water again, the sections were subsequently incubated in Eosin for 1 min.

For immunostaining, sections were first incubated with 3% hydrogen peroxide to block endogenous peroxidase, then heated in sodium citrate buffer to retrieve antigen. Sections were then blocked in Dako Protein Block Serum-Free followed by incubation with specific primary and secondary antibodies

(Table 5). Sections were incubated with DAB reagent (Dako) to detect the targeted proteins.

After either one of the stainings, the slides were dehydrated gradually by a series of increasing concentrations of ethanol until completely dehydrated in absolute ethanol. Lastly, they are soaked in xylene before mounting and observed under a light microscope.

To quantify staining, 20 randomly taken images of 10X fields per section were evaluated by MetaMorph (Molecular Devices) software.

2.2.13 Statistical analysis

All data are presented as mean+SD. The results were analyzed by unpaired Student's *t*-test or ANOVA when appropriate. Statistical calculation was performed using GraphPad Prism software. The animal numbers used for each experiment are indicated in each of the figure legends. P-value less than 0.05 was considered to be statistically significant.

Chapter 3

Identification and characterization of c-JUN-regulated genes

3.1 Background

c-JUN mainly exists in two forms: N-terminal unphosphorylated form and N-terminal phosphorylated form. The N-terminal phosphorylated form of c-JUN generally accumulates in response to various stimuli and is thought to possess higher transcriptional activity (Shaulian *et al*., 2002). However, the transcriptional capability of the N-terminal unphosphorylated c-JUN that usually occurs at low level under unstimulated condition is unclear. Previous studies have revealed that genetic disruption of *c-Jun* leads to embryonic lethality (Hilberg *et al*., 1993, Johnson *et al*., 1993). The expression of the phosphoacceptor mutant c-JUN (*c-Jun^{AA/AA}*), where serines 63 and 73 are changed to alanines, disabling JNP and thus mimicking the N-terminal unphosphorylated form of c-JUN, is sufficient to rescue the embryonic lethal phenotype of the *c-Jun* null mice (Behrens *et al*., 1999). This data suggests that the expression of the genes that are essential for the survival of the embryo and the adult organism can be efficiently regulated even by the N-terminal unphosphorylated form of c-JUN. In other words, c-JUN does not require JNP for some of its functions. Of note, many studies have also demonstrated that under particular stressed conditions, JNP is indeed critical for proper c-JUN function in certain cell types (e.g. neurons) (Behrens *et al*., 1999, Behrens *et al*., 2001, Besirli *et al*., 2005). Collectively, these data suggest that c-JUN can function in a JNP-dependent and -independent manner.

3.2 Transcriptome profiling of $c\text{-}Jun^{+/+}$, $c\text{-}Jun^{-/-}$ and $c\text{-}Jun^{AA/AA}$ embryos

To gain insights into how c-JUN functions in a JNP-dependent and -independent manner, we identified genes that are differentially regulated by N-terminal phosphorylated and unphosphorylated c-JUN. To this end, we employed $c\text{-}Jun^{+/-}$ and $c\text{-}Jun^{AA/+}$ mice and bred them accordingly to obtain $c\text{-}Jun^{+/+}$, $c\text{-}Jun^{-/-}$ and $c\text{-}Jun^{AA/AA}$ mice (Table 9). These mice express wild type c-JUN (c-JUNWT), frameshift non-functional c-JUN and the N-terminal nonphosphorylatable mutant form of c-JUN (c-JUNAA) respectively.

Table 9. Intercross of $c\text{-}Jun^{+/-}$ and $c\text{-}Jun^{AA/+}$ mice illustrated by Punnett squares
$c\text{-}Jun^{+/-}$ mice were intercrossed to obtain $c\text{-}Jun^{+/+}$ and $c\text{-}Jun^{-/-}$ embryos. $c\text{-}Jun^{AA/+}$ mice were intercrossed to obtain $c\text{-}Jun^{+/+}$ and $c\text{-}Jun^{AA/AA}$ embryos.

$c\text{-}Jun^{+/-}$

$c\text{-}Jun^{+/-}$	$c\text{-}Jun^{+}$	$c\text{-}Jun^{-}$
$c\text{-}Jun^{+}$	$c\text{-}Jun^{+/+}$	$c\text{-}Jun^{+/-}$
$c\text{-}Jun^{-}$	$c\text{-}Jun^{+/-}$	$c\text{-}Jun^{-/-}$

$c\text{-}Jun^{AA/+}$

$c\text{-}Jun^{AA/+}$	$c\text{-}Jun^{+}$	$c\text{-}Jun^{AA}$
$c\text{-}Jun^{+}$	$c\text{-}Jun^{+/+}$	$c\text{-}Jun^{AA/+}$
$c\text{-}Jun^{AA}$	$c\text{-}Jun^{AA/+}$	$c\text{-}Jun^{AA/AA}$

We first sought for genes that are regulated differently by c-JUNWT and c-JUNAA proteins under normal physiological condition by using viable and healthy $c\text{-}Jun^{+/+}$, $c\text{-}Jun^{-/-}$ and $c\text{-}Jun^{AA/AA}$ embryos. Previous studies have reported that the morphological defects of the liver and heart arise in $c\text{-}Jun^{-/-}$ embryos at around embryonic day E12.5 (Eferl *et al.*, 1999). Thus we chose embryonic day E11.5 as the evaluation time point to avoid secondary effects (such as gradual loss of embryo viability) confounding the transcriptome profiles of the $c\text{-}Jun^{-/-}$ embryos. We randomly picked (1) 3 $c\text{-}Jun^{-/-}$ embryos with 2 $c\text{-}Jun^{+/+}$ littermate controls from the $c\text{-}Jun^{+/-}$ intercrossing; (2) 3 c-

$Jun^{AA/AA}$ embryos with 2 c-$Jun^{+/+}$ littermate controls from the c-$Jun^{AA/+}$ intercrossing; and generated their transcriptome profiles by performing whole genome expression arrays of each individual embryo. The whole experiment was then repeated with identical numbers and genotypes of embryos as mentioned above. The whole genome expression array used in this study is Affymetrix GeneChip® mouse genome 430 2.0 array. This array is a type of 3' *in vitro* transcription (IVT) expression array that contains 45000 probe sets which covers more than 39000 transcripts and variants from more than 34000 well-characterized mouse genes and UniGene clusters, and thus enables the analysis of gene expressions across the whole mouse genome.
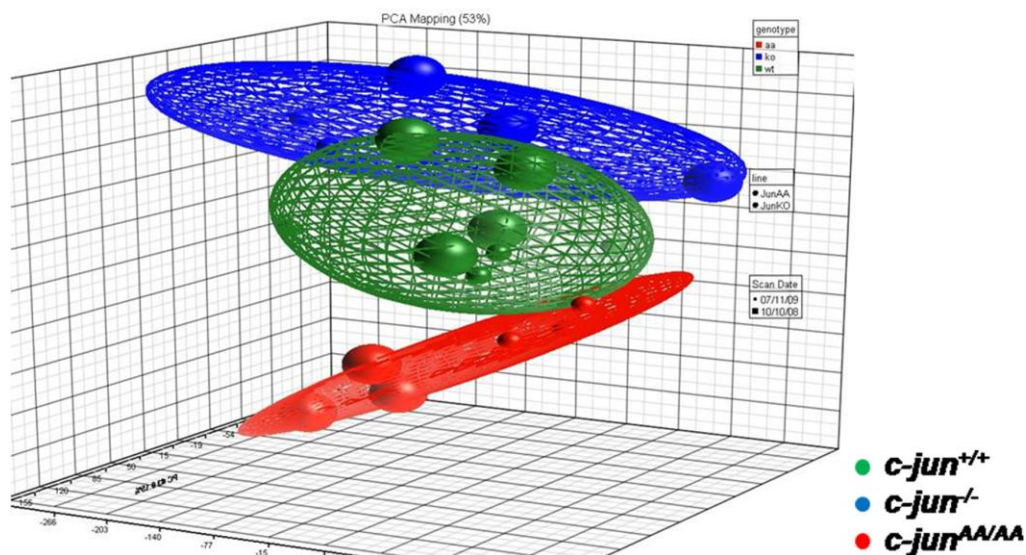
Figure 10. Transcriptome profiles of c-$Jun^{+/+}$, c-$Jun^{-/-}$ and c-$Jun^{AA/AA}$ embryos
Viable E11.5 embryos were used for whole genome expression arrays. Each circle represents one array in PCA mapped scatter plot generated by Partek Genomic Suite software. The embryos are colored by genotype: c-$Jun^{+/+}$ (green), n=8; c-$Jun^{-/-}$ (blue), n=4; c-$Jun^{AA/AA}$ (red), n=4. Circle size represents the experimental duplicates. Ellipsoids are drawn around embryos of the same genotype to illustrate the range of their gene expression profiles.

Principal component analysis (PCA) is a global analysis of the genome instead of any particular gene. It provides an overview of the major factors that influence the overall expression pattern of the experiment. Samples that are closer together denote that their expression patterns are more alike, whereas samples that are far apart imply that their expression profiles are less similar across the whole genome (Downey, 2006). PCA mapping of the transcriptome profiles of all the embryos (Figure 10) revealed that, albeit individual variance, embryos of the same genotype exhibited a rather similar global expression pattern thus could be clustered together whereas embryos of different genotypes displayed a rather dissimilar global expression pattern. These suggested that the major factor contributing to the global expression differences of the embryos was genotype.

To obtain the differential gene expressions between c-$Jun^{+/+}$, c-$Jun^{-/-}$ and c-$Jun^{AA/AA}$ embryos, we performed ANOVA analysis followed by contrasting the transcriptome profiles between (1) c-$Jun^{+/+}$ and c-$Jun^{-/-}$ samples (2) c-$Jun^{+/+}$ and c-$Jun^{AA/AA}$ samples with a statistical cutoff set at FDR <0.05 and FC >1.5. While the PCA plot implied global expression differences between different genotypes, to our surprise, we detected no statistically significant changes in gene expression profiles between c-$Jun^{+/+}$ and c-$Jun^{-/-}$ samples, as well as between c-$Jun^{+/+}$ and c-$Jun^{AA/AA}$ samples (data not shown).

Although the PCA plot indicated interesting differences between the different genotypes, we were unable to obtain statistically significant differentially expressed genes. The reasons behind that could be (1) sample size is not big enough; (2) the E11.5 day embryos is too early to exhibit the gene expression

differences although it is the most ideal time point as morphological defects start to appear at E12.5 day in the *c-Jun* null embryos; (3) organ-specific gene expression differences are nullified due to the dilution effect; (4) the gene expression differences are too subtle to be detected due to low expression level of c-JUN under normal physiological condition.

3.3 Transient and sustained c-JUN activation upon stresses

Although the endogenous levels of both N-terminal unphosphorylated and phosphorylated c-JUN are very low under normal physiological condition, they can be robustly induced by various stimuli (Vogt, 2001). Unfortunately, it is not possible to stimulate viable embryos to induce their endogenous c-JUN levels. We therefore sought to identify the gene expression differences in a more simple system by utilizing primary MEFs isolated from E11.5 *c-Jun*$^{+/+}$, *c-Jun*$^{-/-}$ and *c-Jun*$^{AA/AA}$ embryos, as it is a rather homogenous system and the c-JUN levels can be manipulated by applying stresses.

As c-JUN-deficient cells exhibit severe proliferation defects and undergo very early senescence in conventional cell culture condition (21% O_2) (Johnson *et al*., 1993, Schreiber *et al*., 1999), we couldn't acquire sufficient numbers of *c-Jun*$^{-/-}$ MEFs for further treatment. To overcome this problem, we cultured primary MEFs in low oxygen (3% O_2), which mimics the normal physiological condition as suggested by MacLaren *et al*. (MacLaren *et al*., 2004) and successfully expanded MEFs of all genotypes for several passages. Interestingly, analysis of the cellular proliferation rate by counting the cumulative number of cells over several days revealed that *c-Jun*$^{-/-}$ and *c-*

$Jun^{AA/AA}$ MEFs still showed slightly slower proliferation rates (albeit not significant) compared to c-$Jun^{+/+}$ MEFs in 3% O_2 condition (Figure 11).
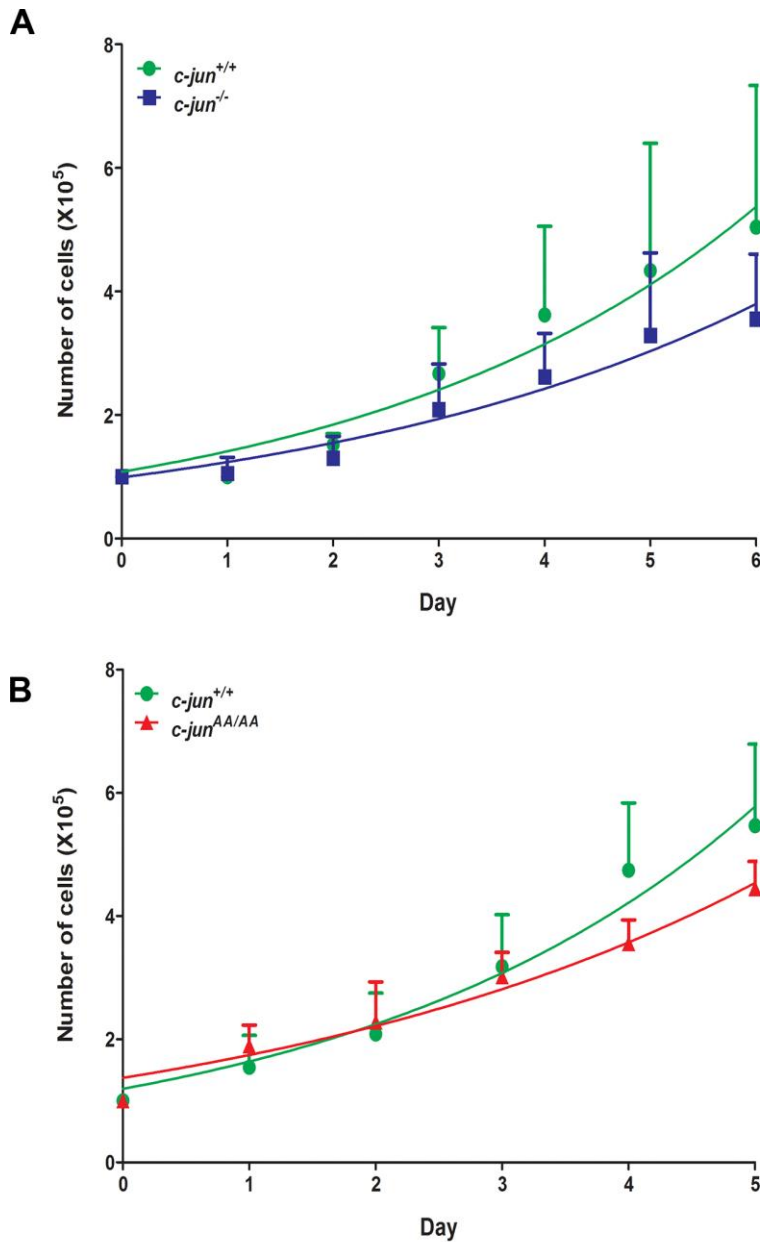
Figure 11. c-$Jun^{+/+}$, c-$Jun^{-/-}$ and c-$Jun^{AA/AA}$ MEFs show comparative proliferation rates in 3% O_2 condition
Cells were seeded at 1.0×10^5 in 6-well plates and cumulative cell numbers were counted daily. Experiments were done in duplicates, mean values of all clones of the same genotype are shown plotted against time, error bars indicate SD. (**A**) Sibling MEFs from the c-$Jun^{+/-}$ mice intercross were used to plot the growth curve: c-$Jun^{+/+}$ (green), n=5; c-$Jun^{-/-}$ (blue), n=5. (**B**) Sibling MEFs from the c-$Jun^{AA/+}$ mice intercross were used plot the growth curve: c-$Jun^{+/+}$ (green), n=5; c-$Jun^{AA/AA}$ (red), n=4.

We treated the early-passaged MEFs with either UV or CDDP to induce c-JUN as well as JNP because both stresses are known to activate c-JUN in a JNK-dependent manner (Kharbanda *et al.*, 1995, Zanke *et al.*, 1996). Next, we investigated the level of serines 63/73 phosphorylated c-JUN, total c-JUN, phosphorylated JNK and total JNK at different treatment time points respectively by immunoblots. As shown in Figure 12A and B, c-JUN expression was very low under unstimulated condition. UV irradiation (Figure 12A) induced an immediate activation of JNK, seen by the rapid increase of the phosphorylated JNK level by 1 hour following UV treatment. However this induction was not sustained overtime. The phosphorylated JNK level decreased back to its original state 4 hours after UV treatment. The total JNK level remained constant all the time. Like its upstream kinase JNK, phosphorylated c-JUN induction was also rapid and transient following UV irradiation, whereas the total c-JUN accumulation occurred in a more sustained manner. In contrast to UV, treatment with CDDP (Figure 12B) did not cause a rapid induction of both c-JUN and JNK. In fact, the phosphorylated forms of c-JUN and JNK were only prominent 4 hours after CDDP treatment. Nevertheless the activation of both c-JUN and JNK was much more prolonged as compared to UV treatment. Congruently, both *c-Jun*$^{+/+}$ and *c-Jun*$^{AA/AA}$ MEFs exhibited similar kinetics of c-JUN and JNK activation. Thus, to ensure the abundance of both total and N-terminal phosphorylated c-JUN in MEFs, we chose 1 and 4 hour for UV treatment, 4 and 7 hour for CDDP treatment for future experiments.
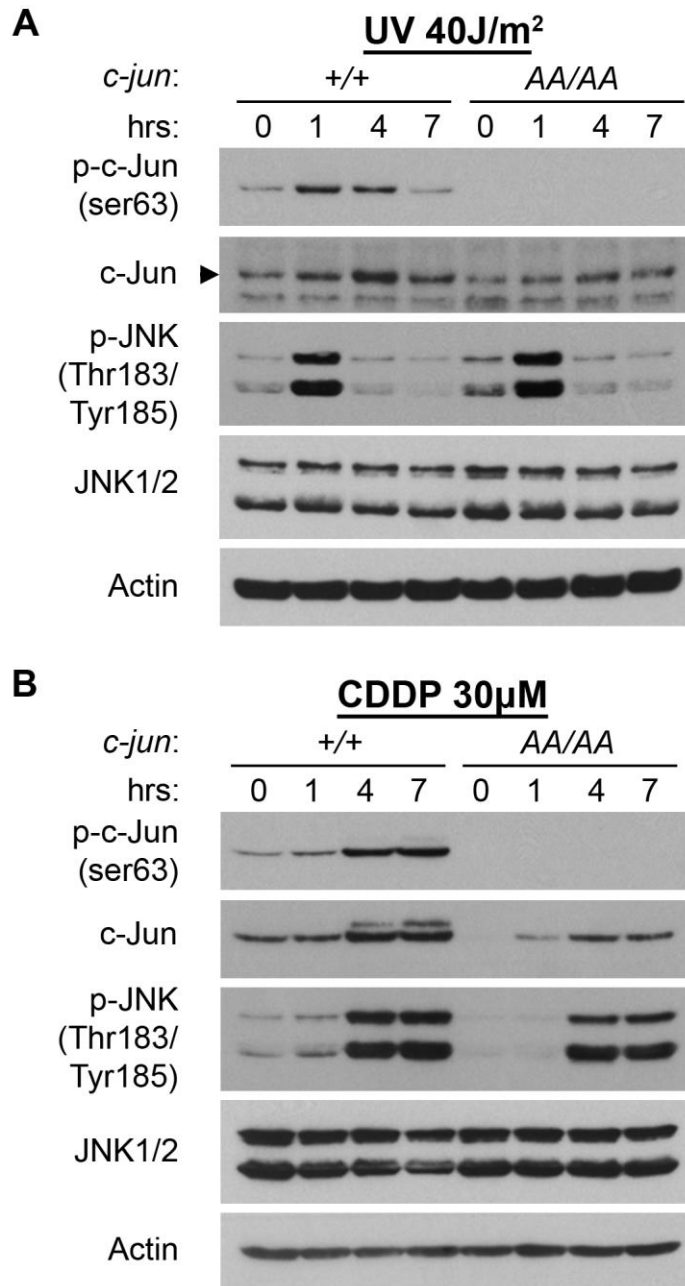
Figure 12. UV and CDDP are transient and sustained c-JUN activating signals
MEFs of the indicated genotypes were isolated from E11.5 day embryos. MEFs were treated with 40 J/m^2 of UV radiation (**A**) or 30 µM of CDDP (**B**) and harvested at the indicated time points. Total cell extracts were prepared and subjected to immunoblot analysis with the indicated antibodies. Actual c-JUN band is indicated by the arrowhead.

3.4 Transcriptome profiling of c-$Jun^{+/+}$, c-$Jun^{-/-}$ and c-$Jun^{AA/AA}$ MEFs

Having determined the appropriate treatments and time points to elevate the endogenous c-JUN and JNP levels, we prepared primary MEFs from littermate E11.5 c-$Jun^{+/+}$ and c-$Jun^{-/-}$ embryos, as well as from littermate E11.5 c-$Jun^{+/+}$ and c-$Jun^{AA/AA}$ embryos and treated them as specified earlier. Four individual MEF clones of each specific c-Jun genotype were used in this experiment. Transcriptome profiles of untreated as well as UV or CDDP-treated MEFs of various c-Jun genotypes were then generated.

PCA mapping of all the samples is shown in Figure 13A. Ellipsoids were drawn according to the specific treatment and time point to facilitate visualization. Interestingly, samples from the same treatment and time point were close enough to be grouped together albeit they bear different genotypes. Moreover, the ranges of individual groups hardly overlapped one another. This data indicated that alterations of stress type and duration resulted in a shift in global gene expression.

Further PCA mapping of untreated and UV-treated samples (Figure 13B, left panel) with ellipsoids drawn around each genotype revealed that c-$Jun^{-/-}$ samples (blue) formed a distinctly separate group with completely no overlap to either c-$Jun^{+/+}$ (green) or c-$Jun^{AA/AA}$ (red) samples, whereas the groups formed by c-$Jun^{+/+}$ and c-$Jun^{AA/AA}$ samples exhibited high degree of overlapping. Likewise, PCA mapping of untreated and CDDP-treated samples (Figure 13B, right panel) also arranged the c-$Jun^{-/-}$ samples (blue) into a completely separate group, far apart from the c-$Jun^{+/+}$ (green) and c-$Jun^{AA/AA}$ (red) samples; while less overlapping was observed in CDDP-treated c-$Jun^{+/+}$
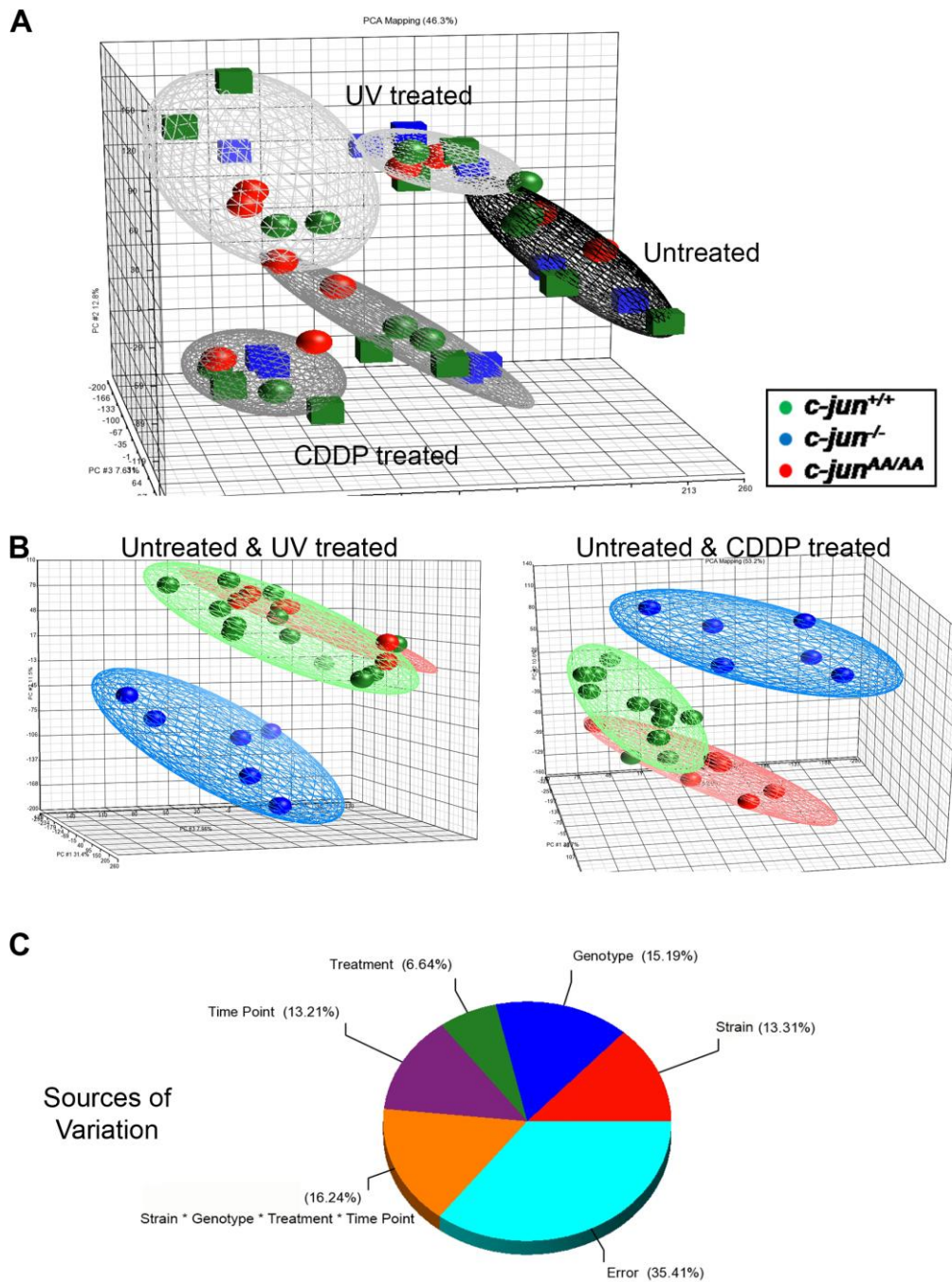
Figure 13. Transcriptome profiles of *c-Jun^{+/+}*, *c-Jun^{-/-}* and *c-Jun^{AA/AA}* MEFs
Untreated and UV/CDDP treated MEFs were used for whole genome expression arrays. PCA mapping of (**A**) all the untreated and treated samples; (**B**) untreated and UV-treated samples (left); untreated and CDDP-treated samples (right). Each circle represents one array. The samples are colored by genotype and ellipsoids are drawn to group samples: untreated (black); UV-treated (light grey); CDDP-treated (dark grey); *c-Jun^{+/+}* (green); *c-Jun^{-/-}* (blue); *c-Jun^{AA/AA}* (red). (**C**) Source of variation indicates the impact of each factor in contributing to the overall gene expression change.

and $c\text{-}Jun^{AA/AA}$ samples as compared to UV-treated samples. These results suggested a profound global gene expression differences between $c\text{-}Jun^{+/+}$ and $c\text{-}Jun^{-/-}$ samples. Strikingly, while $c\text{-}Jun^{+/+}$ and $c\text{-}Jun^{AA/AA}$ samples also exhibited difference in their global gene expression profiles, this difference appeared less profound.

We also performed source of variation analysis to measure the impact of all the known variation factors in affecting the global expression values in this experiment. The known variation factors include mouse strain, genotype, treatment, time point and their interactive effect. The respective contributing percentage of each factor is shown in Figure 13C: mouse strain 13.31%, genotype 15.19%, treatment 6.64%, time point 13.21% and interactive effect 16.24%. While the interactive effect from all the factors contributed the most in global gene expression changes, 'genotype' appeared as the single most influencing factor that caused the global expression alterations, highlighting the significance of c-JUN and JNP in affecting the global gene expression.

Taken together, these data suggested that deletion of c-JUN affects the global transcriptome profiles more dramatically, whereas inactivation of JNP does not affect gene expression as much as absence of c-JUN.

3.5 Identification of c-JUN and JNP-dependent genes

To avoid complications arising from different genetic background, we did not contrast the transcriptome profiles between $c\text{-}Jun^{-/-}$ and $c\text{-}Jun^{AA/AA}$ samples as they were derived from different mouse strains. Instead, we contrasted the transcriptome profiles between littermate $c\text{-}Jun^{+/+}$ and $c\text{-}Jun^{-/-}$ samples and the

transcriptome profiles between littermate $c\text{-}Jun^{+/+}$ and $c\text{-}Jun^{AA/AA}$ samples to obtain genes expressed differently among the $c\text{-}Jun^{+/+}$, $c\text{-}Jun^{-/-}$ and $c\text{-}Jun^{AA/AA}$ samples. Hence, genes expressed differently between $c\text{-}Jun^{+/+}$ and $c\text{-}Jun^{-/-}$ samples were considered as c-JUN-dependent genes, while genes expressed differently between $c\text{-}Jun^{+/+}$ and $c\text{-}Jun^{AA/AA}$ samples were considered to be JNP-dependent genes. As indicated in Table 10, a large number of genes were found to express differentially between $c\text{-}Jun^{+/+}$ and $c\text{-}Jun^{-/-}$ samples. On the contrary, very few genes exhibit differential expression between $c\text{-}Jun^{+/+}$ and $c\text{-}Jun^{AA/AA}$ samples. These results are consistent with our previous findings that absence of JNP does not affect gene expression as much as absence of c-JUN. The complete gene lists are submitted as a soft copy.

Table 10. Number of c-JUN-dependent genes and JNP-dependent genes

Contrast			P-value (FDR)	FC	Number of genes
c-JUN dependent genes	$c\text{-}Jun^{+/+}$ vs. $c\text{-}Jun^{-/-}$	Untreated	<0.05	>2 OR <-2	264
		UV			546
		CDDP			490
JNP dependent genes	$c\text{-}Jun^{+/+}$ vs. $c\text{-}Jun^{AA/AA}$	Untreated	<0.05	>2 OR <-2	14
		UV			7
		CDDP			69

To verify the whole genome expression array data, we selected many c-JUN-dependent genes and JNP-dependent genes and performed qRT-PCR assays by using the same RNA samples used for the whole genome expression

arrays. The quantified gene expression values were normalized to the expression of the housekeeping gene *Gapdh*. To determine whether the expression of these genes were altered by c-JUN or JNP, the relative expression difference (FC) of each individual gene was calculated as follows: (1) littermate $c\text{-}Jun^{+/+}$ versus $c\text{-}Jun^{-/-}$ samples; (2) littermate $c\text{-}Jun^{+/+}$ versus $c\text{-}Jun^{AA/AA}$ samples. The complete qRT-PCR validation results are shown in Table 11 with indications of significance calculated by student t-test.

Table 11. qRT-PCR validation of c-JUN-dependent and JNP-dependent genes

Untreated

Gene Symbol	qRT-PCR			
	$c\text{-}Jun^{+/+}$ vs. $c\text{-}Jun^{-/-}$		$c\text{-}Jun^{+/+}$ vs. $c\text{-}Jun^{AA/AA}$	
	FC	p-value	FC	p-value
9830001H06RIK	-1.006	0.9763 ns	-1.336	0.026 *
Agtr1b	-10.623	0.2346 ns	-2.050	0.1799 ns
Ambra1	-1.507	0.3913 ns	1.231	0.1873 ns
Angptl2	2.147	0.0355 *	1.428	0.0053 **
Arl13b	-1.106	0.6008 ns	-1.088	0.6909 ns
C1qa	15.572	0.0041 **	1.644	0.0354 *
C1qb	27.585	0.0010 **	1.433	0.0151 *
C1qc	22.056	0.0031 **	1.627	0.0148 *
C3ar1	3.290	0.0040 **	1.212	0.6681 ns
Cd14	1.866	0.1601 ns	1.022	0.9702 ns
Cp	-1.166	0.8675 ns	-1.985	0.4496 ns

Dcn	-6.236	0.0287 *	1.095	0.788 ns
Dock11	-1.113	0.5677 ns	2.048	0.0026 **
Dyrk1a	-1.042	0.8176 ns	-1.036	0.7097 ns
Elk3	-1.551	0.1295 ns	1.016	0.927 ns
Emilin2	4.710	0.0017 **	1.095	0.1627 ns
Eml4	-1.248	0.4646 ns	-1.095	0.7071 ns
Erc2	2.667	0.0017 **	1.837	0.0020 **
Fam174b	-3.581	0.0449 *	1.073	0.7963 ns
Fermt3	2.208	0.0226 *	1.035	0.9476 ns
Fgf1	-2.319	0.4214 ns	-1.582	0.3493 ns
Flt4	9.045	0.0376 *	1.883	0.0708 ns
Glt25d1	-1.272	0.0964 ns	1.465	0.0498 *
Gpr1	-1.107	0.7425 ns	1.265	0.1381 ns
Gtf3c1	1.002	0.9917 ns	-1.191	0.2473 ns
Hipk2	-1.766	0.0231 *	1.103	0.1341 ns
Hjurp	-1.086	0.7501 ns	3.100	0.013 *
Il1rl1	8.994	0.0426 *	1.503	0.0526 ns
Il4ra	1.654	0.0548 ns	1.305	0.1432 ns
Kif13b	-1.366	0.4519 ns	-1.141	0.5983 ns
Laptm5	9.841	0.0088 **	1.213	0.3062 ns
Nfia	-2.245	0.2165 ns	1.286	0.4732 ns
Nppb	3.968	0.0403 *	2.182	0.0058 **
Pdgfra	-5.234	0.1584 ns	-1.335	0.6613 ns
Pik3r1	-3.326	0.0394 *	-1.253	0.5262 ns
Sh3rf1	-1.309	0.3562 ns	2.294	0.0014 **
Slc7a2	-1.988	0.2822 ns	-1.273	0.5739 ns

Gene Symbol	FC	p-value	FC	p-value
Sparcl1	-5.293	0.0455 *	1.833	0.1426 ns
Tacc3	1.138	0.5707 ns	-1.207	0.9285 ns
Tbl1xr1	-3.354	0.0658 ns	1.708	0.0662 ns

UV treatment

Gene Symbol	qRT-PCR			
	$c\text{-}Jun^{+/+}$ vs. $c\text{-}Jun^{-/-}$		$c\text{-}Jun^{+/+}$ vs. $c\text{-}Jun^{AA/AA}$	
	FC	p-value	FC	p-value
1500004F05Rik	1.665	0.0751 ns	1.540	0.0367 *
Ablim1	-1.667	0.0881 ns	-1.674	0.0553 ns
Angptl2	2.229	0.0005 ***	1.448	< 0.0001 ***
Arid5b	-1.569	0.2743 ns	1.070	0.8703 ns
BC023969	-1.382	0.1186 ns	2.008	0.1455 ns
Dcn	-5.996	0.0157 *	1.006	0.9760 ns
Glt25d1	-1.124	0.3836 ns	1.303	0.0317 *
Hjurp	-1.174	0.6125 ns	1.426	0.1812 ns
Ica1	2.346	0.0178 *	1.173	0.4785 ns
Nppb	4.026	0.0040 **	1.973	0.0025 **
Plscr2	-2.412	0.0483 *	-1.273	0.2182 ns
Prnd	3.269	0.0250 *	1.146	0.2712 ns
Sparcl1	-2.567	0.0472 *	1.535	0.0534 ns

CDDP treatment

Gene Symbol	qRT-PCR			
	c-Jun$^{+/+}$ vs. *c-Jun*$^{-/-}$		*c-Jun*$^{+/+}$ vs. *c-Jun*$^{AA/AA}$	
	FC	p-value	FC	p-value
2610528A11Rik	1.326	0.3133 ns	1.439	0.3675 ns
Ablim1	-3.379	0.0148 *	-1.283	0.1782 ns
Ampd1	1.398	0.1945 ns	1.377	0.1027 ns
Angptl2	2.621	< 0.0001 ***	1.310	0.0406 *
Arhgap5	-1.616	0.0258 *	-1.062	0.6703 ns
Chd7	1.612	0.2205 ns	1.129	0.4755 ns
Cpeb4	-1.209	0.2999 ns	-1.117	0.3801 ns
Ctrl	1.030	0.8752 ns	1.291	0.0401 *
Cyp1b1	-2.008	0.0677 ns	-2.042	0.1305 ns
Dcn	-6.070	0.0062 **	1.166	0.4826 ns
Depdc1a	-1.345	0.3227 ns	-1.460	0.3314 ns
E030042N06Rik	-1.728	0.0052 **	1.120	0.3958 ns
Elavl1	-1.038	0.7848 ns	1.104	0.2777 ns
Enpp1	-1.211	0.2782 ns	1.141	0.4088 ns
Erc2	1.454	0.1999 ns	1.402	0.0849 ns
Erlin1	-1.003	0.9900 ns	-1.082	0.5917 ns
Gabpb2	-1.310	0.1855 ns	1.095	0.3628 ns
Gdf9	1.191	0.4455 ns	1.751	0.0161 *
Gm5544	1.480	0.0747 ns	1.476	0.0616 ns
Gsto2	1.284	0.4445 ns	2.169	0.0062 **
Glt25d1	-1.380	0.0269 *	1.324	0.0148 *
Hjurp	-1.463	0.1535 ns	1.230	0.4996 ns

Hoxa5	-1.870	0.0957 ns	-1.607	0.0792 ns
Igf2	-1.734	0.3200 ns	2.025	0.0267 *
Itsn1	-1.798	0.0460 *	-1.084	0.6979 ns
Mapk8	-1.958	0.0327 *	-1.476	0.1833 ns
Nasp	-1.014	0.9491 ns	-1.091	0.6368 ns
Nefl	8.173	0.0190 *	1.435	0.1620 ns
Nppb	4.850	0.0193 *	2.645	0.0016 **
Ola1	1.100	0.5384 ns	-1.159	0.1594 ns
Pcmtd2	-1.856	0.0924 ns	-1.472	0.1601 ns
Plscr2	-2.666	0.0422 *	-1.207	0.3485 ns
Pogk	-1.616	0.1489 ns	-1.330	0.2762 ns
Prrc1	-1.613	0.0211 *	1.027	0.8394 ns
Ptger1	-2.566	0.1034 ns	-1.187	0.0879 ns
Pus3	-1.494	0.0551 ns	-1.055	0.7192 ns
Rad21	-1.197	0.4875 ns	-1.657	0.1178 ns
Rcan1	1.477	0.2603 ns	1.452	0.0129 *
Scd2	-1.335	0.3541 ns	-1.409	0.1399 ns
Sdcbp	-1.298	0.0953 ns	-1.063	0.5187 ns
Sema7a	-1.041	0.8923 ns	-1.019	0.9543 ns
Shd	-1.269	0.2309 ns	1.384	0.0413 *
Tigd3	1.266	0.6996 ns	-2.017	0.2143 ns
Tm9sf2	-1.319	0.1988 ns	-1.667	0.0234 *
Tnfrsf11b	-2.531	0.0399 *	-1.227	0.0852 ns
Vwce	1.019	0.8924 ns	1.147	0.4060 ns
Wrn	-1.600	0.2287 ns	-1.544	0.2792 ns
Ywhaz	1.021	0.9215 ns	-1.022	0.8590 ns

Representative genes whose expressions were significantly altered by c-JUN and/or JNP are shown in Figure 14A. Gene *Laptm5* is regulated by c-JUN but not JNP (littermate *c-Jun*$^{+/+}$ versus *c-Jun*$^{-/-}$: FC=9.841 [p=0.0088**]; littermate *c-Jun*$^{+/+}$ versus *c-Jun*$^{AA/AA}$: FC=1.1213 [p=0.3062]). Gene *Hjurp* is regulated by JNP but not c-JUN (littermate *c-Jun*$^{+/+}$ versus *c-Jun*$^{-/-}$: FC=-1.086 [p=0.7501]; littermate *c-Jun*$^{+/+}$ versus *c-Jun*$^{AA/AA}$: FC=3.100 [p=0.013*]). Gene *Erc2* is regulated by both c-JUN and JNP (littermate *c-Jun*$^{+/+}$ versus *c-Jun*$^{-/-}$: FC=2.667 [p=0017**]; littermate *c-Jun*$^{+/+}$ versus *c-Jun*$^{AA/AA}$: FC=1.837 [p=0.0020**]).

We have thus grouped the validated genes with significant FC into three categories based on their expression regulation by c-JUN and/or JNP and is illustrated in Figure 14B. (1) genes such as *Laptm5*, *Flt4*, *Sparcl1* and *Dcn*, come under the category of genes whose transcription was mediated by N-terminal unphosphorylated c-JUN, whereas JNP did not further enhance/suppress their transcription. (2) genes like *Hjurp*, *Sh3rf1*, *Dock11* and *Glt25d1* belong to the category of genes whose transcription was only modulated by N-terminal phosphorylated c-JUN. (3) genes like *C1qa*, *C1qb*, *C1qc*, *Nppb*, *Erc2* and *Angptl2* were classified under the category of genes whose transcription was regulated by both N-terminal unphosphorylated and phosphorylated c-JUN. These data demonstrated that the N-terminal unphosphorylated c-JUN is sufficient to regulate gene transcription.

Intriguingly, while the expression of the second group of genes (e.g. *Hjurp*, *Sh3rf1*, *Dock11*) could be modulated by N-terminal phosphorylated c-JUN, their expression was not affected by absence of c-JUN. One possibility is that

these genes may not be direct targets of c-JUN, but targets of other transcription factors that can only cooperate with N-terminal phosphorylated c-JUN but not N-terminal unphosphorylated c-JUN.

In general, the number of JNP-dependent genes are much lesser than the number of the c-JUN-dependent genes. This suggests that JNP is not critical for c-JUN function in gene transcription in MEFs under both basal and genotoxic stressed conditions. Furthermore, detailed gene descriptions, functions and related diseases of all validated JNP-dependent genes are summarized and shown in Table 12.

The chromatin binding sites of c-JUN have been mapped previously in K562, a human myelogenous leukemia cell line, by using chromatin immunoprecipitation-sequencing technique. Several gene regulatory regions that were bound by c-JUN have thus been identified in normal unstimulated K562 cells (Raha *et al*., 2010). Therefore, we converged the gene lists encompassing c-JUN-dependent genes from our MEFs expression array data with genes whose regulatory regions were found to be bound by c-JUN in the study mentioned above (GSM487425). We discovered many genes that are both bound and regulated by c-JUN and these genes are considered as direct c-JUN targets. The complete list of these genes and their expression differences between $c\text{-}Jun^{+/+}$ and $c\text{-}Jun^{-/-}$ cells are shown in Table 13. However, it is worth mentioning that different cell types exhibit distinct gene expression profiles, hence certain genes that were found to be bound by c-JUN in the K562 genome may not be verified by the MEFs expression array data and vice versa.
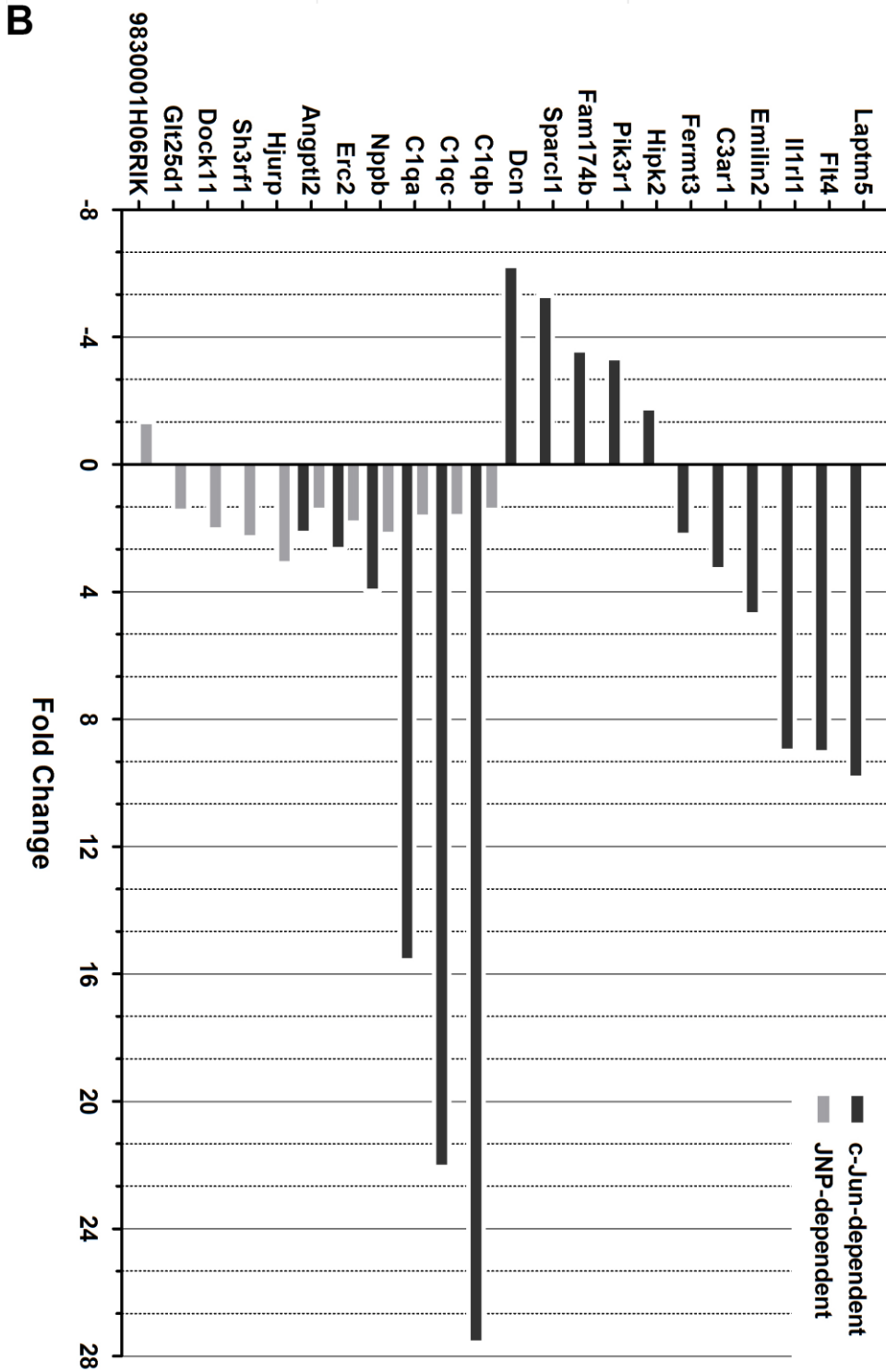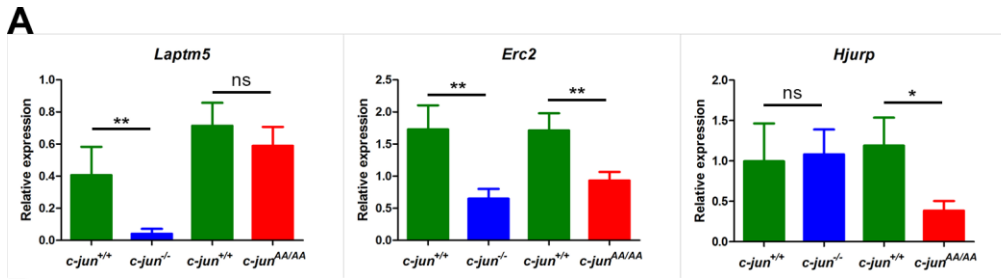
Figure 14. qRT-PCR verification of subset of c-JUN and JNP-dependent genes
$c\text{-}Jun^{+/+}$, $c\text{-}Jun^{-/-}$ and $c\text{-}Jun^{AA/AA}$ MEFs (n=4 for each genotype) used for the whole genome expression arrays were also used for qRT-PCR validation. (**A**) Relative expression of the representative genes. $c\text{-}Jun^{+/+}$ (green); $c\text{-}Jun^{-/-}$ (blue); $c\text{-}Jun^{AA/AA}$ (red). (**B**) FC values of the c-JUN-dependent genes (black) and JNP-dependent genes (grey). FC was calculated by littermate $\frac{c-jun\ +/+}{c-jun\ -/-}$ or littermate $\frac{c-jun\ +/+}{c-junAA\ /AA}$. Positive FC value represents upregulation in $c\text{-}Jun^{+/+}$ samples, negative FC value represents downregulation in $c\text{-}Jun^{+/+}$ samples. All the c-JUN-dependent and/or JNP-dependent genes shown here are statistically significant differentially expressed genes by qRT-PCR verification.

Table 12. Summaries of validated JNP-dependent genes.
Information compiled from NCBI (www.ncbi.nlm.nih.gov) and Genecards (www.genecards.org).

Gene Symbol	Description	Biological functions and processes	Location	Disease associated
Angptl2	Member of the vascular endothelial growth factor family	Participate in the formation of blood vessels Chemotaxis Transformation	Extracellular space Vesicles	Various skin cancer Colorectal cancer
C1qa C1qb C1qc	Subcomponent C1q	Participate in complement system Aging Brain development	Extracellular space Plasma Vesicles	Autoimmune disease Epileptic seizure Hepatic insulin resistance
Ctrl	Serine-type peptidase	Digestion Proteolysis	Extracellular space	Severe acute respiratory syndrome Lymphoblastic lymphoma
Dock11	Rho guanyl-nucleotide exchange factor	Blood coagulation Positive regulation of Rho GTPase	Cytoplasm	Astrocytoma Epithelial cancer
Erc2	PDZ domain binding	Regulates neurotransmitter	Cytoplasm	Melanoma

		Synapse assembly and organization	Axon terminals Synapse	Astrocytoma Epithelial cancer
Gdf9	Member of the TGF-β superfamily	Cytokine and growth factor activity Female gamete generation Oocyte growth	Cytoplasm Extracellular space	Melanoma Ovarian cancer Polycystic ovary syndrome Cachexia
Glt25d1 (Colgalt1)	Procollagen galactosyltransferase	Transferring glycosyl groups ECM organization LPS biosynthesis	Cellular membrane Cytoplasm Endoplasmic reticulum	--
Gsto2	Omega class glutathione S-transferase	Involved in metabolism of xenobiotics and carcinogens	Cytoplasm Vesicles	Barrett's adenocarcinoma Parkinson's disease
Hjurp	Holliday junction recognition protein	Cell cycle DNA binding, histone binding Nucleosome assembly	Cytoplasm Nucleus Centromere	Lung cancer

		Chromosome segregation	Kinetochore	
Igf2	Member of the insulin family of polypeptide growth factors	Involved in development and growth Various metabolic process Cell proliferation Wound healing	Extracellular space Cytoplasm Plasma membrane Vesicles	Metabolic disorder Various types of cancer
Nppb	Cardiac hormone Member of the natriuretic peptide family	Negative regulation of angiogenesis Regulation of blood pressure, blood vessel size, vascular permeability, renal sodium excretion, urine volume	Extracellular space Plasma	Various cardio and renal disorders
Rcan1	Interacts with calcineurin A	Calcium-mediated signaling Central nervous system development Involved in locomotory behaviour Skeletal muscle fiber development	Cytoplasm Nucleus Secretory granules	Hypertrophy Down's syndrome Huntington's disease Alzheimer's disease
Sh3rf1	Contains RING and SH3	Scaffold for JNK signaling pathway	Cytoplasm	Benign paroxysmal

	domains	Protein ubiquitination	Nucleus	positional nystagmus
		Apoptosis	Golgi apparatus	
			Neurites	
Shd	Contains SH2 domain	Protein binding	Cytoplasm	Melanoma; Epithelial cancer
Tm9sf2	Member of the transmembrane 9 superfamily	Transport Ion channel	Nucleus Membrane rafts Vesicles	Cancer Infection by HIV-1

Table 13. List of genes that are both bound and regulated by c-JUN

Gene Symbol	Whole genome expression array ($c\text{-}Jun^{-/-}$ vs. $c\text{-}Jun^{+/+}$)					
	Untreated		UV treated		CDDP treated	
	p-value	FC	p-value	FC	p-value	FC
ABCC1	0.001008	-1.74962	0.000332	-1.58455	0.003726	-1.38341
ACOT7	1.47E-05	-2.19684	3.23E-07	-2.33372	4.62E-07	-2.26038
AMBRA1	0.002423	1.65968	0.948374	-1.00593	0.732739	1.03176
BCAT1	0.009371	-2.19913	0.000345	-2.51374	0.000888	-2.24869
BCL2L1	0.008315	-1.77567	0.223386	-1.17442	0.272625	1.15464
BTG2	0.005207	1.85695	0.774629	-1.03686	0.049749	-1.31589
CAPG	0.001097	-3.40731	0.000188	-3.00195	3.73E-05	-3.81884
CARHSP1	0.004504	-1.51857	3.41E-05	-1.77386	2.57E-05	-1.8087
CAST	0.004526	-1.55207	0.000402	-1.55862	8.40E-05	-1.71887
CDC45	0.002471	-1.73149	0.003679	-1.4398	0.000281	-1.69443
CLASP1	0.001598	1.93861	0.783174	-1.03136	0.291819	1.12925
CPEB3	1.22E-05	2.0981	0.284147	1.07726	0.089902	1.1314
CTPS	0.000968	-1.57903	0.000536	-1.41986	0.065949	-1.15566
CTSB	0.002153	-1.83612	0.00074	-1.65162	0.000333	-1.74887
CUBN	0.004273	-1.64409	0.172043	-1.15105	0.700961	-1.03852
CUX1	0.005759	1.51789	0.012569	1.29193	0.004153	1.36575
DTX4	0.005212	-1.57813	0.814746	-1.02206	0.055231	-1.21748
E2F7	0.006155	-1.97809	0.00076	-1.94489	0.203165	-1.20926
EIF2B3	0.000241	-1.63166	3.87E-06	-1.75848	0.000259	-1.40903
EIF5	0.003027	-1.57006	0.021349	-1.25072	0.07483	-1.17727
EIF6	0.002243	-1.60679	0.000258	-1.57426	0.000546	-1.50812
ELOVL5	0.001959	1.54372	0.000228	1.51222	5.19E-05	1.64349

EPT1	0.00275	-1.72266	0.001016	-1.56218	0.280629	-1.11759
ERC2	0.001084	-2.25708	0.001009	-1.78882	0.111714	-1.24786
FAM115A	0.000379	1.94754	0.161112	1.14584	0.841664	-1.01861
FAM174B	0.001622	3.02345	7.69E-05	3.23388	4.16E-05	3.53927
FGF1	2.32E-06	3.28253	2.49E-07	2.91174	0.593551	1.04947
FILIP1L	0.002346	-2.02685	0.000517	-1.86073	0.012674	-1.45399
FOSL1	0.006757	-4.48834	0.221279	-1.50262	0.249408	-1.46482
FYCO1	0.004602	1.64758	0.346581	1.10079	0.650923	1.04639
GARS	0.000406	-1.55752	4.62E-05	-1.50914	0.000136	-1.43421
GNA12	0.004302	-1.73934	0.004558	-1.47355	0.00644	-1.44135
GNAL	0.00695	-1.61943	0.017318	-1.33218	0.00018	-1.78789
GSN	0.008333	-1.78287	0.000541	-1.86498	0.001553	-1.71075
HCFC1R1	0.000958	1.53624	9.77E-05	1.50646	2.86E-05	1.60802
HIPK2	0.008904	2.03966	0.000541	2.17627	0.000478	2.20486
HN1	7.43E-05	-1.50251	4.79E-06	-1.48548	2.23E-06	-1.53844
HSPA9	9.58E-05	-1.51679	9.18E-06	-1.4744	4.32E-05	-1.38315
IGF1	0.009105	2.7119	0.026656	1.76478	0.008923	2.03003
IL1RL1	0.007225	-20.672	0.000347	-29.3137	0.001005	-18.5516
ITPR3	5.86E-05	-3.53237	1.54E-06	-3.85998	3.73E-05	-2.56457
JAZF1	0.008435	1.80651	0.000503	1.90646	0.001299	1.75948
KIF1B	0.006716	-1.66472	0.001768	-1.56332	0.407314	1.09588
KLK8	0.000455	-7.43455	1.01E-05	-9.55872	1.22E-05	-9.11724
LAPTM5	0.004183	-36.8369	0.000262	-44.8133	0.000283	-43.0941
LASS4	0.004162	1.57242	0.000478	1.55328	0.006363	1.34707
LRRC59	7.28E-05	-1.8398	2.60E-06	-1.88225	4.41E-05	-1.58084
LRRFIP1	0.003256	-2.15935	0.000426	-2.07683	0.187324	-1.22208

LTBP1	0.00153	-2.04244	0.002096	-1.61888	0.261317	-1.14959
MAP3K5	0.00372	2.83462	0.032557	1.62553	0.484692	1.15277
MAPK13	0.000484	-4.23554	5.43E-06	-5.79521	8.57E-06	-5.30763
MASP1	0.001798	-1.55322	0.00019	-1.52788	0.000973	-1.40563
MASTL	0.002686	-2.07678	0.002781	-1.67188	0.045874	-1.34631
MSI2	0.000111	2.27338	0.700273	1.03824	0.755364	-1.0308
MTHFD1L	0.001517	-1.89239	0.000204	-1.80976	0.000456	-1.70551
MYO1D	0.008121	1.75645	0.00321	1.59337	0.000218	1.97642
NADK	0.009931	-1.68656	0.004266	-1.53461	0.001552	-1.65084
NEK2	0.003642	-1.87635	0.002261	-1.61548	0.003436	-1.56704
NFIA	0.001437	3.39338	4.18E-05	3.93483	0.000166	3.18132
NFIC	0.002328	1.50717	0.007213	1.27239	0.837434	1.0152
NOC4L	0.008439	-1.87212	0.025812	-1.42571	0.034732	-1.39262
NR4A1	0.003415	3.6907	0.522112	1.17428	0.70568	1.0987
NR6A1	0.000615	1.62847	0.812334	1.01727	0.547037	1.04475
NUBP1	0.005098	-1.57193	0.000738	-1.53553	0.001285	-1.48646
PANX1	0.009318	-1.93251	0.002935	-1.76232	0.037991	-1.41437
PCOLCE2	0.000597	-8.81131	1.61E-05	-11.1309	0.000171	-6.13249
PHF21A	3.51E-05	1.59752	0.40407	1.04179	0.977752	-1.00134
PIP4K2A	1.76E-08	1.70099	0.924625	-1.00227	0.926157	-1.00222
PLTP	0.007659	1.94857	0.001217	1.88197	0.001633	1.83247
PLXNA2	0.000532	1.97609	0.017219	1.31553	0.423027	1.08367
PPP1R10	0.004679	2.02676	0.825574	-1.0317	0.226489	-1.19456
PRC1	0.000219	-1.57466	0.000641	-1.32113	5.51E-05	-1.46381
PTRH1	2.87E-05	-1.73057	2.38E-06	-1.6725	5.60E-05	-1.43079
RAB30	0.001924	1.51593	0.001093	1.3767	0.073493	1.15154

RAD18	0.000135	-1.70572	0.010687	-1.21847	0.8791	-1.0099
RAI14	0.002116	2.35066	0.89931	1.01928	0.345944	1.15662
RANGAP1	0.008153	-1.57067	0.011204	-1.35132	0.001607	-1.51519
RAPGEF4	0.002865	1.7691	0.015162	1.3512	0.504954	1.07375
RCC1	0.008506	-1.72402	5.03E-05	-2.21794	0.541167	-1.07749
RGS20	0.0032	-4.82135	0.000445	-4.39695	0.003766	-2.95529
RIN1	0.001641	-2.02857	0.002974	-1.57878	0.936046	-1.00969
RORA	0.000603	2.74021	0.003035	1.75522	0.006634	1.6391
RRAS2	5.72E-05	-2.32442	1.43E-06	-2.47795	0.005241	-1.37538
RRM2	0.005652	-1.98131	0.002729	-1.72368	0.031185	-1.41234
SCMH1	7.46E-07	1.70164	0.751197	-1.01135	0.985895	1.00063
SERPINE1	0.009515	-2.43829	0.00435	-2.05904	0.22691	-1.28878
SGK1	0.002582	-4.17961	0.022921	-1.97651	0.152734	-1.48117
SGMS1	0.005583	-1.65222	0.086507	-1.21166	0.409372	1.09087
SLC1A5	0.004537	-2.30127	0.000319	-2.38188	0.001344	-2.03751
SLC20A1	0.007599	-2.13115	0.007638	-1.70669	0.118773	-1.31525
SLC25A13	0.007261	-1.94282	0.036876	-1.40013	0.164709	-1.23323
SMARCAL1	0.00246	1.51216	2.36E-05	1.71209	0.044358	1.18226
SNHG3	0.00098	-2.45641	6.80E-05	-2.45818	4.23E-06	-3.45666
SOX5	0.002125	2.72246	0.243795	1.23818	0.776291	1.05165
SPAG9	0.000244	1.61393	0.831805	-1.01339	0.977326	-1.00178
STIM1	0.003622	1.627	0.006817	1.36272	0.082383	1.19234
STIP1	0.000323	-1.51424	0.000236	-1.35739	0.000407	-1.32918
STK39	0.008745	-1.57682	0.000231	-1.74024	0.001325	-1.54759
STXBP4	0.009539	1.67728	0.836234	1.02457	0.995386	-1.00068
SUSD4	0.000248	2.30549	4.88E-06	2.56619	0.000623	1.6863

TACC1	0.004137	1.86312	0.003657	1.56662	0.021833	1.38121
TAGLN2	0.000244	-2.16119	2.29E-05	-2.06975	7.57E-05	-1.87948
TBX15	0.000193	-3.38674	3.40E-05	-2.90692	0.10777	-1.30532
TIMP1	0.006923	-2.1708	0.001326	-2.03968	0.006492	-1.74069
TMEM151A	0.004204	-2.4674	0.591743	-1.10075	0.448317	-1.14652
TNK2	0.000426	-2.41461	0.00012	-2.08248	0.060092	-1.29185
TOP1	0.005781	1.91729	0.484021	1.10046	0.765547	1.04119
TSPAN18	6.39E-05	-2.60472	0.000627	-1.65728	0.00032	-1.73824
UCK2	0.000347	-1.53989	0.084826	-1.11645	0.303237	-1.0645
USP24	0.000406	-2.14232	0.00021	-1.79903	0.031117	-1.29697
VAT1	0.009979	-1.62168	0.01592	-1.36663	0.109658	-1.20842
VRK2	0.002518	-1.60763	0.001685	-1.42879	0.07409	-1.18219
WHSC1L1	0.006263	1.58344	0.886824	-1.01386	0.517417	1.06532
WNT5B	0.003831	-1.58016	0.002752	-1.4064	0.096571	-1.17178
YDJC	0.009553	-2.04785	0.000127	-2.6014	0.045681	-1.43587
ZCCHC11	0.004173	1.96732	0.86859	-1.02225	0.358543	1.13289

3.6 JNP has subtle effect on genotoxic stress-induced apoptosis

JNP has been established to be essential for c-JUN function in neurons in response to excitotoxic stimuli (Behrens *et al*., 1999). Nevertheless, our data so far suggested that JNP has only minor effect on c-JUN function in MEFs both under basal and genotoxic stressed conditions. To further confirm these results, we treated the *c-Jun*$^{+/+}$ and *c-Jun*$^{AA/AA}$ MEFs with two different doses of UV or CDDP for 24 hours to induce cell death and determined the extent of cellular survival based on annexin V and PI staining.
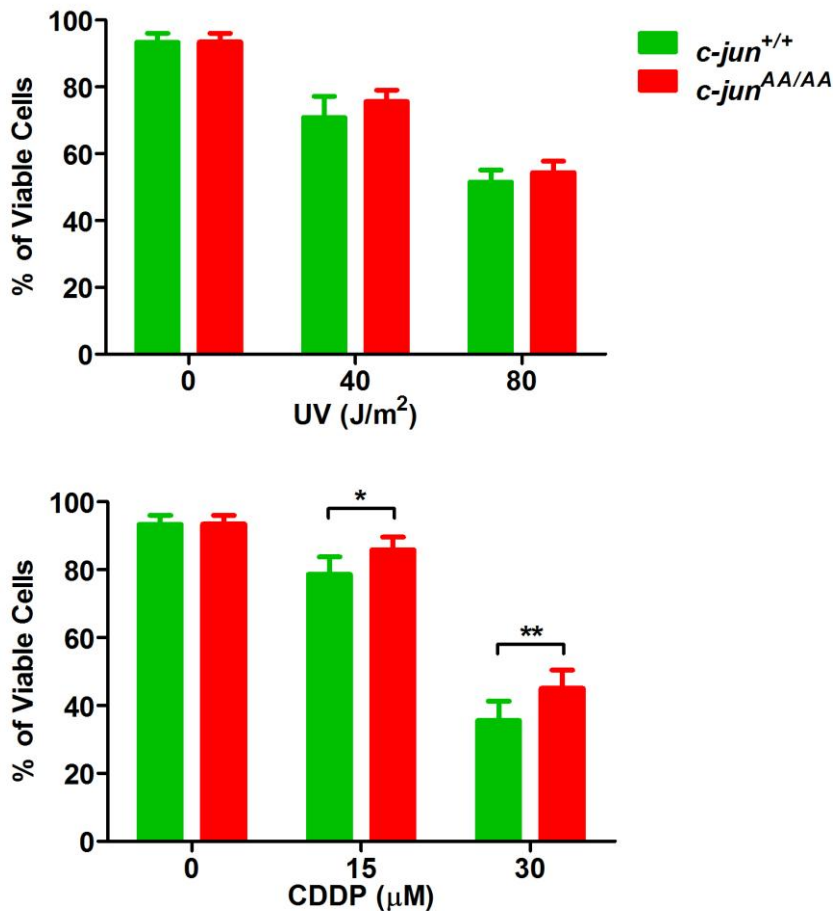
Figure 15. JNP has subtle effect on genotoxic stress-induced apoptosis
MEFs were exposed to 40 J/m^2 and 80 J/m^2 of UV (top) or 15 μM and 30 μM of CDDP (bottom). The percentage of viable cells were determined by Annexin V and PI staining 24 hours post treatment. Sibling MEFs from the *c-Jun*$^{AA/+}$ mice intercross were used: *c-Jun*$^{+/+}$ (green), n=6; *c-Jun*$^{AA/AA}$ (red), n=7. Experiments were done in duplicates, data represents mean+SD. Statistics done by 2-way ANOVA, *P<0.05, **P<0.01.

Treatment with either genotoxic stress led to a decrease in the number of viable cells in both *c-Jun*$^{+/+}$ and *c-Jun*$^{AA/AA}$ MEFs (Figure 15). We observed a small but statistically significant difference in cellular survival between the *c-Jun*$^{+/+}$ and *c-Jun*$^{AA/AA}$ cells in response to CDDP treatment (percentage of viable *c-Jun*$^{+/+}$ versus *c-Jun*$^{AA/AA}$ cells at 15 μM CDDP: 78.6 versus 85.8 [p<0.05]; percentage of viable cells at 30 μM CDDP: 35.5 versus 45.0

[p<0.01]). However, cellular survival between UV-treated c-$Jun^{+/+}$ and c-$Jun^{AA/AA}$ MEFs was similar with no significance difference (percentage of viable c-$Jun^{+/+}$ versus c-$Jun^{AA/AA}$ cells at 40 J/m^2 of UV: 70.9 versus 75.6 [p>0.05]; percentage of viable cells at 80 J/m^2 of UV: 51.6 versus 54.4 [p>0.05]). These data indicated that JNP has subtle effect on c-JUN function in regulating genotoxic stress-induced apoptosis in MEFs.

Thus, consistent with our previous findings that JNP is required only for a small subset of c-JUN target genes transcription, these results pieced together supported that JNP has limited effect in c-JUN function in MEFs even during exposure to genotoxic stresses.

3.7 Stress-regulated c-JUN target genes

Having identified genome-wide c-JUN-dependent genes at basal as well as under stressed conditions, we were interested in dividing and characterizing these genes into different groups based on their expression changes in response to stresses. As c-JUN is one of the immediate early responding proteins to a plethora of stresses (Mechta-Grigoriou *et al*., 2001, Vogt, 2001), this analysis could be an initial step to provide clues in how c-JUN behaves in response to different stresses.

We converged the gene lists encompassing c-JUN-dependent genes under untreated (basal) or UV/CDDP treated (stressed) conditions respectively and identified genes that were common or unique among specific conditions. As illustrated in Figure 16A, many genes were initially expressed differently between c-$Jun^{+/+}$ and c-$Jun^{-/-}$ MEFs at basal level, however their expression

differences were lost/compensated after stress (Group 1). In addition, a large number of genes were regulated by c-JUN at both basal and stressed conditions; they are thus constitutive c-JUN targets regardless of the stress status (Group 2). Moreover, a substantial number of genes did not exhibit expression differences between $c\text{-}Jun^{+/+}$ and $c\text{-}Jun^{-/-}$ MEFs at basal level and began to show expression differences upon stress; therefore these genes are the stress-induced c-JUN-dependent genes (Group 3). The numbers of genes in each individual groups regulated by UV or CDDP respectively are indicated in Figure 16B.
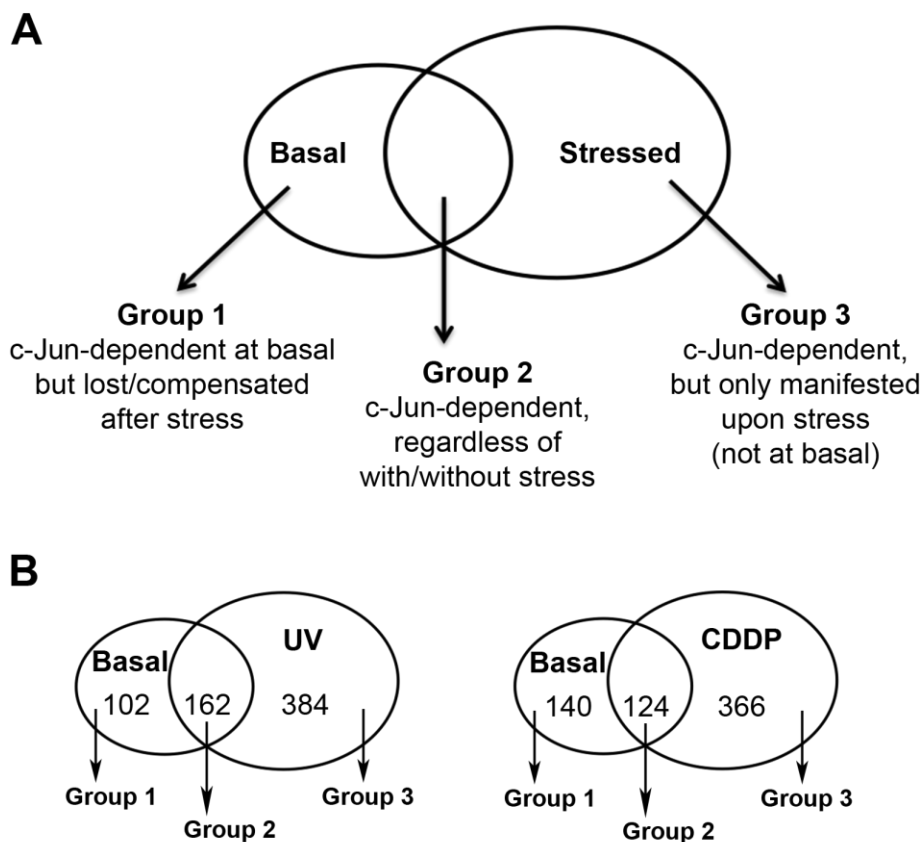

Figure 16. Stress-regulated c-JUN-dependent genes
(**A**) Venn Diagram illustrating the different grouping of c-JUN-dependent genes in response to either with stress or without stress or both. (**B**) Number of genes in each group at basal level and at stressed level with UV or CDDP respectively.

Many c-JUN target genes and their physiological roles have been reported by other groups before. These genes include *Tcf4* (*Tcf7l2*), *Cd44* and *Lgr5*, which have been shown to participate in the intestinal homeostasis and tumorigenesis (Nateri *et al.*, 2005, Sancho *et al.*, 2009, Aguilera *et al.*, 2011). We have also identified these three genes as c-JUN-dependent genes but not JNP-dependent genes. Our results indicate that *Lgr5* is a constitutive c-JUN dependent gene, while *Cd44* and *Tcf4* are stress-induced c-JUN dependent genes. *Cd44* was induced by both UV and CDDP whereas *Tcf4* was only induced by CDDP but no UV (Table 14).

Table 14. Expression of representative known c-JUN target genes

Gene Symbol	Whole genome expression array (c-$Jun^{-/-}$ vs. c-$Jun^{+/+}$)					
	Untreated		UV treated		CDDP treated	
	p-value	FC	p-value	FC	p-value	FC
Lgr5	1.60E-12	23.2618	6.05E-14	14.1647	9.08E-14	13.3876
CD44	0.000375	-1.95634	1.50E-08	-2.75097	5.55E-08	-2.54092
Tcf4	0.049251	1.54561	0.016555	1.46915	4.22E-05	2.15271

To gain further insights into the cellular and molecular functions of the genes in each individual group, we performed gene ontology analysis by IPA software. IPA categorizes gene functions according to scientific publications and can rank the cellular and molecular functions based on the number of genes enriched in each function and their relative expression values. The top enriched cellular and molecular functions of UV and CDDP-regulated genes are shown in Figure 17.
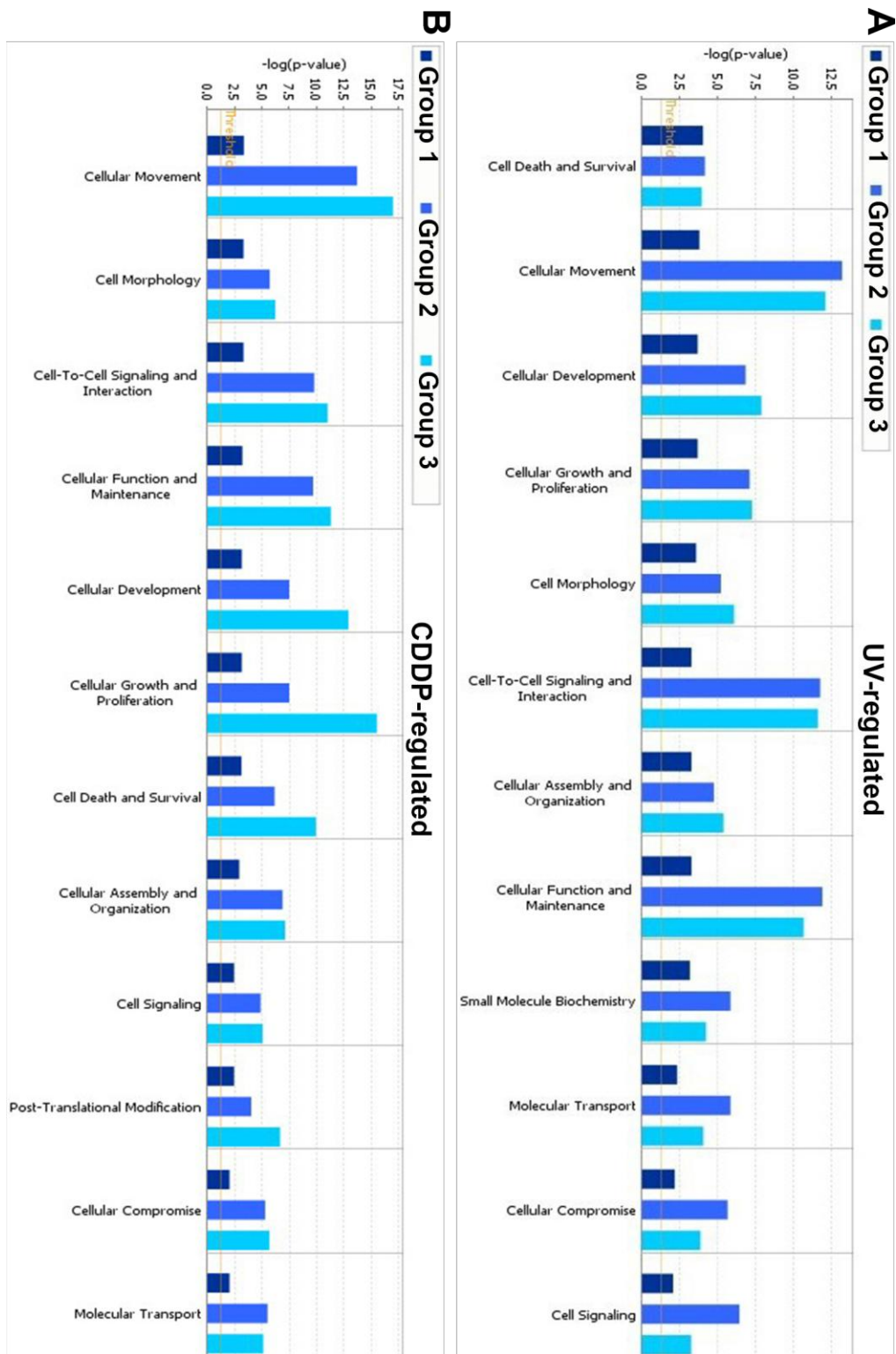
Figure 17. Top c-JUN-regulated molecular and cellular functions suggested by IPA

Different groups of UV-regulated (**A**) and CDDP-regulated (**B**) c-JUN-dependent genes were imported to IPA software for gene ontology analysis. Top molecular and cellular functions calculated by IPA are indicated. X axis represents the -log(p-value), hence the longer the bar, the smaller the p-value (more significant).

Interestingly, the group 1 genes which were only differentially expressed at basal level did not show prominent enrichment in any particular functions; whereas group 2 and 3 genes which were differentially expressed at stressed conditions exhibited obvious functional enrichment. Apparently, the top five cellular and molecular functions in both UV and CDDP-regulated genes are 'Cellular Movement', 'Cell-To-Cell Signaling and Interaction', 'Cellular Function and Maintenance', 'Cellular Development' and 'Cellular Growth and Proliferation'. These data suggest that cells respond similarly to both genotoxic stresses and implicated c-JUN's role in cellular interaction, migration, general maintenance and development.

3.8 Potential biological pathways regulated by c-JUN

We also grossly analyzed the differentially expressed genes between $c\text{-}Jun^{-/-}$ and $c\text{-}Jun^{+/+}$ MEFs at basal, UV and CDDP-treated conditions individually to explore for potential biological processes/pathways that are most deregulated in the absence of c-JUN. Analysis by IPA uncovered many affected canonical pathways and the top five canonical pathways with most significant changes in gene expressions are shown in Figure 18. Among them, IL-10 signaling, complement system and hepatic fibrosis/HSC activation pathways have been consistently found to be affected in untreated as well as in UV/CDDP-treated conditions.

IL-10 is an anti-inflammatory cytokine that functions at different stages of immune response in order to limit the exaggerated or excessive response to protect the host (Saraiva *et al*., 2010). Moreover, measurement of the serum cytokine levels in between the healthy and NAFLD patients has revealed a

characteristic significant increase of TNF-α along with decreasing of IL-10 in accordance with the severity of NAFLD (Zahran *et al.*, 2013, Paredes-Turrubiarte *et al.*, 2015). Previous studies have proposed a role for c-JUN in regulating IL-10 expression in certain immune cell types (Jones *et al.*, 2005, Wang *et al.*, 2005), suggesting that c-JUN may be able to modulate the IL-10 levels in NAFLD patients.
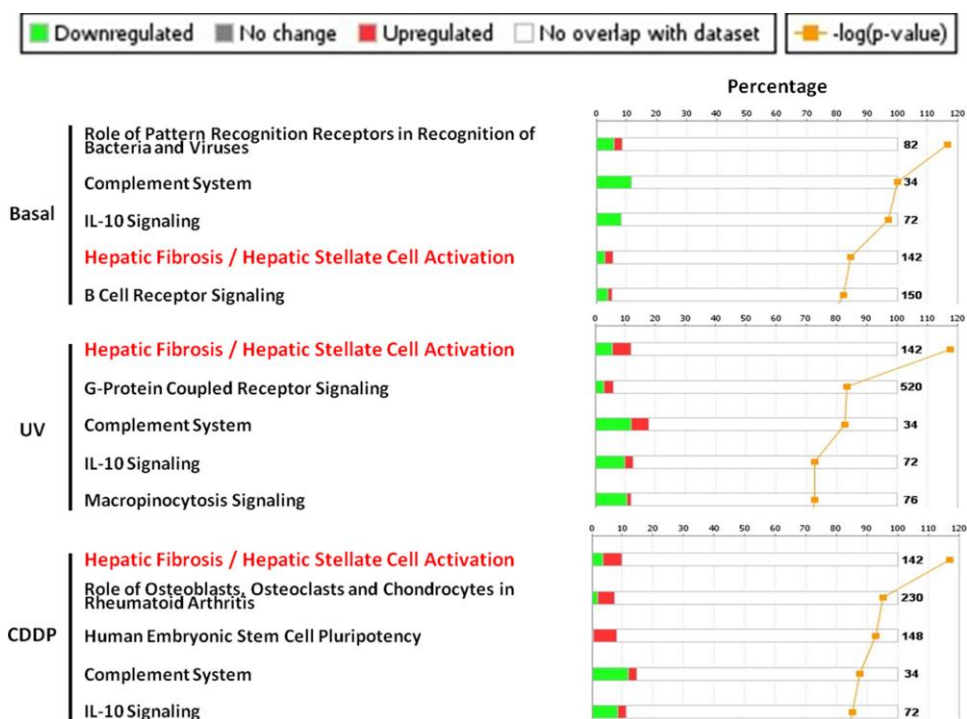

Figure 18. Top c-JUN-regulated canonical pathways suggested by IPA
Basal and UV/CDDP regulated c-JUN-dependent genes were uploaded to IPA for canonical pathway analysis. X axis shows the percentage of the molecules affected in the indicated pathway: the open bar indicates the total number of molecules in the indicated pathway, while the colored bar indicates the affected molecules (red, upregulated in c-$Jun^{-/-}$ cells; green, downregulatd in c-$Jun^{-/-}$ cells). Significance is shown by -log(p-value) in orange dots, i.e. higher -log(p-value) indicates more significance.

While the association between c-JUN and IL-10 signaling is known, two pathways with possible novel association with c-JUN have been uncovered - the complement system and hepatic fibrosis/HSC activation pathway.

The complement system is part of the immune system consisting of numerous serum proteins as well as many soluble or membrane-bound receptors. It functions in recognizing an array of molecules such as pathogens to initiate inflammatory responses for host defense (Markiewski *et al.*, 2007). The C1q complex is the first component of the classical complement pathway and is composed of 18 polypeptide chains of three subunits (6 C1qa, 6 C1qb and 6 C1qc) (Nayak *et al.*, 2012). C1q has been found to play an important role in the clearance of apoptotic cells in the situation of overwhelming apoptosis or impaired phagocytosis (Trouw *et al.*, 2008). Interestingly, we found that expressions of all the three subunits were strongly reduced in *c-Jun*^{-/-} MEFs (Table 11), suggesting that loss of c-JUN may affect the clearance of apoptotic cells during acute or chronic tissue damage.

Hepatic fibrosis usually results from chronic liver diseases with an inflammatory microenvironment while NASH is one of its main risk factor (Bataller *et al.*, 2005). HSC, as the most fibrogenic cell type, can be potently activated by signals (e.g. ROS and pro-inflammatory cytokines) emitted from dying/apoptotic hepatocytes and various type of activated immune cells (Friedman, 2008a). c-JUN has been found to promote hepatocyte and hematopoietic cell survival in various liver pathological conditions (Eferl *et al.*, 1999, Hasselblatt *et al.*, 2007, Fuest *et al.*, 2012), suggesting that c-JUN may be involved in HSC activation and hepatic fibrosis development.

Taken together, these potential c-JUN-regulated biological processes/pathways suggest some potential functions of c-JUN in regulating tissue inflammation and homeostasis especially in the liver.

Chapter 4

Role of c-JUN in hepatic fibrosis

4.1 Background

c-JUN is widely expressed in a variety of tissues and it plays a pivotal role in liver physiology, especially in embryonic liver development, adult liver regeneration and tumorigenesis. However its role in liver fibrosis has not been defined as yet (Jochum *et al*., 2001, Eferl *et al*., 2003b). Our results from the canonical pathway analysis on genome-wide c-JUN-dependent genes suggest that c-JUN is involved in HSC activation and hepatic fibrosis pathway under normal physiological status. Interestingly, this pathway appeared as the top most affected pathway during stressed conditions, highlighting the association of c-JUN with HSC activation and hepatic fibrosis. It is therefore conceivable that c-JUN has a potential role in liver fibrosis development. Furthermore, JNK/c-JUN signaling has been implicated in the progression of NASH, a high risk factor associated with liver fibrosis (Seki *et al*., 2012). JNK signaling has also been demonstrated to modulate HSC activation and liver fibrogenesis, while both total c-JUN and N-terminal phosphorylated c-JUN have been found to be strongly augmented during hepatic fibrogenesis (Kluwe *et al*., 2010, Zhao *et al*., 2014). A recent transcriptome-wide gene expression analysis on NASH mice induced by a high fat and cholesterol diet further proposed that c-JUN is the central protein connecting many other deregulated proteins to facilitate the development of NASH (Dorn *et al*., 2014).

4.2 Increased baseline HSC activation in *c-Jun*$^{-/-}$ embryos

Since HSC is the major fibrogenic cell type and its activation and transdifferentiation into myofibroblast-like cell is the key step in hepatic fibrogenesis, we first examined whether systemic *c-Jun* deletion, which
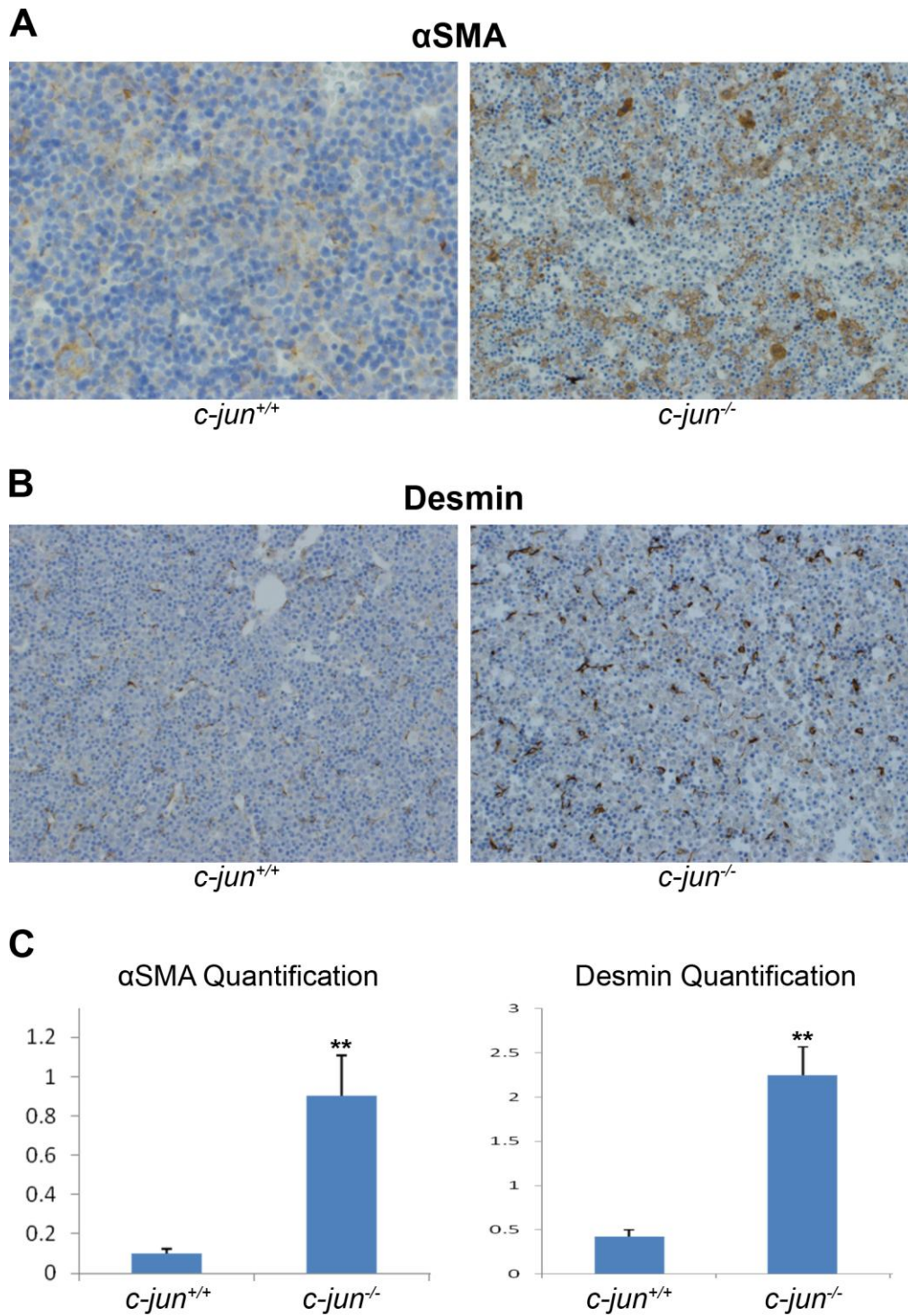
Figure 19. Increased baseline HSC activation in *c-Jun*^{-/-} embryos
(**A, B**) IHC staining for αSMA (**A**) and Desmin (**B**) in representative E13.5 *c-Jun*^{+/+}
(left) and *c-Jun*^{-/-} (right) embryos. (**C**) Quantitative αSMA (left) and Desmin (right)
IHC data from all embryos (n≥4 per genotype). Data represents mean+SD, **P<0.01.
Data in collaboration with Dr Anna Mae Diehl from Duke University.

caused extensive fetal liver apoptosis, would activate the HSCs in embryos. It has been reported that $c\text{-}Jun^{-/-}$ fetuses began to show liver morphological abnormalities at E13.0 and the very low fetal liver c-JUN expression also increased about three-fold at E13.5; suggesting that c-JUN gains significance in the liver around E13.5 (Eferl *et al.*, 1999). We therefore chose E13.5 $c\text{-}Jun^{+/+}$ and $c\text{-}Jun^{-/-}$ embryos to investigate their baseline HSC status.

Two classical HSC markers, αSMA and desmin, were assessed by immunohistochemistry (IHC). As expected, the proportion of αSMA-positive and desmin-positive cells, representing activated HSCs, increased dramatically in $c\text{-}Jun^{-/-}$ embryos in comparison to $c\text{-}Jun^{+/+}$ embryos (Figure 19). These data strongly indicate that loss of c-JUN resulted in HSC activation and accumulation; impling that $c\text{-}Jun^{-/-}$ mice may exhibit spontaneous congenital fibrosis. Thereby, we hypothesized that c-JUN is involved in hepatic fibrosis development.

4.3 Inactivation of c-JUN in HSCs

To investigate the role of c-JUN in adult liver fibrosis, we first conditionally deleted c-JUN in adult murine HSCs. Kinoshita *et al.* have demonstrated that the *Col1a2* promoter is an effective and specific promoter to drive the *Cre* recombinase expression in activated HSCs (Kinoshita *et al.*, 2007). We therefore employed Col-CreER ($Col\text{-}CreER^{tg}$) transgenic mice, in which the Cre recombinase is fused to a modified estrogen receptor (ER) ligand binding domain and the resulting CreER fusion protein is controlled by the *Col1a2* promoter (Zheng *et al.*, 2002). The $Col\text{-}CreER^{tg}$ transgenic mice were then sequentially crossed with $c\text{-}Jun^{f/f}$ mice to obtain $c\text{-}Jun^{f/f};Col\text{-}CreER^{tg}$ and $c\text{-}$

$Jun^{f/f}$;Col-$CreER^{ntg}$ (equivalent to and here on designated as c-$Jun^{f/f}$) mice (Table 15). As 4-hydroxytamoxifen, a metabolite of the tamoxifen, is required to activate the CreER fusion protein, both c-$Jun^{f/f}$;Col-$CreER^{tg}$ and c-$Jun^{f/f}$ mice were administrated with equal doses of tamoxifen to avoid confounding phenotypes.

Table 15. Sequential crossing of *Col-CreER^{tg}* transgenic mice with *c-Jun^{f/f}* mice illustrated by Punnett squares

Col-CreER^{tg}

		c-Jun^+;Col-$CreER^{tg}$	c-Jun^+;Col-$CreER^{ntg}$
c-$Jun^{f/f}$	c-Jun^f	c-$Jun^{f/+}$;Col-$CreER^{tg}$	c-$Jun^{f/+}$;Col-$CreER^{ntg}$
	c-Jun^f	c-$Jun^{f/+}$;Col-$CreER^{tg}$	c-$Jun^{f/+}$;Col-$CreER^{ntg}$

c-Jun^{f/+};*Col-Cre^{tg}*

		c-Jun^f; Col-$CreER^{tg}$	c-Jun^f; Col-$CreER^{ntg}$	c-Jun^+; Col-$CreER^{tg}$	c-Jun^+; Col-$CreER^{ntg}$
c-$Jun^{f/f}$	c-Jun^f	c-$Jun^{f/f}$; Col-$CreER^{tg}$	c-$Jun^{f/f}$; Col-$CreER^{ntg}$	c-$Jun^{f/+}$; Col-$CreER^{tg}$	c-$Jun^{f/+}$; Col-$CreER^{ntg}$
	c-Jun^f	c-$Jun^{f/f}$; Col-$CreER^{tg}$	c-$Jun^{f/f}$; Col-$CreER^{ntg}$	c-$Jun^{f/+}$; Col-$CreER^{tg}$	c-$Jun^{f/+}$; Col-$CreER^{ntg}$

c-Jun^{f/f};*Col-CreER^{tg}*

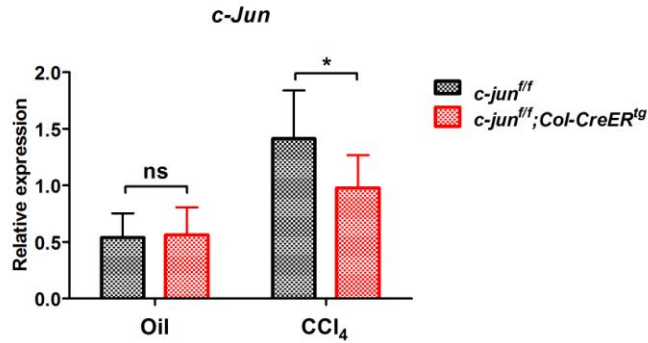|		c-Jun^f;Col-$CreER^{tg}$	c-Jun^f;Col-$CreER^{ntg}$
c-$Jun^{f/f}$	c-Jun^f	c-$Jun^{f/f}$;Col-$CreER^{tg}$	c-$Jun^{f/f}$;Col-$CreER^{ntg}$
	c-Jun^f	c-$Jun^{f/f}$;Col-$CreER^{tg}$	c-$Jun^{f/f}$;Col-$CreER^{ntg}$

Figure 20. c-JUN inactivation in HSCs
Both *c-Jun^{f/f}* and *c-Jun^{f/f};Col-CreER^{tg}* mice were administrated with tamoxifen. In addition, mice were treated with CCl_4 (n=8 for each genotype) to induce c-JUN expression; or with oil (n=5 for each genotypes) as vehicle control. Whole liver fractions were used to examine c-JUN expression by qRT-PCR. Experiments were done in duplicates, data represents mean+SD. Statistics done by t-test, *P<0.05.

c-JUN inactivation was assessed by whole liver qRT-PCR (Figure 20). Interestingly, c-JUN level was markedly augmented in both *c-Jun^{f/f}* and *c-Jun^{f/f};Col-CreER^{tg}* mice following CCl_4 treatment as compared to oil treatment, indicating that hepatic c-JUN expression can be induced in response to liver damage. However, oil-treated *c-Jun^{f/f}* and *c-Jun^{f/f};Col-CreER^{tg}* mice exhibited almost equivalent levels of c-JUN expression, suggesting inadequate c-JUN inactivation in oil-treated mice probably due to the *Col1a2* promoter which could only modestly drive Cre expression in quiescent HSCs (Kinoshita *et al.*, 2007). Nevertheless, liver damage can activate HSC (Bataller *et al.*, 2005) and the *Col1a2* promoter can then competently drive Cre expression in activated HSCs (Kinoshita *et al.*, 2007). Hence, we observed significantly less c-JUN induction in *c-Jun^{f/f};Col-CreER^{tg}* mice than in *c-Jun^{f/f}* mice by CCl_4. This indicates a successful c-JUN inactivation in activated HSCs. Notably, HSCs only comprise approximately 10% of the total liver resident cells (Geerts, 2001). The efficient induction of

111

c-JUN expression by CCl$_4$ in *c-Jun$^{f/f}$;Col-CreER^{tg}* mice can therefore be attributed to other liver cell types which harbor the intact *c-Jun* gene.

4.4 Loss of c-JUN in HSCs aggravates fibrosis

We next investigated the consequences of c-JUN inactivation in HSCs on fibrosis progression in a CCl$_4$ intoxication model. CCl$_4$ is a classical hepatotoxicant that causes pericentral injury. Its metabolism by hepatocyte cytochrome P450 2E1 generates highly reactive free radical metabolites which results in lipid peroxidation and hepatocellular membrane disruption (Manibusan *et al*., 2007). Therefore, it has been widely used experimentally to induce hepatic fibrosis (Iredale, 2007).
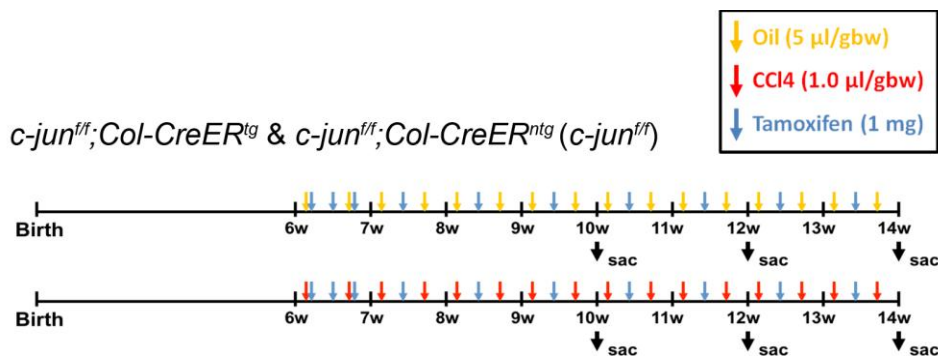

Figure 21. Detailed injection and harvesting scheme for *c-Jun$^{f/f}$;Col-CreER^{tg}* and *c-Jun$^{f/f}$* mice
c-Jun$^{f/f}$;Col-CreER^{tg} and *c-Jun$^{f/f}$;Col-CreER^{ntg}* (*c-Jun$^{f/f}$*) mice were injected twice per week with the indicated dosage of oil (yellow) or CCl$_4$ (red) for 4 weeks, 6 weeks or 8 weeks respectively. In addition, tamoxifen (blue) was also fed to all the experimental mice along with the oil or CCl$_4$ treatment. All mice were harvested 48-72 hour after the last injection.

We subjected equal numbers of six-week-old male and female *c-Jun$^{f/f}$;Col-CreER^{tg}* and *c-Jun$^{f/f}$* mice to 4, 6 and 8 weeks of treatment with either CCl$_4$ (1 µl/gbw) or olive oil (vehicle control) (Figure 21). 8-10 mice were collected per

genotype, treatment and time period. All liver specimens collected in this experiment were then analyzed by Sirius Red staining to assess the fibrosis and by H&E staining to evaluate the overall liver morphology. Sirius Red can directly stain the collagen proteins in the ECM and has long been considered as the 'gold standard' for assessing liver fibrosis (Bataller *et al.*, 2005). The degree of fibrosis was determined by quantitative measurement of the percentage of Sirius Red positive regions over the whole liver by Metamorph software because it appeared more accurate than various semi-quantitative scoring systems.

Light microscopy images of Sirius Red and H&E staining from representative liver specimens are shown in Figure 22 A to C. Sirius Red staining revealed that all the oil-treated mice, regardless of their genotypes, did not form any fibrotic septa; whereas all mice with time course CCl_4 treatment showed extensive formation of fibrotic septa. Quantification of the Sirius Red positive area (fibrotic area) over the whole liver (Figure 22D) revealed that approximately 3% of the liver area appeared Sirius Red positive in 4 weeks CCl_4-treated *c-Jun^{f/f}* and *c-Jun^{f/f};Col-CreER^{tg}* mice, which is approximately a four-fold increase over the oil-treated controls. No major difference on the degree of fibrosis was detected between these two genotypes. Interestingly, with prolonged CCl_4 treatment, we began to observe significantly more fibrosis developing in *c-Jun^{f/f};Col-CreER^{tg}* mice. In the 6 weeks treatment group, the average fibrotic area in *c-Jun^{f/f};Col-CreER^{tg}* mouse livers was approximately 30% larger than in *c-Jun^{f/f}* mouse livers. As shown in Figure 22 B and D, the percentage of Sirius Red positive regions was 5.00% in *c-Jun^{f/f};Col-CreER^{tg}* livers compared to 3.87% in *c-Jun^{f/f}* livers (p<0.01). The
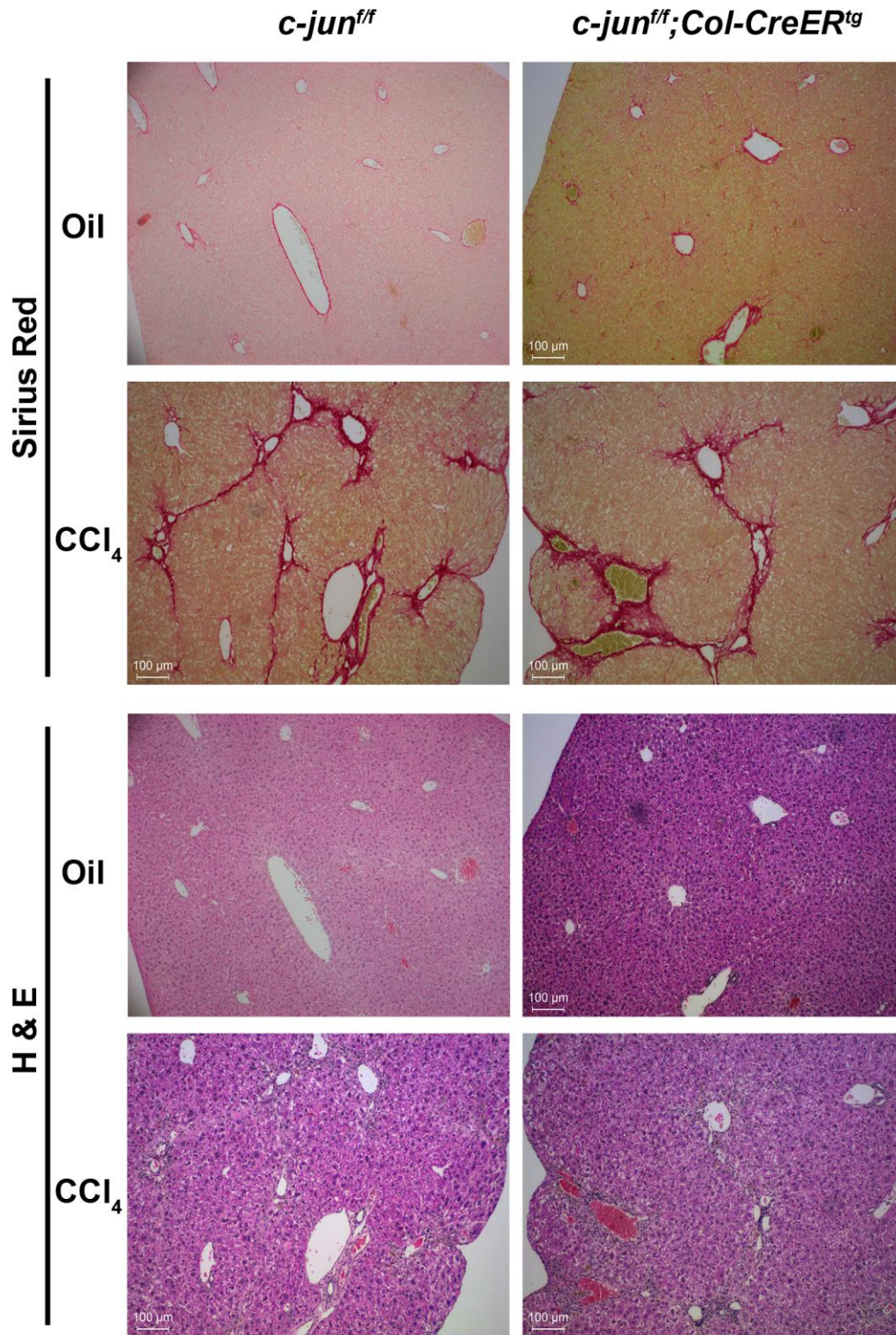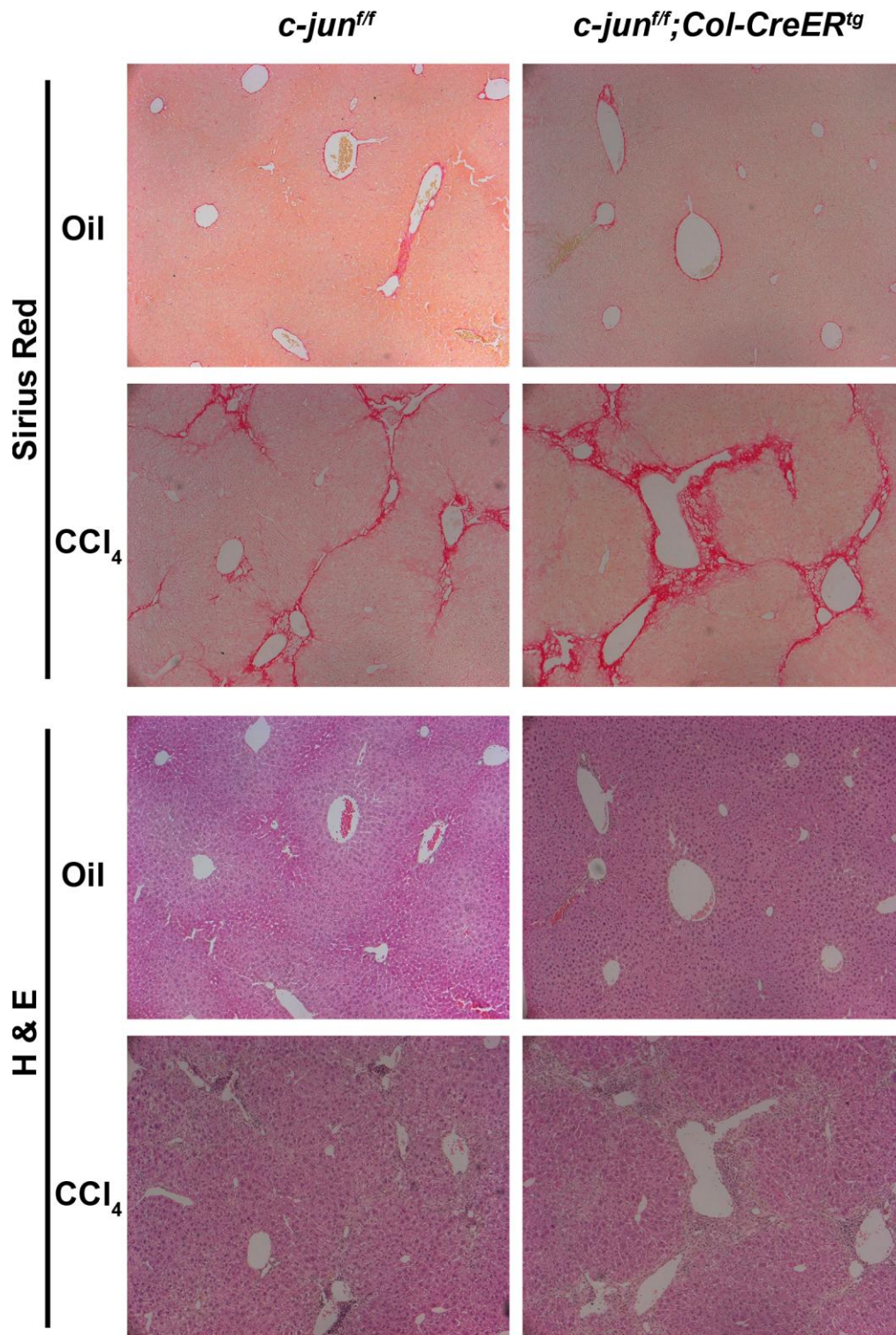
113

A <u>4 Weeks Fibrosis Progression</u>

B

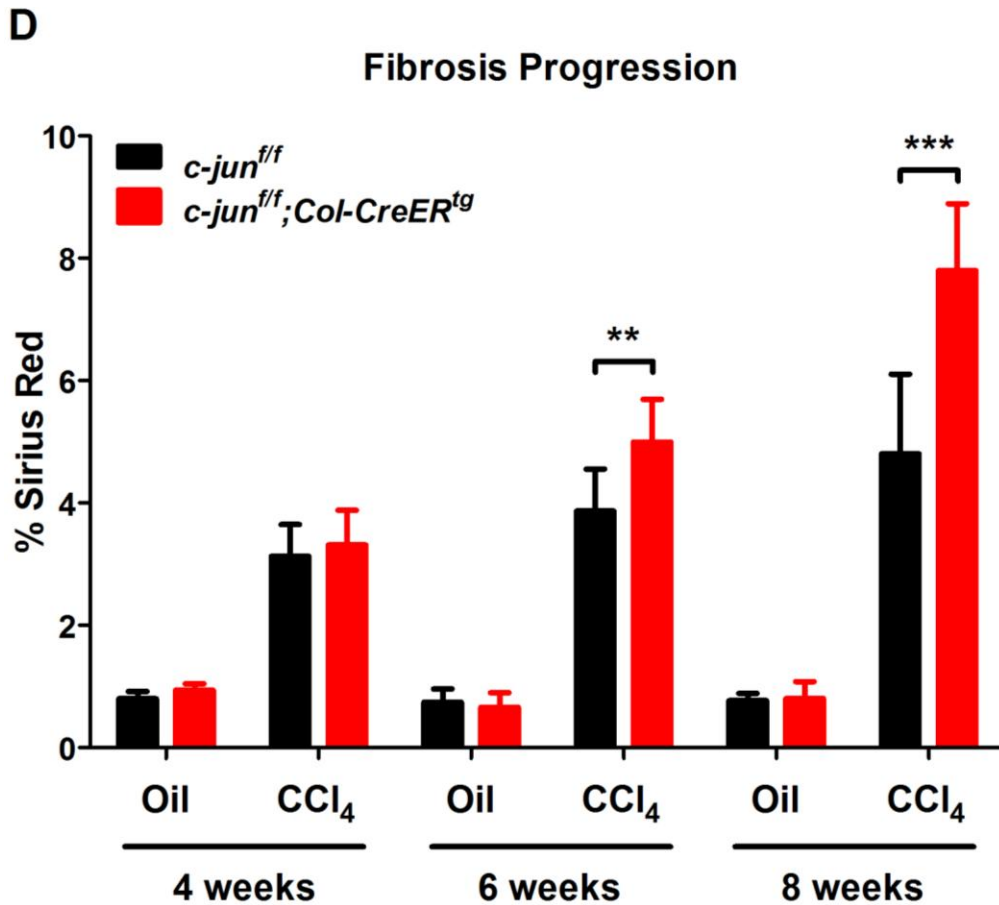## 6 Weeks Fibrosis Progression

C

D
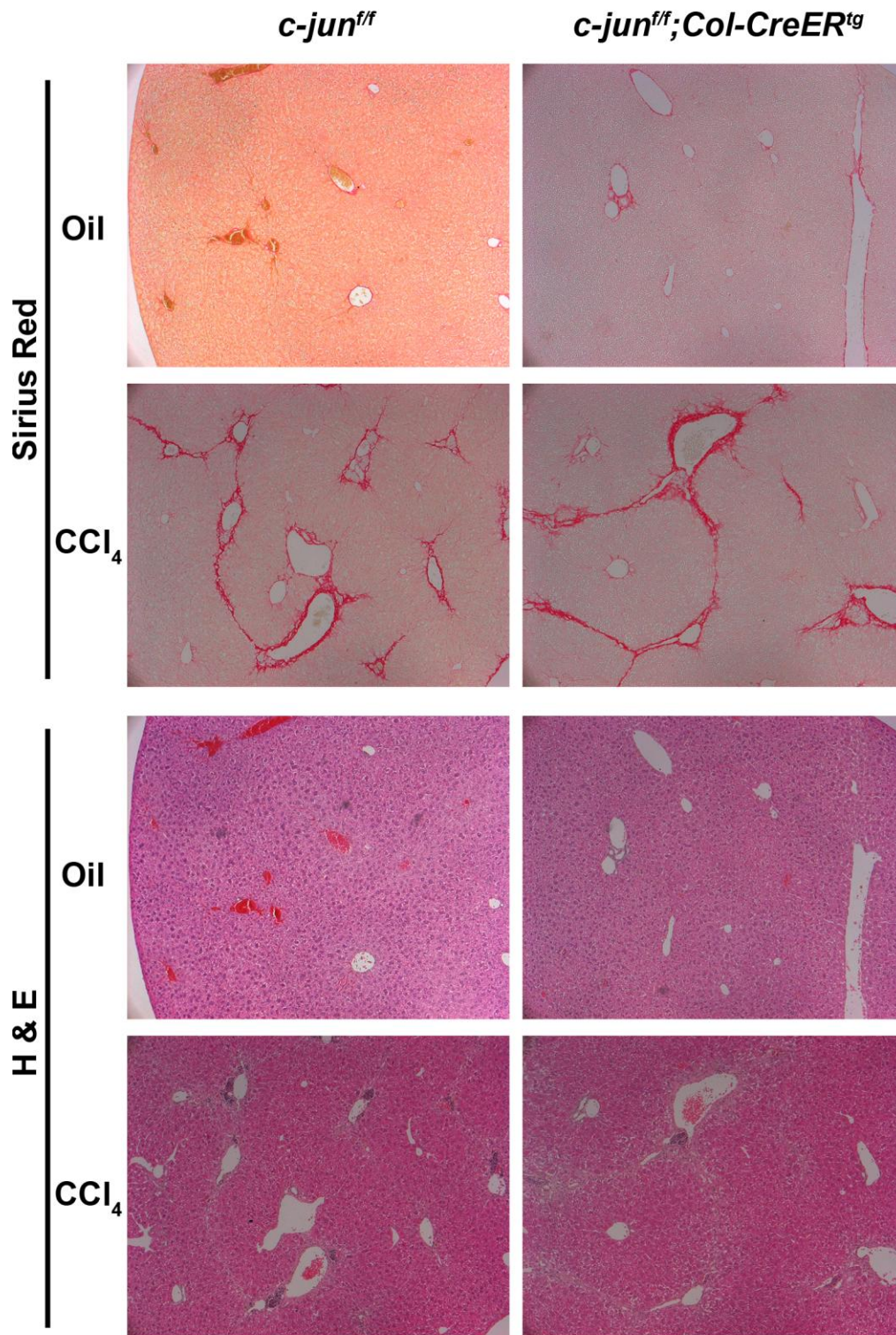
Fibrosis Progression

Figure 22. Loss of c-JUN in HSCs aggravates fibrosis
$c\text{-}Jun^{f/f}$ (left) and $c\text{-}Jun^{f/f};Col\text{-}CreER^{tg}$ (right) mice were treated with oil or CCl_4 for 4 weeks (**A**), 6 weeks (**B**) and 8 weeks (**C**) respectively. Number of mice: n≥5 in Oil-treated group per time period; n≥8 in CCl_4-treated group per time period. (**A to C**) Sirius Red (top panels) and H&E (bottom panels) staining of liver sections from representative mice (10X magnification). (**D**) Quantification of fibrosis based on Sirius Red staining by 20 randomly chosen fields (10X) from four individual liver lobes per mouse. Data represents mean+SD. Statistics done by 2-way ANOVA, **p<0.01, ***P<0.001.

difference in fibrogenesis was even more pronounced in the 8 weeks treatment group. The $c\text{-}Jun^{f/f};Col\text{-}CreER^{tg}$ mouse livers contain 7.80% fibrotic region whereas the $c\text{-}Jun^{f/f}$ mouse livers contain only 4.80% fibrotic region in average; demonstrating about 60% more hepatic fibrosis developed in $c\text{-}Jun^{f/f};Col\text{-}CreER^{tg}$ mice over the control genotype. Moreover, the fibrotic scars formed in $c\text{-}Jun^{f/f};Col\text{-}CreER^{tg}$ mice at this stage were much broader

(Figure 22C), suggesting an increase in matrix stiffness compared to the control genotype. These data clearly demonstrated that the loss of c-JUN in HSCs strongly promoted fibrosis progression; indicating that c-JUN functions in activated HSCs to limit fibrosis development during chronic liver injury.

4.5 c-JUN deletion in HSCs potentiates HSC activation

As the fibrogenic process is consecutive to HSC activation, we next examined whether c-JUN deletion in HSC could affect its activation. Hepatic expression of three classical activated HSC markers, *αSMA*, *Desmin* and *Vimentin*, were assessed by whole liver qRT-PCR (Figure 23A). CCl_4 potently stimulated the expression of all three markers in both *c-Jun^{f/f}* and *c-Jun^{f/f};Col-CreER^{tg}* mice as compared to oil-treated mice. Remarkably, as expected, *c-Jun^{f/f};Col-CreER^{tg}* mice showed significantly higher levels of HSC markers induction than *c-Jun^{f/f}* mice, indicating a greater extent of HSC activation in these mice.

Activated HSCs can produce large amount of fibrillar ECM proteins. The most-studied and increased ECM protein during fibrogenesis is type I collagen (Bataller *et al*., 2005, Tsukada *et al*., 2006, Friedman, 2008b). Type I collagen is a heterotrimeric protein composing of two α1 and one α2 chains encoded by *Col1a1* and *Col1a2* genes respectively. Its increase is directly reflected by an increase in *Col1a1* and *Col1a2* mRNA levels (Tsukada *et al*., 2006). Thus, we analyzed hepatic *Col1a1* and *Col1a2* expressions (Figure 23B) and found substantial upregulation of both genes (more than 20-fold increase of *Col1a1* expression and more than 10-fold increase of *Col1a2* expression) after repetitive exposure to CCl_4 as compared to oil which act as control. Strikingly, the augmentation of both *Col1a1* and *Col1a2* genes were approximately two
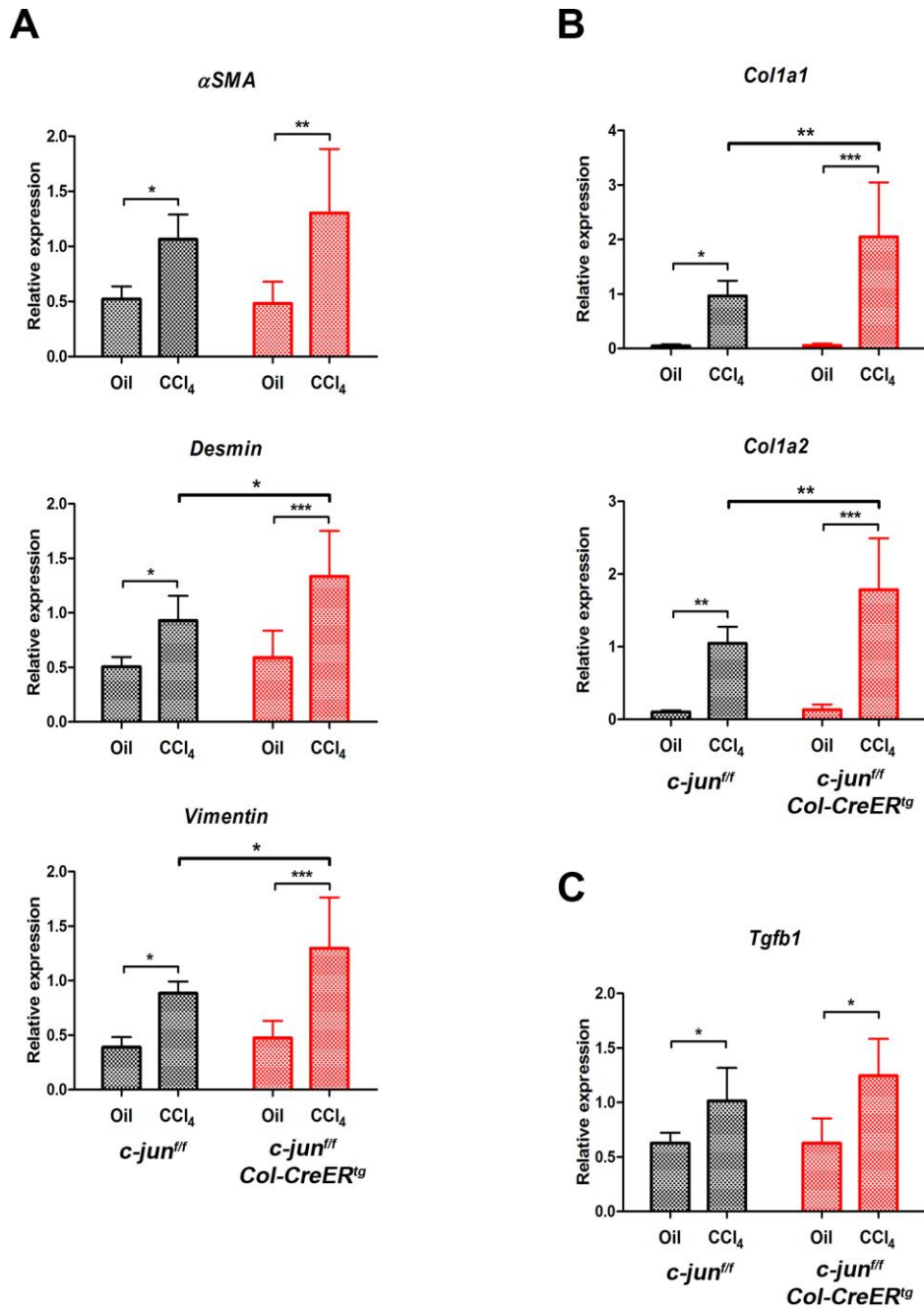
Figure 23. c-JUN deletion in HSCs potentiates HSC activation
Whole liver RNA extracts from 8 weeks oil (n=5 per genotype) or CCl_4 (n=8 per genotype) treated *c-Jun$^{f/f}$* and *c-Jun$^{f/f}$;Col-CreER^{tg}* mice were used to determine activated HSC markers and fibrogenic genes expression by qRT-PCR (normalized against *Gapdh*). (**A**) Activated HSC markers α-SMA, Desmin and Vimentin mRNA As levels. (**B**) Type I Collagen mRNA levels. (**C**) TGF-β1 mRNA level. Experiments were done in duplicates, data represents mean+SD. Statistics done by 2-way ANOVA, *p<0.5, **p<0.01, ***P<0.001.

times higher in CCl$_4$-treated *c-Jun^{f/f};Col-CreER^{tg}* mice than in CCl$_4$-treated *c-Jun^{f/f}* mice. This data is consistent with the previous Sirius Red staining results showing that *c-Jun^{f/f};Col-CreER^{tg}* mouse livers contain significantly larger fibrotic regions. This further corroborates a stronger HSC profibrogenic activity in these mice.

Another key fibrogenic marker is TGF-β1 (encoded by *Tgfb1*). TGF-β1 is the most potent fibrogenic cytokine expressed in nonparenchymal liver cells mainly HSCs and Kupffer cells (De Bleser *et al.*, 1997, Bataller *et al.*, 2005). In HSCs, TGF-β1 function to stimulate their activation and fibrogenesis (e.g. promotes collagen synthesis and inhibits collagen degradation) (Bataller *et al.*, 2005). As shown in Figure 23C, hepatic TGF-β1 expression seemed to be comparable between *c-Jun^{f/f};Col-CreER^{tg}* and *c-Jun^{f/f}* mice. However, we used whole liver fractions to evaluate TGF-β1 expression while hepatocytes being the most abundant cell type in the liver do not express it (De Bleser *et al.*, 1997). Therefore, there could be a dilution effect and thus purification of HSCs is needed for an accurate evaluation of TGF-β1 expression in these mice.

Taken together, these data strongly demonstrated that *c-Jun^{f/f};Col-CreER^{tg}* mice, which harbor genetic inactivation of c-JUN in activated HSCs, contained more activated HSCs and maintained greater fibrogenic activity.

4.6 Inactivation of c-JUN in hepatocytes and hematopoietic cells

Liver is a multicellular organ where cell-to-cell signaling and interaction orchestrate to regulate its normal function as well as injury responses. Given

the complexity of hepatic fibrosis and the involvement of different liver cell types, we next ablated *c-Jun* in other liver cell types without affecting it in HSCs to obtain a more complete picture of how c-JUN regulates hepatic fibrosis. We crossed *c-Jun^{f/f}* mice with *Mx-Cre^{tg}* transgenic mice, which carry the *Cre* transgene under the control of an interferon-inducible *Mx1* promoter (Kuhn *et al*., 1995), in an identical way as the sequential breeding of *c-Jun^{f/f}* mice and *Col-CreER^{tg}* transgenic mice. The progeny littermate *c-Jun^{f/f};Mx-Cre^{tg}* and *c-Jun^{f/f};Mx-Cre^{ntg}* (equivalent to and here on designated as *c-Jun^{f/f}*) mice were used for subsequent experiments. As Poly I/C is required to induce the interferon production in order to activate *Cre* transgene expression, all experimental mice were administrated with Poly I/C to avoid confounding phenotypes. The expressed Cre recombinase can robustly delete *c-Jun* in both hepatocytes and hematopoietic cells in the liver (Maeda *et al*., 2005). As shown in Figure 24, c-JUN expression was significantly impaired in both oil and CCl₄-treated *c-Jun^{f/f};Mx-Cre^{tg}* mice.
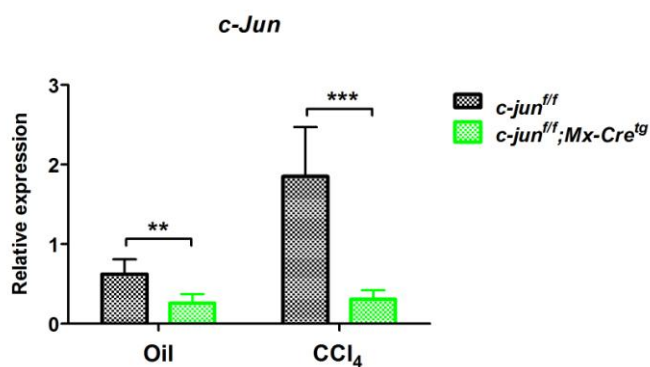

Figure 24. c-JUN inactivation in hepatocytes and hematopoietic cells
Both *c-Jun^{f/f}* and *c-Jun^{f/f};Mx-Cre^{tg}* mice were administrated with Poly I/C. In addition, mice (n=8 for each genotype) were treated with CCl₄ to induce c-JUN expression; or with oil (n≥5 for each genotype) as vehicle control. Whole liver fractions were used to examine c-JUN expression by qRT-PCR. Experiments were done in duplicates, data represents mean+SD. Statistics done by t-test, **P<0.01, ***P<0.001.

4.7 Loss of c-JUN in hepatocytes and hematopoietic cells ameliorates fibrosis

We went on to investigate the effect of c-JUN in hepatocytes and hematopoietic cells in hepatic fibrosis. We again subjected six-week-old *c-Jun^{f/f}* and *c-Jun^{f/f};Mx-Cre^{tg}* mice of balanced genders to the same dose and time periods of oil or CCl$_4$ treatment. Of note, sufficient doses of poly I/C were administrated prior to oil and CCl$_4$ treatment to ensure efficient c-JUN inactivation in *c-Jun^{f/f};Mx-Cre^{tg}* mice before the induction of fibrosis (Figure 25).
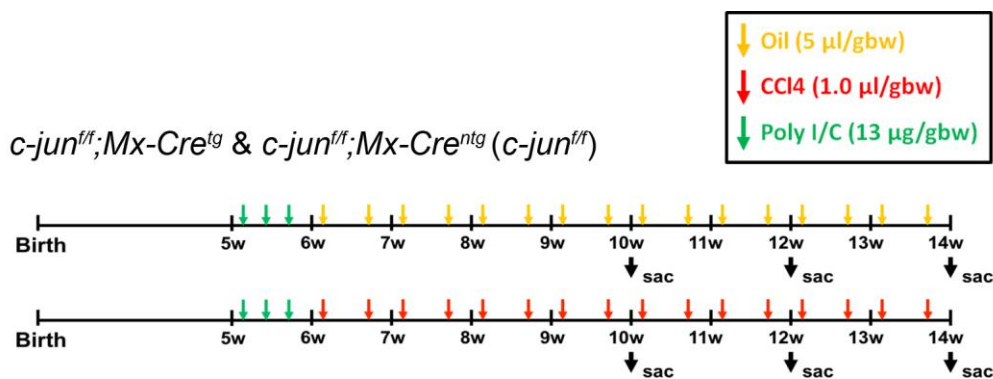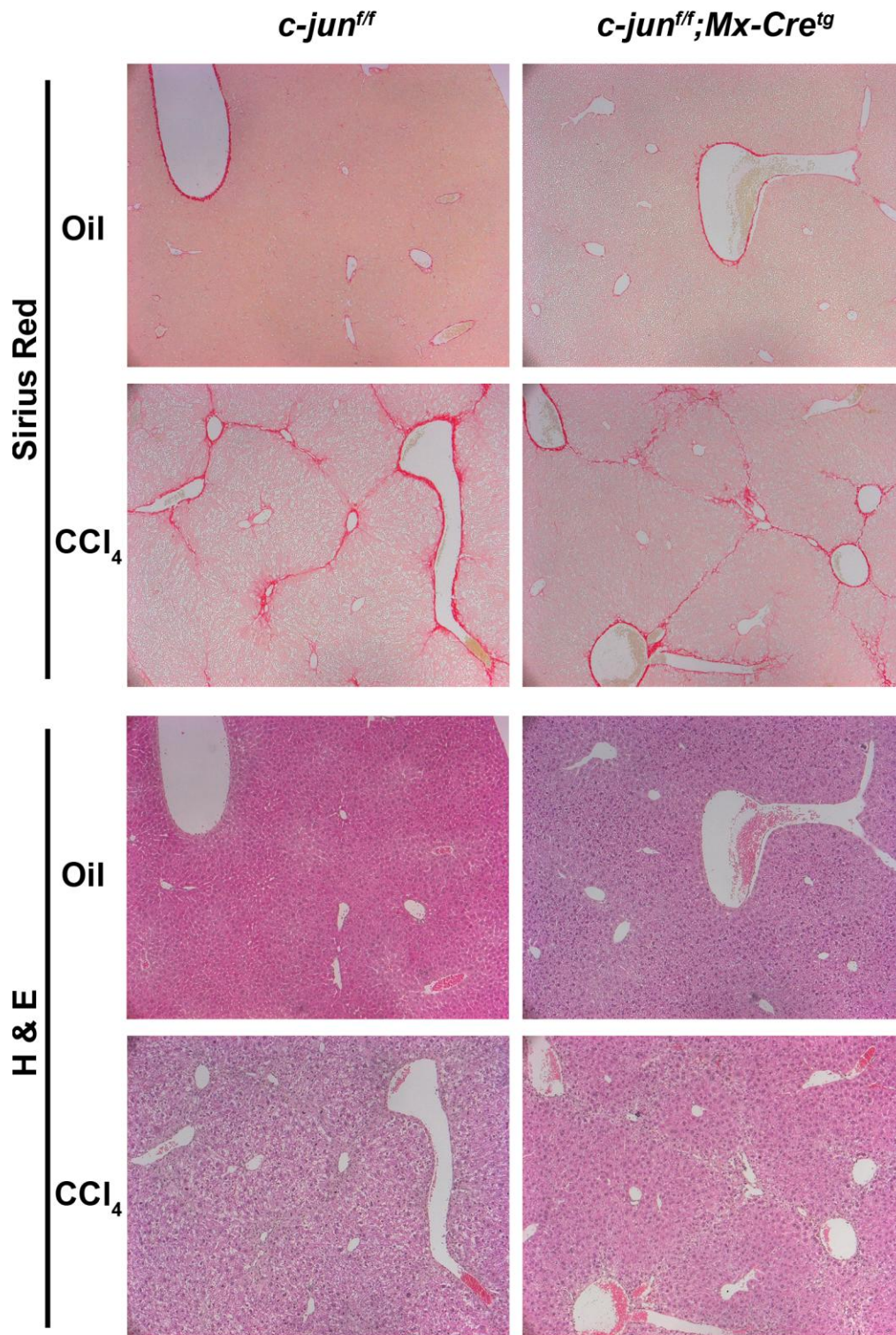

Figure 25. Detailed injection and harvesting scheme for *c-Jun^{f/f};Mx-Cre^{tg}* and *c-Jun^{f/f}* mice
c-Jun^{f/f};Mx-Cre^{tg} and *c-Jun^{f/f};Mx-Cre^{ntg}* (*c-Jun^{f/f}*) mice were injected twice per week with the indicated dosage of oil (yellow) or CCl$_4$ (red) for 4 weeks, 6 weeks or 8 weeks respectively. In addition, indicated dosage of Poly I/C (green) was injected to all the experimental mice before the first week of the oil or CCl$_4$ treatment. All mice were then harvested at 48 to 72 hour after the last injection.

Liver fibrosis and overall morphology were also evaluated by Sirius Red and H&E staining respectively; representative histology pictures are depicted in Figure 26. As expected, the protocol produced 100% fibrosis in all CCl$_4$-treated mice. Surprisingly, we observed small but significantly less fibrosis developing in *c-Jun^{f/f};Mx-Cre^{tg}* mice throughout all three time periods we

A

<u>4 Weeks Fibrosis Progression</u>

| | *c-jun^{f/f}* | *c-jun^{f/f};Mx-Cre^{tg}* |

Sirius Red — Oil, CCl$_4$

H & E — Oil, CCl$_4$

123

B <u>6 Weeks Fibrosis Progression</u>

c-jun^{f/f}   *c-jun^{f/f};Mx-Cre^{tg}*

Sirius Red — Oil, CCl_4

H & E — Oil, CCl_4

124

C

c-jun^{f/f}   *c-jun^{f/f};Mx-Cre^{tg}*

Sirius Red — Oil, CCl₄

H & E — Oil, CCl₄

D
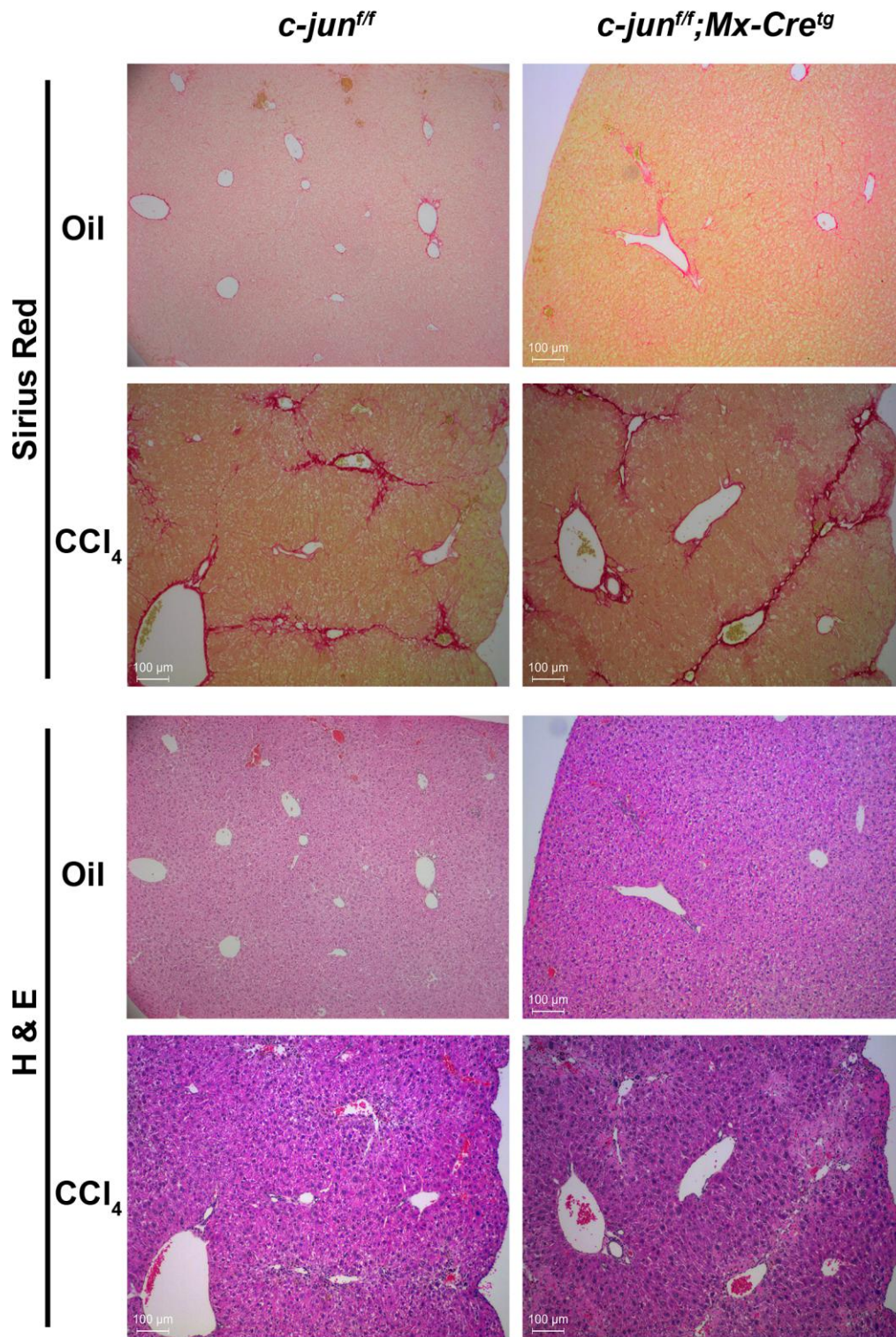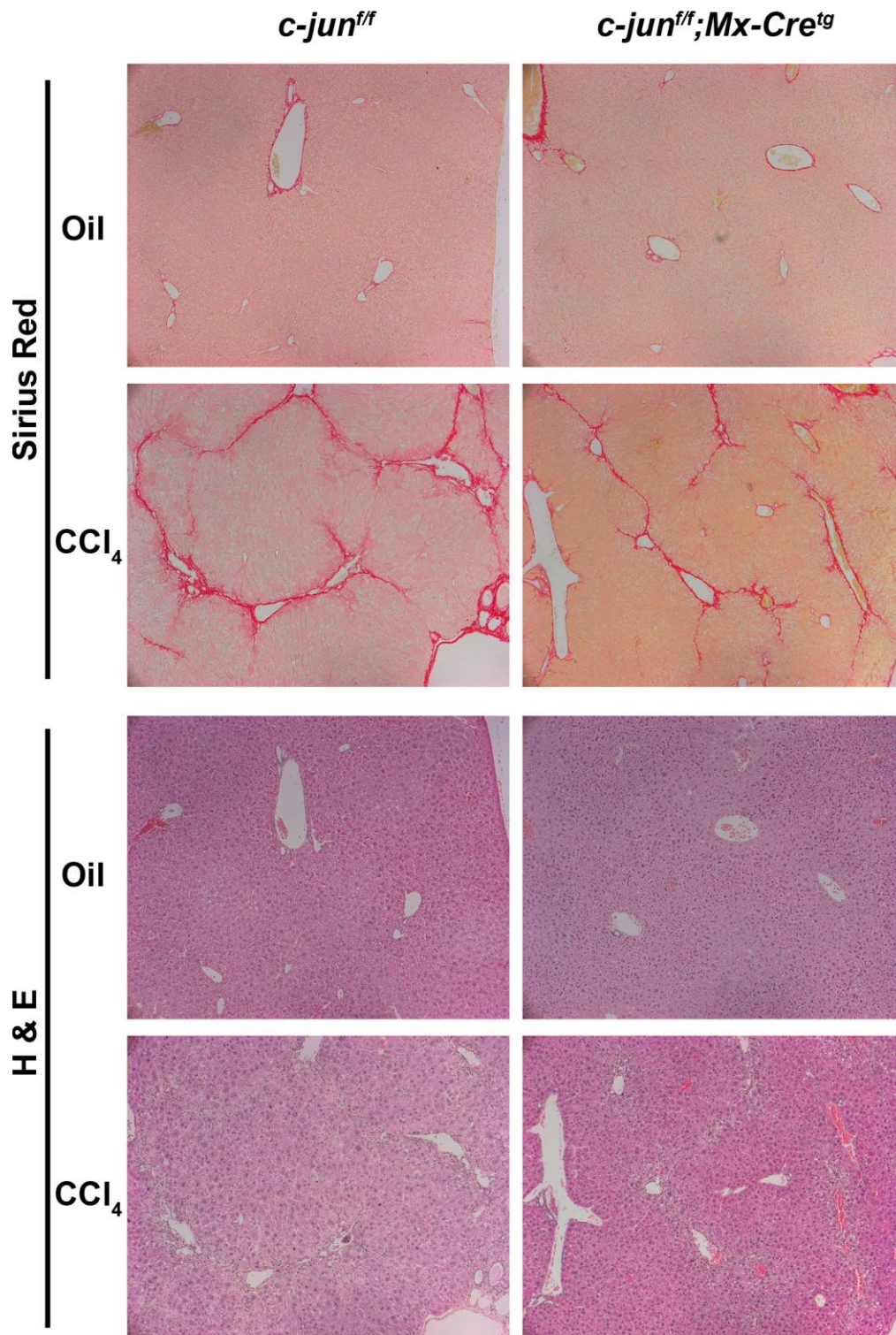
Figure 26. Loss of c-JUN in hepatocytes and hematopoietic cells ameliorates fibrosis
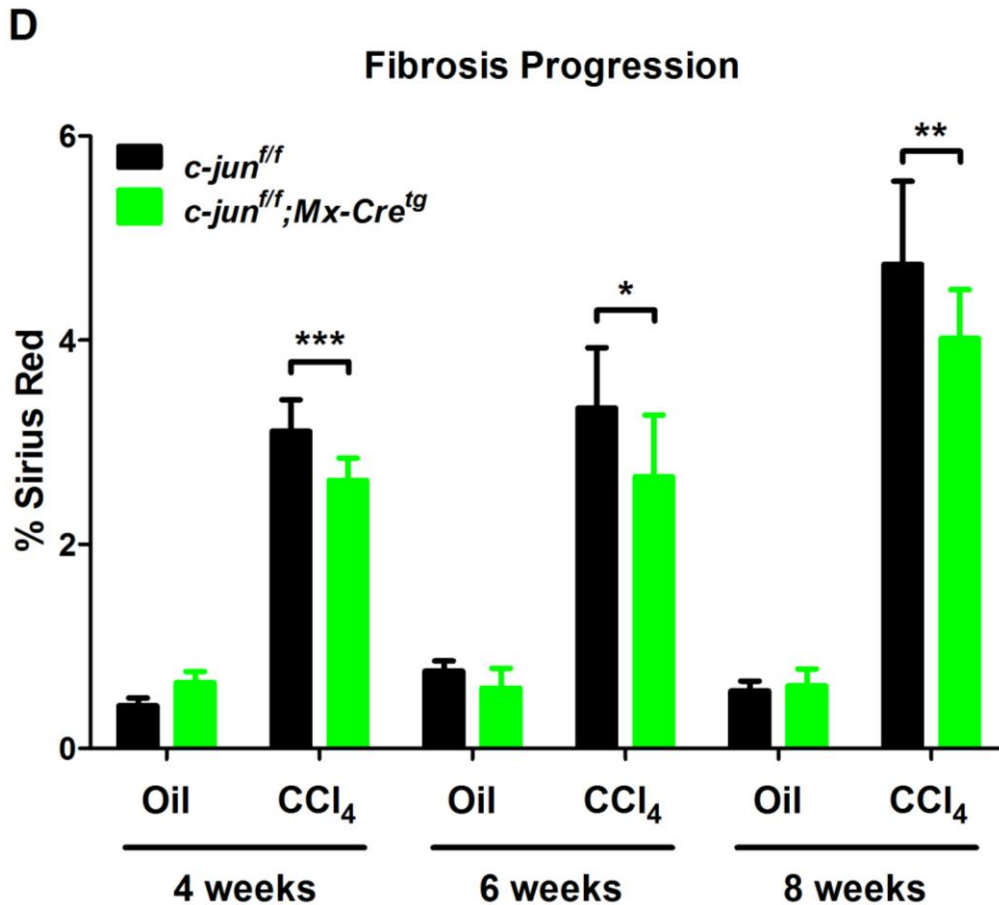*c-Jun$^{f/f}$* (left) and *c-Jun$^{f/f}$;Mx-Cre^{tg}* (right) mice were treated with oil or CCl$_4$ for 4 weeks (**A**), 6 weeks (**B**) and 8 weeks (**C**) respectively. Number of mice: n≥7 in oil-treated group per time period; n≥8 in CCl$_4$-treated group per time period. (**A to C**) Sirius Red (top panels) and H&E (bottom panels) staining of liver sections from representative mice (10X magnification). (**D**) Quantification of fibrosis based on Sirius Red staining by 20 randomly chosen fields (10X) from four individual liver lobes per mouse. Data represents mean+SD. Statistics done by 2-way ANOVA, *P<0.5, **p<0.01, ***P<0.001.

have analyzed (*c-Jun$^{f/f}$;Mx-Cre^{tg}* versus *c-Jun$^{f/f}$*; percentage of Sirius Red positive regions upon 4 weeks CCl$_4$ treatment: 2.63 versus 3.11 [p<0.001]; percentage of Sirius Red positive regions upon 6 weeks CCl$_4$ treatment: 2.66 versus 3.34 [p<0.05]; percentage of Sirius Red positive regions upon 8 weeks CCl$_4$ treatment: 4.02 versus 4.74 [p<0.01]). These data demonstrated a persistent 15~20% less fibrotic areas in CCl$_4$-treated *c-Jun$^{f/f}$;Mx-Cre^{tg}* over the

control c-$Jun^{f/f}$ mice; indicating that ablation of c-JUN in hepatocytes and hematopoietic cells limits fibrosis progression. Intriguingly, these data revealed a completely opposite role of c-JUN in hepatocytes and hematopoietic cells as compared to in HSCs during the progression of fibrosis.

4.8 c-JUN deletion in hepatocytes and hematopoietic cells attenuates HSC activation

As paracrine signaling plays an important role in stimulating and maintaining HSC activation, we next sought to investigate whether inactivation of c-JUN in hepatocytes and hematopoietic cells would affect HSC activation during liver injury. By comparing the hepatic expression of *αSMA*, *Desmin* and *Vimentin* genes between c-$Jun^{f/f}$ and c-$Jun^{f/f}$;Mx-Cre^{tg} mice, we again observed significant induction of all three HSC activation markers in both genotypes generated by CCl$_4$ treatment (Figure 27A), indicating that the inactivation of c-JUN in hepatocytes and hematopoietic cells does not impair HSC activation in response to liver injury. However, we noticed that the extent of the inductions of these HSC activation markers was significantly reduced in c-$Jun^{f/f}$;Mx-Cre^{tg} mice (Figure 27A). These results revealed that inactivating c-JUN in hepatocytes and hematopoietic cells, but not in HSCs, can result in lower HSC activation; highlighting the importance of paracrine signaling in regulating HSC fate.

Moreover, analysis of the hepatic *Col1a1* and *Col1a2* expressions revealed that the overall increase of type I collagen synthesis (both *Col1a1* and *Col1a2* mRNA levels) during chronic CCl$_4$-induced fibrogenesis was approximately 50% less in c-$Jun^{f/f}$;Mx-Cre^{tg} mice as compared to c-$Jun^{f/f}$ mice (Figure 27B).

127
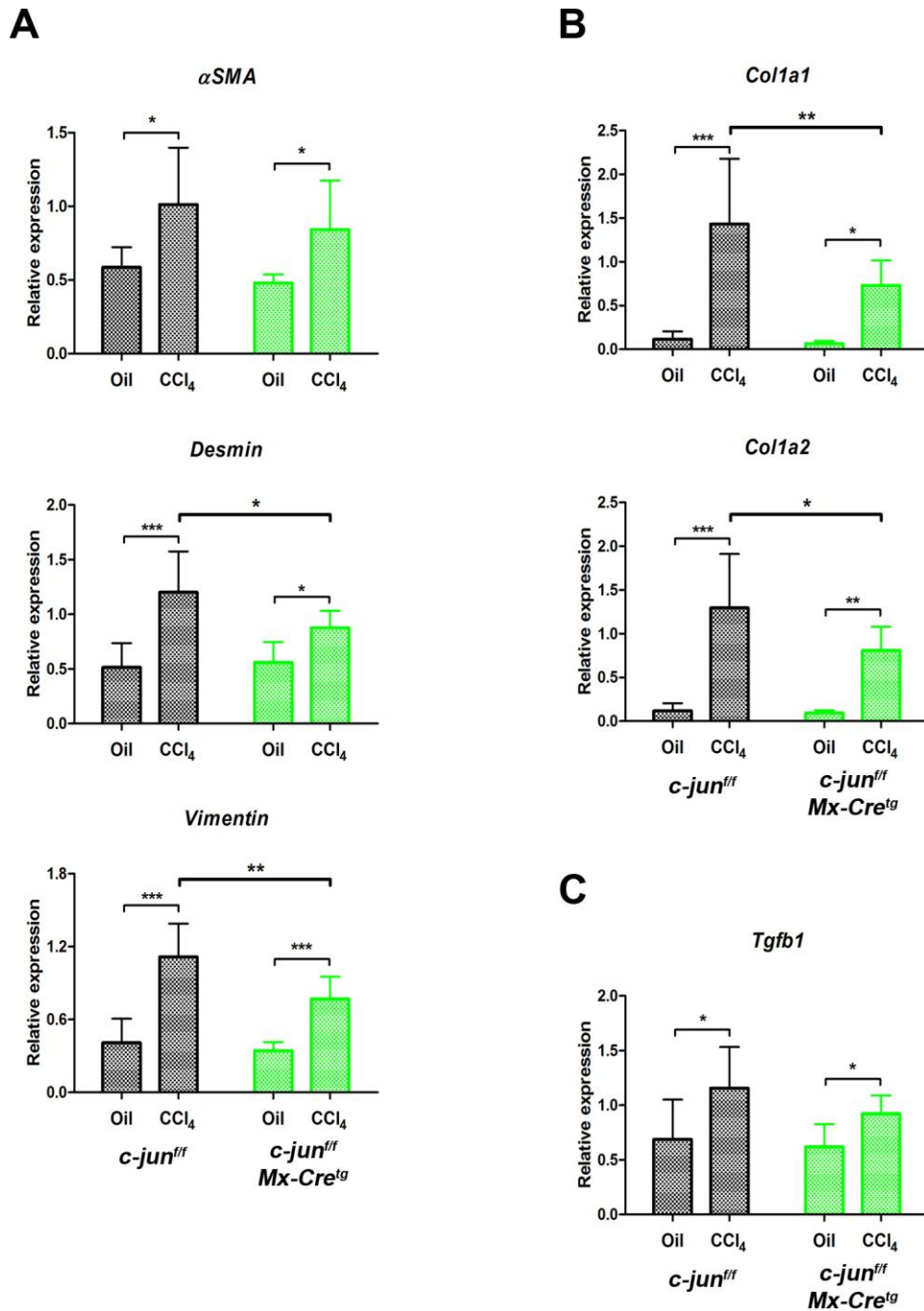
Figure 27. c-JUN deletion in hepatocytes and hematopoietic cells attenuates HSC activation

Whole liver RNA extracts from 4 weeks oil (n≥5 per genotype) or CCl₄ (n=8 per genotype) treated *c-Jun^{f/f}* and *c-Jun^{f/f};Mx-Cre^{tg}* mice were used to determine activated HSC markers and fibrogenic genes expression by qRT-PCR (normalized against *Gapdh*). (**A**) Activated HSC markers α-SMA, Desmin and Vimentin mRNA levels. (**B**) Type I Collagen mRNA levels. (**C**) TGF-β1 mRNA level. Experiments were done in duplicates, data represents mean+SD. Statistics done by 2-way ANOVA, *p<0.5, **p<0.01, ***P<0.001.

This data is consistent with the Sirius Red quantification results that *c-Jun^{f/f};Mx-Cre^{tg}* livers contain significantly less collagen deposition, suggesting a reduced HSC activity in these mice.

Moreover, hepatic TGF-β1 expression was similar between *c-Jun^{f/f};Mx-Cre^{tg}* and *c-Jun^{f/f}* mice (Figure 27C). Considering the fact that TGF-β1 is mainly expressed in the nonparenchymal cells (De Bleser *et al.*, 1997), cell type-specific expression of TGF-β1 needs to be defined to better understand the hepatic microenvironment.

These data together clearly manifested that inactivating c-JUN in hepatocytes and hematopoietic cells but not in HSCs led to reduced HSC activation and fibrogenesis by an unknown mechanism. This probably contributed to reduced fibrosis progression in *c-Jun^{f/f};Mx-Cre^{tg}* mice.

4.9 Increased expression of Hh pathway components in c-JUN-deficient cells and mice

The fact that activated HSCs tend to accumulate in *c-Jun^{-/-}* embryos as well as in mice with HSC-specific c-JUN deletion (*c-Jun^{f/f};Col-CreER^{tg}*), but not in mice with hepatocytes and hematopoietic cells-specific c-JUN deletion (*c-Jun^{f/f};Mx-Cre^{tg}*), suggests a c-JUN-mediated cell-autonomous mechanism for HSC to regulate its own activation.

Studies have reported active Hh signaling in HSCs but not in liver parenchymal cells as HSCs are Hh-responsive cells while hepatocytes are not. HSC can produce biologically active Hh ligands. These ligands in turn activate Hh signaling in HSC via autocrine thereby promote its activation and

viability (Sicklick *et al*., 2005, Yang *et al*., 2008). Inhibition of active Hh signaling by pharmacologic inhibitor cyclopamine considerably reduced HSC activation both *in vitro* and *in vivo* (Sicklick *et al*., 2005). Moreover, Hh ligands can mediate cytokine (such as PDGF-BB)-induced HSC proliferation. Inhibition of active Hh signaling by pharmacologic inhibitors or neutralizing antibodies drastically blocked the mitogenic effect of cytokines to HSC (Yang *et al*., 2008).

Interestingly, we have identified Gli2 as a c-JUN-dependent gene from our whole genome expression array data in primary MEFs. Gli2 is a Hh activated transcription factor whose function is to transactivate Hh-target gene expression therefore serving as a marker for active Hh signaling (Grzelak *et al*., 2015). Hence, we validated *Gli2* expression by qRT-PCR and detected approximately two-fold higher *Gli2* level in c-JUN-deficient MEFs (Figure 28). This suggests that c-JUN can suppress Gli2 expression and prompted us to hypothesize that c-JUN may modulate HSC activation by interfering with active Hh signaling in HSCs.
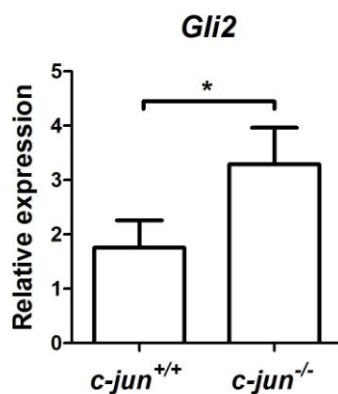
Figure 28. c-JUN downregulates *Gli2* expression
c-Jun$^{+/+}$ and *c-Jun*$^{-/-}$ MEFs (n≥4 per genotype) were used for qRT-PCR analysis of *Gli2* expression. Data represents mean+SD, *P<0.05.
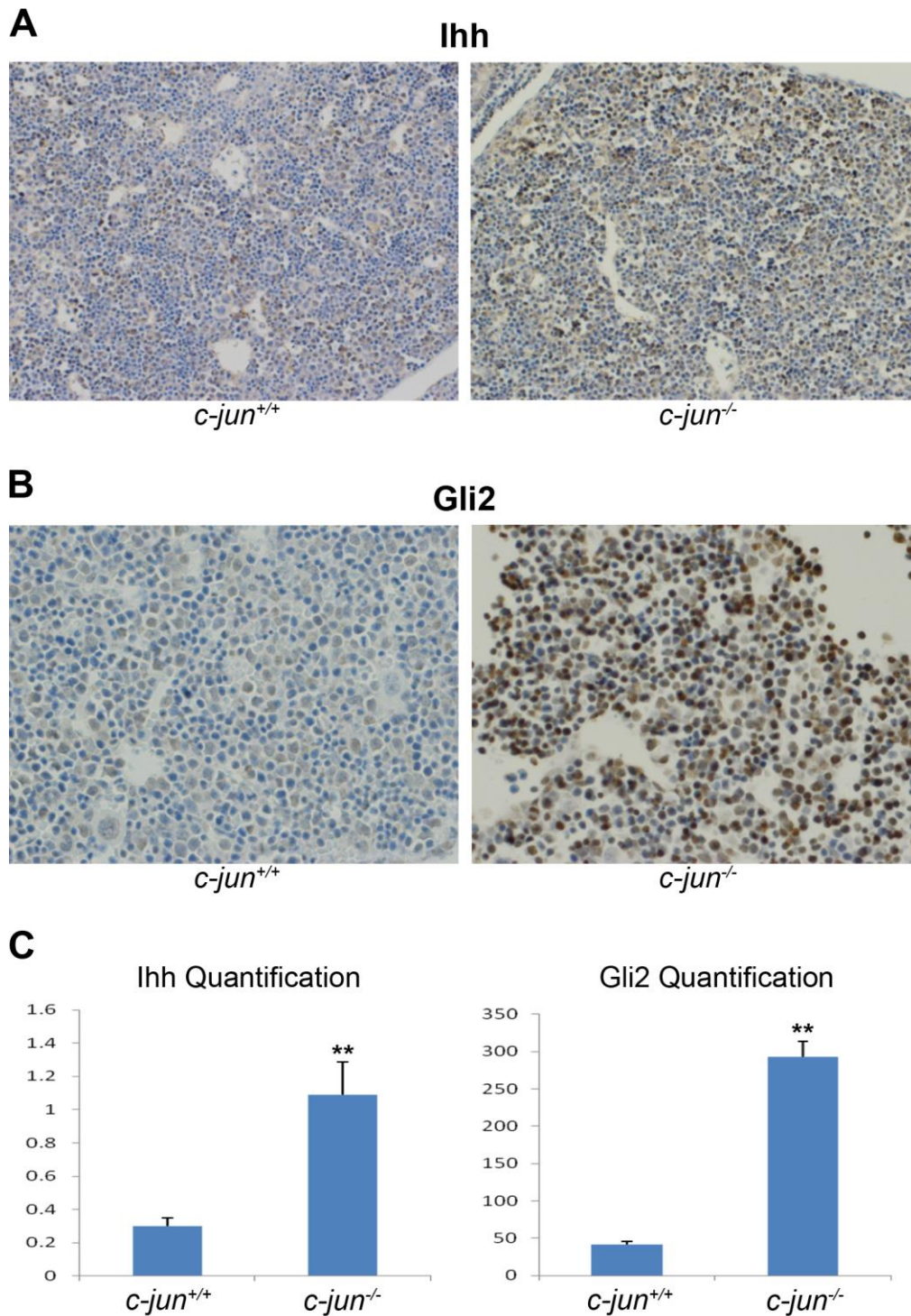
Figure 29. Increased expression of Hh pathway components in *c-Jun*^{-/-} embryos
(A, B) IHC staining for Ihh **(A)** and Gli2 **(B)** in representative E13.5 *c-Jun*^{+/+} (left) and *c-Jun*^{-/-} (right) embryos. **(C)** Quantitative Ihh (left) and Gli2 (right) IHC data from all embryos (n≥4 per genotype). Data represents mean+SD, **P<0.01. Data in collaboration with Dr Anna Mae Diehl from Duke University.

131

We thus investigated whether Hh signaling was generally more active in *c-Jun*^{-/-} background by comparing the expression of Hh pathway components in *c-Jun*^{+/+} and *c-Jun*^{-/-} embryos. As expected, IHC staining revealed vastly higher amount of Ihh, a Hh ligand, as well as Gli2 transcription factor in *c-Jun*^{-/-} embryos than in *c-Jun*^{+/+} embryos (Figure 29). These data indicate that Hh signaling is greatly augmented in the absence of c-JUN and strongly suggest a possible mechanism in modulating HSC activation through the crosstalk between c-JUN and Hh signaling.

Chapter 5

Discussion

5.1 Identification and characterization of c-JUN-regulated genes

c-JUN is the central molecule of the AP-1 transcription factor complex and acts as a convergence point of many signaling cascades to control corresponding target gene transcription in different cellular programs (Shaulian *et al*., 2001, Shaulian *et al*., 2002, Eferl *et al*., 2003b). Historically, JNK-mediated JNP was thought to be essential for c-JUN function. However, since *c-Jun*^AA/AA mice were viable and fertile with no major defects, this conventional thought has been changed (Behrens *et al*., 1999). Till date, mounting evidence have reported that JNP is important but not absolutely required for multiple aspects of c-JUN functions including cell proliferation, apoptosis and transformation (Behrens *et al*., 1999, Behrens *et al*., 2001, Besirli *et al*., 2005). Hence, it is now well accepted that JNP only partially contributes to c-JUN activity. Researchers have therefore tried different attempts to investigate how c-JUN functions in JNP-dependent and -independent manner. Behrens *et al*. have embarked on this subject by screening proteins from a brain library that interact differently with N-terminal phosphorylated and unphosphorylated forms of c-JUN in order to dissect their roles in different biological processes (Nateri *et al*., 2004). By this approach, they successfully identified and characterized several such proteins including Fbw7, TCF4, Bag1-L, RACO-1 and Mbd3 (Nateri *et al*., 2004, Nateri *et al*., 2005, Da Costa *et al*., 2010, Davies *et al*., 2010, Aguilera *et al*., 2011). As c-JUN is a transcription factor, we, on the other hand, focused on identifying target genes that are differentially regulated by N-terminal phosphorylated and unphosphorylated c-JUN. The data presented from this study demonstrate that globally JNP is required only for a small subset of c-JUN target gene

134

transcription. Moreover, we have also shown that JNP has subtle effect on c-JUN functions in response to genotoxic stresses.

5.1.1 Absence of c-JUN has a greater impact on gene expression than the absence of JNP

Our main goal was to identify genes that are regulated differently by N-terminal phosphorylated and unphosphorylated c-JUN. To elucidate this question, we have generated transcriptome profiles of $c\text{-}Jun^{+/+}$, $c\text{-}Jun^{-/-}$ and $c\text{-}Jun^{AA/AA}$ samples prepared from both viable embryos and primary MEFs, with or without stresses, to seek for differentially expressed genes.

Although we did not detect any gene showing statistically significant difference in expression in E11.5 embryos carrying different c-JUN genotypes, we have indeed successfully identified a large number of genes in cultured primary MEFs whose expression were significantly altered in the presence or absence of c-JUN (c-JUN-dependent genes). Interestingly, the number of c-JUN-dependent genes is doubled after UV/CDDP stimulation as compared to the unstimulated condition, indicating that the transcriptional activity of c-JUN is significantly augmented during stress. Moreover, we have also identified fewer genes whose expression were significantly modulated by JNP (JNP-dependent genes) and validated all by qRT-PCR. Surprisingly, the maximum gene expression difference caused by JNP (FC between $c\text{-}Jun^{+/+}$ and $c\text{-}Jun^{AA/AA}$ MEFs) was only about 3-fold. Whereas we detected up to 28-fold expression difference caused by c-JUN (FC between $c\text{-}Jun^{+/+}$ and $c\text{-}Jun^{-/-}$ MEFs) amongst the selected c-JUN-dependent genes validated by qRT-PCR. As we have detected visibly abundant N-terminal phosphorylated c-JUN

135

protein by immunoblots, especially after stress, this suggests that the presence of this N-terminal phosphorylated form of c-JUN does not contribute much to its function in transcriptional regulation, both in the number of genes and in the extent of gene activation/suppression. These findings provide a novel view on how c-JUN functions as a transcription factor: the N-terminal unphosphorylated c-JUN is sufficient to induce/suppress most of its target gene transcription, while the function of JNP in regulating transcription is limited to only a small subset of genes by further enhancing their transcription.

5.1.2 Activities of c-JUN and JNP are insignificant at E11.5 day of embryonic development

The reason for not obtaining any c-JUN and JNP-dependent genes in E11.5 embryos is probably due to insignificant activities of c-JUN and JNP at this stage of embryonic development. Previous studies have already demonstrated that liver is the most affected organ during embryonic development in the c-JUN null embryos. However, *c-Jun*^{-/-} livers do not show deregulated expressions of the corresponding genes (including hepatoblast differentiation markers, growth regulators and known AP-1 targets) as well as morphological abnormalities until E12.5 (Eferl *et al*., 1999). While liver abnormalities cannot be detected, embryos at this stage already exhibit heart abnormalities, indicating that the E12.5 day embryos are not healthy (Eferl *et al*., 1999). Hence, E11.5 appeared as a better time point that precluded all detectable abnormalities in order to identify c-JUN-dependent genes under normal physiological condition. Moreover, JNP has no impact on c-JUN activity

under normal physiological condition as well. *c-Jun*[AA/AA] mice do not exhibit any overt defects that are found in the *c-Jun*^{-/-} mice (Behrens *et al*., 1999). These reports, together with our data suggest that under normal physiological condition, when all *c-Jun*^{+/+}, *c-Jun*^{-/-} and *c-Jun*[AA/AA] mice are grossly normal, c-JUN and JNP do not cause detectable differences at both morphological and genomic levels.

5.1.3 N-terminal unphosphorylated c-JUN possesses transcriptional activity

The fact that the expression of only a minimal number of genes are affected by JNP suggests that the c-JUNAA protein acquires comparable transcriptional ability and is able to regulate c-JUN target gene transcription to a similar extent as c-JUNWT. This could be due to a compensatory effect by phosphorylation on other residues such as threonines 91/93 by JNKs (Reddy *et al*., 2013). In fact, previous reports have proposed that c-JUNAA or even c-JUN4A (4 JNK phosphoacceptor sites, serines 63/73 and threonines 91/93, are mutated to alanines) protein can activate various promoters such as TRE by luciferase assays (Behrens *et al*., 1999, Davies *et al*., 2010). These findings in accordance with our data together support that N-terminal unphosphoryated c-JUN can mediate gene transcription.

The mechanism of how N-terminal unphosphorylated c-JUN (c-JUNAA as well as c-JUN4A) mediates gene transcription has been proposed to be through the cooperation with several newly discovered c-JUN interacting proteins. In recent years Behrens and his coworkers have identified many proteins that can interact with c-JUN with regard to the JNP status; among them RACO-1 and Mbd3 have been delineated to be able to interact with N-

137

terminal unphosphorylated c-JUN and thereby regulate gene transcription (Davies *et al*., 2010, Aguilera *et al*., 2011). RACO-1 is a novel RING-domain-containing protein widely expressed in many cell lines of different tissue origin. It can interact with and act as a coactivator to enhance transcriptional activity of both wild type and N-terminal unphosphorylated c-JUN with similar efficiency. Importantly, the cooperation between RACO-1 and N-terminal unphosphorylated c-JUN is mediated by the Raf/MEK/ERK pathway instead of the JNK pathway, highlighting the importance of c-JUN function in a JNP-independent manner (Davies *et al*., 2010). Mbd3 is a subunit of nucleosome remodeling and histone deacetylation (NuRD) complex that mediates gene repression. Mbd3 only interacts with the N-terminal unphosphorylated form of c-JUN, but not with the N-terminal phosphorylated form of c-JUN. Therefore the N-terminal unphosphorylated c-JUN recruits the NuRD complex, containing Mbd3, by specifically interacting with Mbd3 and functions to repress its transcriptional activity. JNP, on the other hand, by activated JNK signaling can release the N-terminal phosphorylated c-JUN from this inhibitory complex (Aguilera *et al*., 2011).

Collectively, previous reports together with our data strongly support that c-JUN can regulate gene activation/repression in a JNP-independent manner. JNP can modulate only a small subset of c-JUN target gene transcription and is generally not required for most of c-JUN target gene transcription.

5.1.4 JNP has mild effect on MEFs proliferation and genotoxic stress-induced apoptosis

Besides the limited effect of JNP in modulating c-JUN responsive gene transcription, we have also demonstrated that JNP exerts mild effect on c-JUN in regulating MEFs proliferation and genotoxic stress-induced apoptosis.

By culturing primary MEFs in low oxygen (3% oxygen), we found that both $c\text{-}Jun^{-/-}$ and $c\text{-}Jun^{AA/AA}$ MEFs grew appreciably with only slightly slower proliferation rates than $c\text{-}Jun^{+/+}$ MEFs, indicating that both c-JUN and JNP exhibit subtle effect on MEFs proliferation. Consistent with our observation, the sizes of the viable $c\text{-}Jun^{-/-}$ and $c\text{-}Jun^{AA/AA}$ fetuses were indistinguishable from the wild type fetuses (Hilberg *et al*., 1993, Johnson *et al*., 1993, Behrens *et al*., 1999), implicating that differences in c-JUN and JNP do not significantly affect *in vivo* development. However, a number of studies have addressed this question before and reported contrasting results. By maintaining cells under conventional culture condition (21% oxygen), those studies reported that $c\text{-}Jun^{-/-}$ cells exhibited severe proliferation defect with a premature senescence phenotype, while $c\text{-}Jun^{AA/AA}$ cells showed partial and clear proliferation defect compare to wild type cells (Johnson *et al*., 1993, Behrens *et al*., 1999, Schreiber *et al*., 1999). Intriguingly, it has been suggested that the cellular proliferation defect is due to the hyperoxic stress experienced during conventional culture condition (21% oxygen), as cells *in vivo* are only exposed to a maximal of 5% oxygen (MacLaren *et al*., 2004). Thus, our culture condition, being similar to the physiological oxygen level, should better reflect the *in vivo* proliferation rates. Therefore, we believe that

JNP has only a mild effect on proliferation of MEFs under normal physiological condition.

Similarly, JNP shows mild effect on MEFs apoptosis in response to UV and CDDP. We found that $c\text{-}Jun^{AA/AA}$ MEFs were significantly and modestly more resistant to CDDP exposure compared to $c\text{-}Jun^{+/+}$ MEFs. On the other hand, we detected no significant resistance of $c\text{-}Jun^{AA/AA}$ MEFs to UV-induced apoptosis. This suggests that UV and CDDP trigger apoptosis by different mechanisms. It has been shown before that $c\text{-}Jun^{AA/AA}$ MEFs are partially protected from cellular apoptosis in response to UV (Behrens $et\ al.$, 1999). Again the difference in the observation is probably due to different cell culture conditions (oxygen levels). Moreover, $c\text{-}Jun^{+/+}$ and $c\text{-}Jun^{AA/AA}$ MEFs also exhibited similar degree of apoptosis in response to other stress such as alkylating agent MNNG (Behrens $et\ al.$, 1999). Taken together, JNP exerts subtle effect on cellular apoptosis in MEFs and in a stress-dependent manner.

5.1.5 JNP is not absolutely required for c-JUN stability

JNK-mediated phosphorylation is an important mechanism for c-JUN stabilization (Karin $et\ al.$, 1997). We have shown by immunoblots that both UV and CDDP strongly activate JNK and c-JUN. Interestingly, we note that c-JUNAA which lacks JNP can still be stabilized by both stresses, which is represented by its increased steady-state levels. This observation suggests that there should be JNP-independent mechanism that contributes to c-JUN abundance, probably through increased transcription and/or other post-translational modifications. In fact, phosphorylation at threonines 91/93 is also important for c-JUN turnover. For example, the E3 ligase Fbw7 that

specifically regulates the N-terminal phosphorylated c-JUN turnover could also target c-JUNAA efficiently for proteasomal degradation. However, the c-JUN4A mutant could resist the Fbw7-mediated degradation (Nateri *et al.*, 2004), suggesting that phosphorylation at threonines 91/93 is also important for c-JUN stabilization. Therefore, in conclusion, our data shows that JNP exerts subtle effect but is not absolutely required for both c-JUN activity and stability.

5.1.6 The significance of JNP is dependent on the cell type and stimulus

We have demonstrated the limited involvement of JNP in c-JUN action in MEFs mainly in response to genotoxic stresses. Of note, the limited effect of JNP on c-JUN activity is not restricted to MEFs. Previous studies from other groups have also revealed that JNP is not required for several critical c-JUN functions especially in the liver. These include embryonic hepatogenesis and liver regeneration in response to PH (Behrens *et al.*, 1999, Behrens *et al.*, 2002).

Nevertheless, JNP is not always dispensable for c-JUN function, since the impact of JNP on c-JUN activity appears to depend on cell type and/or stimulus. JNK signaling, a mediator of JNP, plays crucial roles in multiple biological processes in lymphocytes and neurons. The N-terminal phosphorylated c-JUN thereby serves as an important effector molecule of the JNK signaling at least in T cells and neurons. *In vitro* studies have revealed that lack of JNP could partially protect cellular apoptosis induced by (1) anti-CD3 antibody and TNF-α but not Fas and UV in thymocytes (Behrens *et al.*, 2001) and (2) trophic factor deprivation and several DNA damage agents such

as Ara-C and etoposide in sympathetic neurons and CGNs (Besirli *et al.*, 2005). Importantly, JNK-mediated phosphorylation at c-JUN threonines 91/93 rather than serines 63/73 has been reported as the more responsive regulatory sites for the pro-apoptotic activity of c-JUN in CGNs (Reddy *et al.*, 2013). Moreover, *in vivo* studies have shown that mice lacking of JNP exhibited (1) reduced anti-CD3 induced thymocyte apoptosis (Behrens *et al.*, 2001) and (2) resistance to kainic acid but not to pentylenetetrazole induced epileptic seizures (Behrens *et al.*, 1999). All these findings clearly demonstrate that JNP is important but not always crucial for c-JUN function even in T cells and neurons, highlighting that the impact of JNP is also in a stimulus-dependent manner.

Furthermore, evidence regarding the significance of JNP have also been corroborated in transformed cells. p73 was found to cooperates preferentially with AP-1 dimers that are composed of c-JUN and FRA1 (Vikhanskaya *et al.*, 2007) or c-JUN and c-FOS (Subramanian *et al.*, 2015) in a JNP-dependent manner to promote cancer cell proliferation and survival. Transcription factor TCF4 has been identified to preferentially interact with the N-terminal phosphorylated form of c-JUN, together with Wnt activated cofactor β-catenin to form a ternary complex to regulate intestinal tumorigenesis triggered by mutant APC. Importantly, the cooperation between TCF4 and phosporylated c-JUN only occurred in HCT116 and SW480 colon cancer cells but not in NIH3T3 fibroblast (Nateri *et al.*, 2005), again emphasizing the importance of JNP in a cell-type specific manner.

Taken together, our data in line with data from other groups strongly indicate that the significance of JNP in c-JUN functions is both cell/tissue type and stimulus-dependent. In MEFs and with genotoxic stresses like UV and CDDP, JNP appears to have a minor effect on c-JUN function and stability.

5.2 Role of c-JUN in hepatic fibrosis

The liver functions as a metabolic and detoxification organ that constantly processes endogenous and exogenous substances to maintain the system homeostasis. Increased risk of hepatocellular damage occurs during overloading of nutrients and/or xenobiotics. Therefore, appropriate repair is essential in maintaining healthy liver architecture and function (Kuntz *et al.*, 2008). Repair of damaged liver is a complex wound healing process that engages a range of resident and infiltrating cell types in the liver and is generally accompanied by some level of fibrosis. While successful liver repair ends with fibrosis resolution, repetitive injury and repair generally leads to sustained fibrosis (Friedman, 2008b). Liver fibrosis/cirrhosis is commonly associated with diseases such as NASH and HCC, which not only affects liver function but also limits the treatment options of these diseases (Bataller *et al.*, 2005, Friedman, 2008b). Therefore, developing antifibrotic therapies is urged to improve the clinical outcomes. Since mounting clinical and experimental evidences support that fibrosis and even cirrhosis are reversible, understanding the mechanisms underlying hepatic fibrosis is fundamental to facilitate the research and development of antifibrotic therapies (Bataller *et al.*, 2005, Friedman *et al.*, 2006). Despite the tremendous increase in knowledge of the molecular and cellular basis of hepatic fibrosis over years, in terms of

proteins, signaling pathways and cell types participating in hepatic fibrosis development, the precise mechanism of fibrosis is incompletely understood.

The identification of HSC as the main collagen-producing cell type was a big breakthrough in understanding the mechanism of hepatic fibrosis. Activated HSCs are only present in injured but not healthy liver (Bataller *et al*., 2005, Kisseleva *et al*., 2011). As we observed significantly more activated HSCs in *c-Jun* null mouse embryos, we particularly investigated the relevance of c-JUN in HSC activation and hepatic fibrosis. Our study shows for the first time that c-JUN is directly involved in HSC activation and hepatic fibrosis development. Most strikingly, we have also found that c-JUN plays contrary roles in different liver cell types in regulating HSC activation and hepatic fibrosis progression.

5.2.1 c-JUN actions in HSCs promotes hepatic fibrosis progression and HSC activation

To investigate the direct effect of c-JUN in HSC activation and hepatic fibrosis progression, we specifically inactivated c-JUN in activated HSCs and examined fibrosis progression by chronic CCl_4 injection. Interestingly, HSC-specific c-JUN deletion resulted in severely increased fibrosis progression as compared to the control genotype mice. Moreover, the increased fibrosis was also accompanied by significantly more activated HSCs as determined by classical activated HSC markers. These results suggest that c-JUN functions to restrict HSC activation in a cell-autonomous manner thereby limiting fibrosis progression.

The molecular mechanism of how c-JUN functions in HSC to restrict its own activation is unknown. HSC activation occurs as a result of a complex network of paracrine and autocrine signaling which is stimulated by liver injury. The factors involved in these paracrine and autocrine signaling in injured livers include cytokines (e.g. TGF-β, TNF-α), growth factors (e.g. PDGF, EGF) and Hh ligands (e.g. Shh, Ihh) etc. (Friedman, 2008a, Omenetti *et al.*, 2011). Therefore, it is likely that c-JUN acts to regulate HSC activation by targeting signaling pathways related to these factors. Serendipitously, we found that c-JUN can down-regulate *Gli2* transcription. Gli2 is a Hh-regulated transcription factor at the distal end of the Hh signaling cascade and functions to control transcription of the Hh-responsive genes (Choi *et al.*, 2011, Omenetti *et al.*, 2011). This exciting finding suggests a novel mechanism to modulate Hh signaling activity by c-JUN. Previous study has reported the regulation of *Gli2* transcription by TGF-β (Dennler *et al.*, 2007), highlighting the existence of the 'non-canonical' Hh signaling. Our finding that c-JUN can suppress Gli2 abundance has thus led to a hypothesis that c-JUN may regulate HSC activation by intervening via the Hh signaling arm in HSC. This hypothesis has been further corroborated by detection of high levels of Hh pathway components (Ihh and Gli2 proteins) in the *c-Jun*$^{-/-}$ embryos.

Liver injury can trigger the production of Hh ligands thereby activating Hh signaling rapidly in HSCs. Initiation of Hh signaling in HSCs can be via both autocrine and paracrine mechanisms depending on the source of the Hh ligands, as HSCs as well as other liver parenchymal and nonparenchymal cells can produce active Hh ligands during liver injury. Active Hh signaling in HSC is crucial for its viability and growth (Omenetti *et al.*, 2011). Therefore,

145

modulating Hh signaling in HSCs can be an efficient mechanism to regulate HSC accumulation and activity during liver injury and repair. Furthermore, once activated, Hh signaling tends to auto-amplify its activation thus further augmenting the activated HSC population. However, overactivation of Hh signaling also promotes fibrogenesis during liver injury and repair (Omenetti *et al*., 2011). Taken together, our data strongly imply a potential mechanism for c-JUN to regulate HSC activation as well as hepatic fibrosis progression through constraining the active Hh signaling in the HSCs. Further investigation is needed to justify this model.

5.2.2 Crosstalk between c-JUN and Hh signaling in other tissue

Both c-JUN and several Hh pathway components (Ptc, Smo, Gli1 and Gli2) have been strongly implicated in skin carcinogenesis (Hahn *et al*., 1996, Johnson *et al*., 1996b, Xie *et al*., 1998, Grachtchouk *et al*., 2000, Nilsson *et al*., 2000, Angel *et al*., 2001, Zenz *et al*., 2006). Two studies have already built a link between c-JUN and Hh signaling in the skin cells (Laner-Plamberger *et al*., 2009, Schnidar *et al*., 2009). By *in vitro* assays, c-JUN has been shown as a direct target of both Gli1 and Gli2 and can cooperate with Gli1/2 at the chromatin level to regulate a subset of Gli target gene expression in human keratinocytes. Moreover, physical interaction of the N-terminal phosphorylated c-JUN with Gli2 but not with Gli1 has been reported. In fact, the oncogenic transformation by simultaneous activation of EGFR and Gli1/2 requires c-JUN. Unfortunately, in both studies, Gli1 and Gli2 were either expressed under doxycycline-inducible promoter or transiently overexpressed.

Hence, it is not possible to assess whether c-JUN can downregulate Gli2 expression in those experimental settings.

We have identified that c-JUN can downregulate Gli2 transcription and there are remarkably high levels of Gli2 in c-JUN null embryos. Thus, in conjunction with the above mentioned findings that c-JUN is a direct target of Gli2 and can cooperate with Gli2 to regulate certain target gene expression, there is a strong implication of some auto-regulatory loop between c-JUN and Gli2. Such an auto-regulatory loop exists between c-JUN and EGFR: c-JUN can positively regulate EGFR transcription while EGFR can activate c-JUN via MAPK signaling (Zenz *et al*., 2003, Zenz *et al*., 2006). Furthermore, both c-JUN and Hh signaling have been identified to participate in PH-induced liver regeneration. Nevertheless, the functions of c-JUN and Hh signaling in liver regeneration have been attributed to different liver cell types (parenchymal cells vs. non-parenchymal cells). Interestingly, inhibition of either pathway has resulted in impaired liver regeneration (Behrens *et al*., 2002, Swiderska-Syn *et al*., 2014). Hence It is of crucial importance to elucidate the functional relationship between c-JUN and Hh signaling, at least in the skin and liver.

5.2.3 c-JUN plays a dual role in HSC activation and fibrogenesis

Hepatic repair and fibrosis development engage almost all the cell types in the liver. Both hepatocytes and hematopoietic cells (such as Kupffer cells) are found to be important in activating HSCs and facilitating fibrosis development (Bataller *et al*., 2005, Friedman, 2008a, Friedman, 2008b). ROS released from the dead/dying hepatocytes and pro-inflammatory cytokines (especially TGF-

β) produced from resident/infiltrating inflammatory cells are all potent inducers for HSC activation (Friedman, 2000, Friedman, 2008a, Friedman, 2008b).

We have thus inactivated c-JUN specifically in hepatocytes and hematopoietic cells but not in HSCs to investigate the effect of c-JUN on HSC activation and fibrogenesis in a non-cell-autonomous manner. Surprisingly, we observed a completely contrary phenotype as both HSC activation and fibrosis progression were significantly reduced in livers where c-JUN has been inactivated in hepatocytes and hematopoietic cells. Apparently, c-JUN plays a dual role in hepatic fibrosis development and in different liver cell types, i.e. anti-fibrotic in HSCs and pro-fibrotic in hepatocytes and hematopoietic cells (Figure 30).

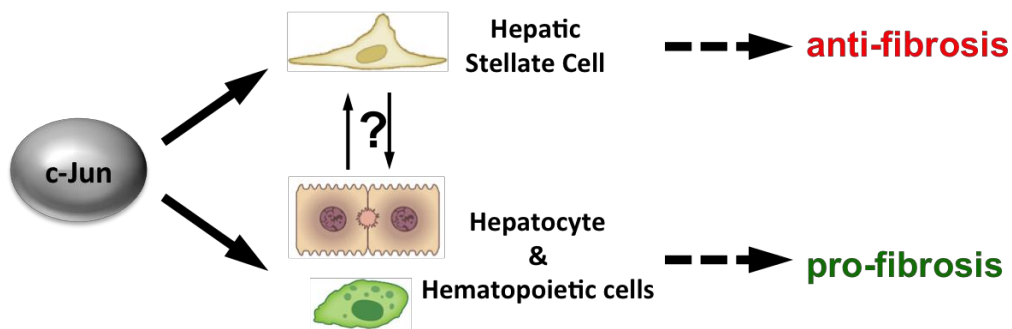**Figure 30. c-JUN plays a dual role in hepatic fibrosis development and in different liver cell types**
c-JUN exerts anti-fibrotic function in HSC: loss of c-Jun in HSCs promotes fibrosis development and enhances HSC activation. c-JUN exerts pro-fibrotic function in hepatocytes and hematopoietic cells: loss of c-Jun in hepatocytes and hematopoietic cells limits fibrosis progression and reduces HSC activation.

The phenotype of one protein exhibiting opposite functions in different cell types has been reported before, examples like JNK, NFκB and EGFR have been demonstrated to play an anti-tumorigenic function in hepatocytes but a pro-tumorigenic function in Kupffer cells in the DEN-induced HCC model (Maeda *et al*., 2005, Das *et al*., 2011, Lanaya *et al*., 2014). These studies together with our findings highlight the importance of the microenvironment, paracrine signaling and interactions between different cell types in liver pathology. This therefore adds the complexity to the molecular basis of how different liver cell types contribute to hepatic fibrosis development.

5.2.4 c-JUN functions in hepatocytes

Liver damage usually causes hepatocyte death followed by proliferation to compensate for the loss of liver parenchyma. Historically, the impact of c-JUN in the liver has been emphasized particularly on its roles in regulating both hepatocyte survival and proliferation.

Many studies have underscored the function of c-JUN in promoting hepatocyte survival especially during early stages of liver pathogenesis. Absence of c-JUN in hepatocytes invariably resulted in markedly increased hepatocyte death upon various pathological stimuli including DEN, TNF-α, Con A and sustained endoplasmic reticulum stress (Eferl *et al*., 2003a, Hasselblatt *et al*., 2007, Fuest *et al*., 2012, Min *et al*., 2012). The mechanisms by which c-JUN promotes hepatocyte survival are largely stimulus dependent: such as by antagonizing p53 and its pro-apoptotic target *noxa* upon TNF-α treatment (Eferl *et al*., 2003a) or by induction of *nos2* expression and subsequent nitric oxide production upon Con A treatment (Hasselblatt *et al*.,

149

2007). In our model, CCl_4 is used as the pathological stimulus. Administration of CCl_4 induces inflammation and thereby activates the release of inflammatory mediators such as TNF-α and nitric oxide (Morio *et al.*, 2001). As both TNF-α and nitric oxide are directly associated with c-JUN functions in promoting hepatocyte survival, we can expect a higher grade of hepatocyte injury and death in the *c-Jun$^{f/f}$;Mx-Cre^{tg}* mice, which will be assessed in the future.

Increased hepatocyte death is generally considered to contribute to the hepatic accumulation of the activated inflammatory cells as well as activated HSCs, which leads to increased fibrosis (Syn *et al.*, 2009). Whereas, on the contrary, we have observed less activated HSCs and less fibrosis in the *c-Jun$^{f/f}$;Mx-Cre^{tg}* mice. These data impling that (1) there may be other inflammatory mediator(s) that is/are regulated by c-JUN in hepatocyte and/or hematopoietic cells which play(s) critical role; (2) c-JUN's role in hematopoietic cells is more important in regulating HSC activation and fibrogenesis.

5.2.5 c-JUN activity in hematopoietic cells

In a DEN-induced mouse HCC model, inactivation of certain genes such as JNK, NFκB or EGFR in hepatocyte alone (by using Albumin-Cre) or in both hepatocytes and hematopoietic cells (by using Mx-Cre) have resulted in completely opposite effect in HCC progression (Maeda *et al.*, 2005, Das *et al.*, 2011, Lanaya *et al.*, 2014), emphasizing the decisive role of the hematopoietic cells in liver pathogenesis. However, several studies inactivating c-JUN in either hepatocyte alone (by using Alfp-Cre) or in both hepatocytes and hematopoietic cells (by using Mx-Cre) under various pathological conditions

have exhibited identical phenotypes. These include liver regeneration stimulated by PH (Behrens *et al.*, 2002, Stepniak *et al.*, 2006), acute liver hepatitis caused by Con A (Hasselblatt *et al.*, 2007) and liver carcinogenesis initiated by DEN (Eferl *et al.*, 2003a). Moreover, although whole body c-JUN knockout caused extensive apoptosis of both fetal hepatocytes and hematopoietic cells, the *c-Jun*$^{-/-}$ fetal liver cells were able to reconstitute all hematopoietic compartments (spleen, thymus and bone marrow) of lethally irradiated adult recipient mice (Eferl *et al.*, 1999).

In order to dissect the compound pro-fibrotic effect of c-JUN in both hepatocytes and hematopoietic cells during hepatic fibrosis progression, it will be necessary to inactivate c-JUN specifically in either hepatocyte or hematopoietic cell. Yet more experiments such as the measurement of hepatic cell death and cytokine production are also needed to determine how c-JUN functions in hepatocytes and hematopoietic cells affects HSC activation.

5.2.6 JNK signaling in hepatic fibrosis

JNKs (JNK1 and JNK2) have been identified to play key roles in various types of liver diseases (e.g. NAFLD, NASH and HCC) as well as diseases associated with liver functions (e.g. insulin resistance and obesity) (Seki *et al.*, 2012). Since the above mentioned pathological conditions are usually accompanied with chronic liver injury and certain degrees of liver fibrosis, some studies have investigated the direct effect of JNKs in hepatic fibrosis in the CCl$_4$ and/or BDL models and found that JNK1 plays a more predominant role in liver repair and fibrogenesis (Kluwe *et al.*, 2010, Hong *et al.*, 2013, Zhao *et al.*, 2014).

Activated JNKs are expressed in hepatocytes, inflammatory cells and myofibroblasts in humans and mice with chronic liver diseases (Seki *et al*., 2012, Cubero *et al*., 2015). Interestingly, mice with whole body knockout of JNK1 exhibited significant protection whereas mice with hepatocyte-specific knockout of JNK1 were not protected from liver injury and fibrosis compared to wild type mice in both CCl$_4$ and BDL-induced fibrosis models. It has thus been suggested that JNK1 functions in the non-parenchymal cells promotes HSC activation and fibrogenesis (Zhao *et al*., 2014). Consistently, JNK1 in hematopoietic cells also promotes HCC development (Das *et al*., 2011). c-JUN being the main downstream effector of the JNK signaling pathway and a dual regulator in different liver cell types in fibrosis progression, its activity in the liver should be investigated together with JNKs. Nevertheless, c-JUN can function in a JNK-dependent and -independent manner and even show opposite effect in certain circumstances such as in regulating HCC development. Mice with hepatocyte-specific deletion of c-JUN protects against (Eferl *et al*., 2003a, Min *et al*., 2012) whereas mice with hepatocyte-specific deletion of JNK1 promotes liver tumor development (Das *et al*., 2011) in the DEN-induced HCC model. Hence the functions of c-JUN and JNK in hepatic fibrosis needs to be carefully examined especially in different liver cell types.

5.2.7 Clinical significance and future direction

As activated HSCs are the major collagen producing cells, their cell fate (quiescence, activation, senescence or death) can affect the degree of hepatic fibrosis. Thus HSC is currently the primary target in antifibrotic therapy

152

development (Kisseleva *et al*., 2011). Identification of targetable molecules and pathways responsible for HSC activation would be beneficial in exploring effective antifibrotic therapies. We have discovered that c-JUN can regulate HSC activation in both cell-autonomous and non-cell-autonomous manner. Our data suggest that molecules and pathways associated with c-JUN (e.g. JNK and Hh) are attractive druggable targets that may help to slow or halt the fibrosis progression. In addition, our data has also raised the importance that different cell types participate differently in the fibrosis development. Hence, an effective antifibrotic therapy should meet both criteria: targeting the right molecule(s) and in the right cell type(s). Taken these considerations, using commercially available drugs such as Hh inhibitors to treat the fibrotic mice of different *c-Jun* genotypes may help to identify effective antifibrotic molecules as well as to differentiate the antifibrotic effect in different liver cell types. Furthermore, whether inactivation of *c-Jun* in different liver cell types would affect hepatic fibrosis reversion is another interesting question to be investigated in future.
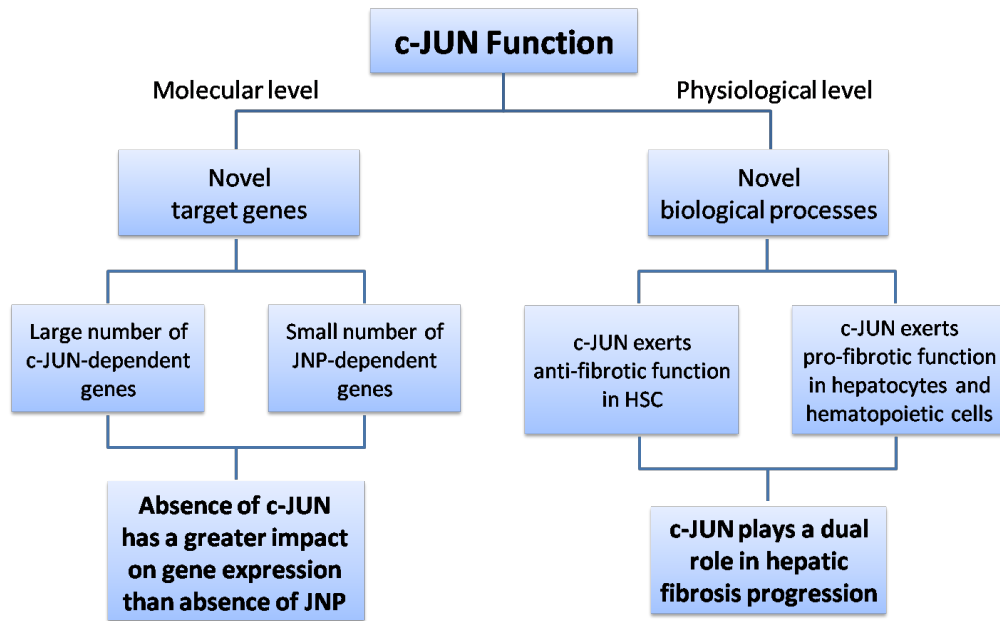
Chapter 6

Conclusion

Figure 31. Mechanistic insights into the function of c-JUN at both the molecular and physiological levels

This study has investigated the functions of c-JUN at both the molecular and physiological levels (Figure 31). In the first part, we have identified, validated and analyzed genes that are regulated by c-JUN and JNP under both basal and stressed conditions in a whole genome scale. We have thus uncovered many novel genes and several potential biological pathways that may be regulated by c-JUN and/or JNP. This study has contributed to a novel view that the N-terminal unphosphorylated c-JUN can function as a transcription factor and is sufficient to regulate its target gene expression; further advancing the knowledge of how c-JUN functions in a JNP-dependent and -independent manner and influences the cellular behaviors in response to stimuli such as genotoxic stresses.

In the second part, we have specifically investigated c-JUN functions in liver fibrosis, as the top pathway identified from the first part. Though c-JUN is well-known for its role in liver physiology including embryonic hepatogenesis, adult liver regeneration, inflammatory liver diseases and HCC initiation, its role in liver fibrosis is relatively unknown. Till date, no studies have reported any effect of c-JUN on hepatic fibrosis yet. Our study shows for the first time that c-JUN plays a dual role in different liver cell types in HSC activation and hepatic fibrosis development. More importantly, our study has provided a better understanding of the role of c-JUN in fibrosis initiation and progression, by the use of the inducible and cell type-specific loss-of-function models. The advantages of these models are (1) it allows the mice to develop normally in the presence of c-JUN until the induction of fibrosis; (2) it only inactivates c-JUN in certain cell type(s) while keeping c-JUN intact in the remaining of the body; (3) it examines c-JUN functions at the physiological level as studies using transgenic or overexpression models may reflect the functions of c-JUN at rather a supraphysiological level. The complete mechanism of how c-JUN regulates HSC activation and fibrosis progression has yet to be elucidated, but the data shown here strongly point to the crosstalk between c-JUN and Hh signaling as a potential mechanism in this biological process. Our findings could therefore benefit the future development of the antifibrotic therapies.

Chapter 7

Bibliography

Adler, V., Franklin, C.C. and Kraft, A.S. (1992). Phorbol esters stimulate the phosphorylation of c-Jun but not v-Jun: regulation by the N-terminal delta domain. *Proceedings of the National Academy of Sciences of the United States of America* **89,** 5341-5345.

Aguilera, C., Nakagawa, K., Sancho, R., Chakraborty, A., Hendrich, B. and Behrens, A. (2011). c-Jun N-terminal phosphorylation antagonises recruitment of the Mbd3/NuRD repressor complex. *Nature* **469,** 231-235.

Angel, P., Allegretto, E.A., Okino, S.T., Hattori, K., Boyle, W.J., Hunter, T. and Karin, M. (1988a). Oncogene jun encodes a sequence-specific trans-activator similar to AP-1. *Nature* **332,** 166-171.

Angel, P., Hattori, K., Smeal, T. and Karin, M. (1988b). The jun proto-oncogene is positively autoregulated by its product, Jun/AP-1. *Cell* **55,** 875-885.

Angel, P. and Karin, M. (1991). The role of Jun, Fos and the AP-1 complex in cell-proliferation and transformation. *Biochimica et biophysica acta* **1072,** 129-157.

Angel, P., Szabowski, A. and Schorpp-Kistner, M. (2001). Function and regulation of AP-1 subunits in skin physiology and pathology. *Oncogene* **20,** 2413-2423.

Asrih, M. and Jornayvaz, F.R. (2015). Metabolic syndrome and nonalcoholic fatty liver disease: Is insulin resistance the link? *Molecular and cellular endocrinology.*

Bakiri, L., Lallemand, D., Bossy-Wetzel, E. and Yaniv, M. (2000). Cell cycle-dependent variations in c-Jun and JunB phosphorylation: a role in the control of cyclin D1 expression. *The EMBO journal* **19,** 2056-2068.

Bakiri, L., Matsuo, K., Wisniewska, M., Wagner, E.F. and Yaniv, M. (2002). Promoter specificity and biological activity of tethered AP-1 dimers. *Molecular and cellular biology* **22,** 4952-4964.

Bakiri, L. and Wagner, E.F. (2013). Mouse models for liver cancer. *Molecular oncology* **7,** 206-223.

Barila, D., Mangano, R., Gonfloni, S., Kretzschmar, J., Moro, M., Bohmann, D. and Superti-Furga, G. (2000). A nuclear tyrosine phosphorylation circuit: c-Jun as an activator and substrate of c-Abl and JNK. *The EMBO journal* **19,** 273-281.

Bataller, R. and Brenner, D.A. (2005). Liver fibrosis. *The Journal of clinical investigation* **115,** 209-218.

Behrens, A., Jochum, W., Sibilia, M. and Wagner, E.F. (2000). Oncogenic transformation by ras and fos is mediated by c-Jun N-terminal phosphorylation. *Oncogene* **19,** 2657-2663.

Behrens, A., Sabapathy, K., Graef, I., Cleary, M., Crabtree, G.R. and Wagner, E.F. (2001). Jun N-terminal kinase 2 modulates thymocyte apoptosis and T cell activation through c-Jun and nuclear factor of activated T cell (NF-AT). *Proceedings of the National Academy of Sciences of the United States of America* **98,** 1769-1774.

Behrens, A., Sibilia, M., David, J.P., Mohle-Steinlein, U., Tronche, F., Schutz, G. and Wagner, E.F. (2002). Impaired postnatal hepatocyte proliferation and liver regeneration in mice lacking c-jun in the liver. *The EMBO journal* **21,** 1782-1790.

Behrens, A., Sibilia, M. and Wagner, E.F. (1999). Amino-terminal phosphorylation of c-Jun regulates stress-induced apoptosis and cellular proliferation. *Nature genetics* **21,** 326-329.

Berry, M.N. and Edwards, A.M. (2000) The hepatocyte review, Springer Science & Business Media.

Besirli, C.G., Wagner, E.F. and Johnson, E.M., Jr. (2005). The limited role of NH2-terminal c-Jun phosphorylation in neuronal apoptosis: identification of the nuclear pore complex as a potential target of the JNK pathway. *The Journal of cell biology* **170,** 401-411.

Bogoyevitch, M.A., Ngoei, K.R., Zhao, T.T., Yeap, Y.Y. and Ng, D.C. (2010). c-Jun N-terminal kinase (JNK) signaling: recent advances and challenges. *Biochimica et biophysica acta* **1804,** 463-475.

Bohmann, D., Bos, T.J., Admon, A., Nishimura, T., Vogt, P.K. and Tjian, R. (1987). Human proto-oncogene c-jun encodes a DNA binding protein with structural and functional properties of transcription factor AP-1. *Science* **238,** 1386-1392.

Bossy-Wetzel, E., Bakiri, L. and Yaniv, M. (1997). Induction of apoptosis by the transcription factor c-Jun. *The EMBO journal* **16,** 1695-1709.

Boulton, T.G., Yancopoulos, G.D., Gregory, J.S., Slaughter, C., Moomaw, C., Hsu, J. and Cobb, M.H. (1990). An insulin-stimulated protein kinase similar to yeast kinases involved in cell cycle control. *Science* **249,** 64-67.

Boyle, W.J., Smeal, T., Defize, L.H., Angel, P., Woodgett, J.R., Karin, M. and Hunter, T. (1991). Activation of protein kinase C decreases phosphorylation of c-Jun at sites that negatively regulate its DNA-binding activity. *Cell* **64,** 573-584.

Cargnello, M. and Roux, P.P. (2011). Activation and function of the MAPKs and their substrates, the MAPK-activated protein kinases. *Microbiology and molecular biology reviews : MMBR* **75,** 50-83.

Chang, L. and Karin, M. (2001). Mammalian MAP kinase signalling cascades. *Nature* **410,** 37-40.

Chinenov, Y. and Kerppola, T.K. (2001). Close encounters of many kinds: Fos-Jun interactions that mediate transcription regulatory specificity. *Oncogene* **20,** 2438-2452.

Choi, S.S., Omenetti, A., Syn, W.K. and Diehl, A.M. (2011). The role of Hedgehog signaling in fibrogenic liver repair. *The international journal of biochemistry & cell biology* **43,** 238-244.

Coleman, W.B. and Tsongalis, G.J. (2009) Molecular pathology: the molecular basis of human disease, academic Press.

Colotta, F., Polentarutti, N., Sironi, M. and Mantovani, A. (1992). Expression and involvement of c-fos and c-jun protooncogenes in programmed cell death induced by growth factor deprivation in lymphoid cell lines. *The Journal of biological chemistry* **267,** 18278-18283.

Cuadrado, A. and Nebreda, A.R. (2010). Mechanisms and functions of p38 MAPK signalling. *The Biochemical journal* **429,** 403-417.

Cubero, F.J., Zhao, G., Nevzorova, Y.A., Hatting, M., Al Masaoudi, M., Verdier, J., *et al.* (2015). Haematopoietic cell-derived Jnk1 is crucial for chronic inflammation and carcinogenesis in an experimental model of liver injury. *Journal of hepatology* **62,** 140-149.

Da Costa, C.R., Villadiego, J., Sancho, R., Fontana, X., Packham, G., Nateri, A.S. and Behrens, A. (2010). Bag1-L is a phosphorylation-dependent coactivator of c-Jun during neuronal apoptosis. *Molecular and cellular biology* **30,** 3842-3852.

Das, M., Garlick, D.S., Greiner, D.L. and Davis, R.J. (2011). The role of JNK in the development of hepatocellular carcinoma. *Genes & development* **25,** 634-645.

Davies, C.C., Chakraborty, A., Cipriani, F., Haigh, K., Haigh, J.J. and Behrens, A. (2010). Identification of a co-activator that links growth factor signalling to c-Jun/AP-1 activation. *Nature cell biology* **12,** 963-972.

Davis, R.J. (2000). Signal transduction by the JNK group of MAP kinases. *Cell* **103,** 239-252.

De Bleser, P.J., Niki, T., Rogiers, V. and Geerts, A. (1997). Transforming growth factor-beta gene expression in normal and fibrotic rat liver. *Journal of hepatology* **26,** 886-893.

Dennler, S., Andre, J., Alexaki, I., Li, A., Magnaldo, T., ten Dijke, P., *et al*. (2007). Induction of sonic hedgehog mediators by transforming growth factor-beta: Smad3-dependent activation of Gli2 and Gli1 expression in vitro and in vivo. *Cancer research* **67,** 6981-6986.

Dorn, C., Engelmann, J.C., Saugspier, M., Koch, A., Hartmann, A., Muller, M., *et al*. (2014). Increased expression of c-Jun in nonalcoholic fatty liver disease. *Laboratory investigation; a journal of technical methods and pathology* **94,** 394-408.

Downey, T. (2006). Analysis of a multifactor microarray study using Partek genomics solution. *Methods in enzymology* **411,** 256-270.

Eferl, R., Ricci, R., Kenner, L., Zenz, R., David, J.P., Rath, M. and Wagner, E.F. (2003a). Liver tumor development. c-Jun antagonizes the proapoptotic activity of p53. *Cell* **112,** 181-192.

Eferl, R., Sibilia, M., Hilberg, F., Fuchsbichler, A., Kufferath, I., Guertl, B., *et al*. (1999). Functions of c-Jun in liver and heart development. *The Journal of cell biology* **145,** 1049-1061.

Eferl, R. and Wagner, E.F. (2003b). AP-1: a double-edged sword in tumorigenesis. *Nature reviews. Cancer* **3,** 859-868.

Estus, S., Zaks, W.J., Freeman, R.S., Gruda, M., Bravo, R. and Johnson, E.M., Jr. (1994). Altered gene expression in neurons during programmed cell death: identification of c-jun as necessary for neuronal apoptosis. *The Journal of cell biology* **127,** 1717-1727.

Fausto, N. (2000). Liver regeneration. *Journal of hepatology* **32,** 19-31.

Forbes, S.J. and Parola, M. (2011). Liver fibrogenic cells. *Best practice & research. Clinical gastroenterology* **25,** 207-217.

Friedman, S.L. (2000). Molecular regulation of hepatic fibrosis, an integrated cellular response to tissue injury. *The Journal of biological chemistry* **275,** 2247-2250.

Friedman, S.L. (2008a). Hepatic stellate cells: protean, multifunctional, and enigmatic cells of the liver. *Physiological reviews* **88,** 125-172.

Friedman, S.L. (2008b). Mechanisms of hepatic fibrogenesis. *Gastroenterology* **134,** 1655-1669.

Friedman, S.L. and Bansal, M.B. (2006). Reversal of hepatic fibrosis -- fact or fantasy? *Hepatology* **43,** S82-88.

Fuest, M., Willim, K., MacNelly, S., Fellner, N., Resch, G.P., Blum, H.E. and Hasselblatt, P. (2012). The transcription factor c-Jun protects against sustained hepatic endoplasmic reticulum stress thereby promoting hepatocyte survival. *Hepatology* **55,** 408-418.

Gao, B., Lee, S.M. and Fang, D. (2006). The tyrosine kinase c-Abl protects c-Jun from ubiquitination-mediated degradation in T cells. *The Journal of biological chemistry* **281,** 29711-29718.

Gao, M., Labuda, T., Xia, Y., Gallagher, E., Fang, D., Liu, Y.C. and Karin, M. (2004). Jun turnover is controlled through JNK-dependent phosphorylation of the E3 ligase Itch. *Science* **306,** 271-275.

Geerts, A. (2001). History, heterogeneity, developmental biology, and functions of quiescent hepatic stellate cells. *Seminars in liver disease* **21,** 311-335.

Grachtchouk, M., Mo, R., Yu, S., Zhang, X., Sasaki, H., Hui, C.C. and Dlugosz, A.A. (2000). Basal cell carcinomas in mice overexpressing Gli2 in skin. *Nature genetics* **24,** 216-217.

Grzelak, C.A., Sigglekow, N.D. and McCaughan, G.W. (2015). GLI2 as a marker of hedgehog-responsive cells. *Hepatology* **61,** 1770.

Gupta, S., Campbell, D., Derijard, B. and Davis, R.J. (1995). Transcription factor ATF2 regulation by the JNK signal transduction pathway. *Science* **267,** 389-393.

Hahn, H., Wicking, C., Zaphiropoulous, P.G., Gailani, M.R., Shanley, S., Chidambaram, A., *et al*. (1996). Mutations of the human homolog of Drosophila patched in the nevoid basal cell carcinoma syndrome. *Cell* **85,** 841-851.

Hai, T. and Curran, T. (1991). Cross-family dimerization of transcription factors Fos/Jun and ATF/CREB alters DNA binding specificity. *Proceedings of the National Academy of Sciences of the United States of America* **88,** 3720-3724.

Ham, J., Babij, C., Whitfield, J., Pfarr, C.M., Lallemand, D., Yaniv, M. and Rubin, L.L. (1995). A c-Jun dominant negative mutant protects sympathetic neurons against programmed cell death. *Neuron* **14,** 927-939.

Hasenfuss, S.C., Bakiri, L., Thomsen, M.K., Hamacher, R. and Wagner, E.F. (2014a). Activator Protein 1 transcription factor Fos-related antigen 1 (Fra-1) is dispensable for murine liver fibrosis, but modulates xenobiotic metabolism. *Hepatology* **59,** 261-273.

Hasenfuss, S.C., Bakiri, L., Thomsen, M.K., Williams, E.G., Auwerx, J. and Wagner, E.F. (2014b). Regulation of steatohepatitis and PPARgamma signaling by distinct AP-1 dimers. *Cell metabolism* **19,** 84-95.

Hasselblatt, P., Rath, M., Komnenovic, V., Zatloukal, K. and Wagner, E.F. (2007). Hepatocyte survival in acute hepatitis is due to c-Jun/AP-1-dependent expression of inducible nitric oxide synthase. *Proceedings of the National Academy of Sciences of the United States of America* **104,** 17105-17110.

Heindryckx, F., Colle, I. and Van Vlierberghe, H. (2009). Experimental mouse models for hepatocellular carcinoma research. *International journal of experimental pathology* **90,** 367-386.

Hernandez-Gea, V. and Friedman, S.L. (2011). Pathogenesis of liver fibrosis. *Annual review of pathology* **6,** 425-456.

Hibi, M., Lin, A., Smeal, T., Minden, A. and Karin, M. (1993). Identification of an oncoprotein- and UV-responsive protein kinase that binds and potentiates the c-Jun activation domain. *Genes & development* **7,** 2135-2148.

Hilberg, F., Aguzzi, A., Howells, N. and Wagner, E.F. (1993). c-jun is essential for normal mouse development and hepatogenesis. *Nature* **365,** 179-181.

Hong, I.H., Park, S.J., Goo, M.J., Lee, H.R., Park, J.K., Ki, M.R., *et al*. (2013). JNK1 and JNK2 regulate alpha-SMA in hepatic stellate cells during CCl4 -induced fibrosis in the rat liver. *Pathology international* **63,** 483-491.

Iredale, J.P. (2007). Models of liver fibrosis: exploring the dynamic nature of inflammation and repair in a solid organ. *The Journal of clinical investigation* **117,** 539-548.

Jochum, W., Passegue, E. and Wagner, E.F. (2001). AP-1 in mouse development and tumorigenesis. *Oncogene* **20,** 2401-2412.

Johnson, P.F. and McKnight, S.L. (1989). Eukaryotic transcriptional regulatory proteins. *Annual review of biochemistry* **58,** 799-839.

Johnson, R., Spiegelman, B., Hanahan, D. and Wisdom, R. (1996a). Cellular transformation and malignancy induced by ras require c-jun. *Molecular and cellular biology* **16,** 4504-4511.

Johnson, R.L., Rothman, A.L., Xie, J., Goodrich, L.V., Bare, J.W., Bonifas, J.M., *et al*. (1996b). Human homolog of patched, a candidate gene for the basal cell nevus syndrome. *Science* **272,** 1668-1671.

Johnson, R.S., van Lingen, B., Papaioannou, V.E. and Spiegelman, B.M. (1993). A null mutation at the c-jun locus causes embryonic lethality and retarded cell growth in culture. *Genes & development* **7,** 1309-1317.

Jones, E.A. and Flavell, R.A. (2005). Distal enhancer elements transcribe intergenic RNA in the IL-10 family gene cluster. *Journal of immunology* **175,** 7437-7446.

Jung, Y., Witek, R.P., Syn, W.K., Choi, S.S., Omenetti, A., Premont, R., *et al*. (2010). Signals from dying hepatocytes trigger growth of liver progenitors. *Gut* **59,** 655-665.

Karin, M. (1995). The regulation of AP-1 activity by mitogen-activated protein kinases. *The Journal of biological chemistry* **270,** 16483-16486.

Karin, M. (1998). Mitogen-activated protein kinase cascades as regulators of stress responses. *Annals of the New York Academy of Sciences* **851,** 139-146.

Karin, M., Liu, Z. and Zandi, E. (1997). AP-1 function and regulation. *Current opinion in cell biology* **9,** 240-246.

Kharbanda, S., Ren, R., Pandey, P., Shafman, T.D., Feller, S.M., Weichselbaum, R.R. and Kufe, D.W. (1995). Activation of the c-Abl tyrosine kinase in the stress response to DNA-damaging agents. *Nature* **376,** 785-788.

Kinoshita, K., Iimuro, Y., Fujimoto, J., Inagaki, Y., Namikawa, K., Kiyama, H., *et al*. (2007). Targeted and regulable expression of transgenes in hepatic stellate cells and myofibroblasts in culture and in vivo using an

adenoviral Cre/loxP system to antagonise hepatic fibrosis. *Gut* **56,** 396-404.

Kisseleva, T. and Brenner, D.A. (2011). Anti-fibrogenic strategies and the regression of fibrosis. *Best practice & research. Clinical gastroenterology* **25,** 305-317.

Klein, I., Cornejo, J.C., Polakos, N.K., John, B., Wuensch, S.A., Topham, D.J., *et al*. (2007). Kupffer cell heterogeneity: functional properties of bone marrow derived and sessile hepatic macrophages. *Blood* **110,** 4077-4085.

Kluwe, J., Pradere, J.P., Gwak, G.Y., Mencin, A., De Minicis, S., Osterreicher, C.H., *et al*. (2010). Modulation of hepatic fibrosis by c-Jun-N-terminal kinase inhibition. *Gastroenterology* **138,** 347-359.

Kolbus, A., Herr, I., Schreiber, M., Debatin, K.M., Wagner, E.F. and Angel, P. (2000). c-Jun-dependent CD95-L expression is a rate-limiting step in the induction of apoptosis by alkylating agents. *Molecular and cellular biology* **20,** 575-582.

Kovary, K. and Bravo, R. (1991). The jun and fos protein families are both required for cell cycle progression in fibroblasts. *Molecular and cellular biology* **11,** 4466-4472.

Krauss, G. (2014) Biochemistry of Signal Transduction and Regulation, Wiley.

Kuhn, R., Schwenk, F., Aguet, M. and Rajewsky, K. (1995). Inducible gene targeting in mice. *Science* **269,** 1427-1429.

Kuntz, E. and Kuntz, H. (2008). Hepatology: Textbook and Atlas: History, Morphology, Biochemistry, Diagnostics, Clinic. *Therapy. Berlin, Heidelberg: Springer,* 7.

Lanaya, H., Natarajan, A., Komposch, K., Li, L., Amberg, N., Chen, L., *et al*. (2014). EGFR has a tumour-promoting role in liver macrophages during hepatocellular carcinoma formation. *Nature cell biology* **16,** 972-981, 971-977.

Laner-Plamberger, S., Kaser, A., Paulischta, M., Hauser-Kronberger, C., Eichberger, T. and Frischauf, A.M. (2009). Cooperation between GLI and JUN enhances transcription of JUN and selected GLI target genes. *Oncogene* **28,** 1639-1651.

Levine, A.J. (1997). p53, the cellular gatekeeper for growth and division. *Cell* **88,** 323-331.

Li, G., Gustafson-Brown, C., Hanks, S.K., Nason, K., Arbeit, J.M., Pogliano, K., *et al*. (2003). c-Jun is essential for organization of the epidermal leading edge. *Developmental cell* **4,** 865-877.

Liu, P., Kimmoun, E., Legrand, A., Sauvanet, A., Degott, C., Lardeux, B. and Bernuau, D. (2002). Activation of NF-kappa B, AP-1 and STAT transcription factors is a frequent and early event in human hepatocellular carcinomas. *Journal of hepatology* **37,** 63-71.

Lodish, H. (2004) Molecular Cell Biology, W. H. Freeman.

Loomba, R. and Sanyal, A.J. (2013). The global NAFLD epidemic. *Nature reviews. Gastroenterology & hepatology* **10,** 686-690.

MacLaren, A., Black, E.J., Clark, W. and Gillespie, D.A. (2004). c-Jun-deficient cells undergo premature senescence as a result of spontaneous DNA damage accumulation. *Molecular and cellular biology* **24,** 9006-9018.

Maeda, S., Kamata, H., Luo, J.L., Leffert, H. and Karin, M. (2005). IKKbeta couples hepatocyte death to cytokine-driven compensatory proliferation that promotes chemical hepatocarcinogenesis. *Cell* **121,** 977-990.

Maki, Y., Bos, T.J., Davis, C., Starbuck, M. and Vogt, P.K. (1987). Avian sarcoma virus 17 carries the jun oncogene. *Proceedings of the National Academy of Sciences of the United States of America* **84,** 2848-2852.

Manibusan, M.K., Odin, M. and Eastmond, D.A. (2007). Postulated carbon tetrachloride mode of action: a review. *Journal of environmental science and health. Part C, Environmental carcinogenesis & ecotoxicology reviews* **25,** 185-209.

Manning, A.M. and Davis, R.J. (2003). Targeting JNK for therapeutic benefit: from junk to gold? *Nature reviews. Drug discovery* **2,** 554-565.

Markiewski, M.M. and Lambris, J.D. (2007). The role of complement in inflammatory diseases from behind the scenes into the spotlight. *The American journal of pathology* **171,** 715-727.

Mechta-Grigoriou, F., Gerald, D. and Yaniv, M. (2001). The mammalian Jun proteins: redundancy and specificity. *Oncogene* **20,** 2378-2389.

Michelotti, G.A., Xie, G., Swiderska, M., Choi, S.S., Karaca, G., Kruger, L., *et al.* (2013). Smoothened is a master regulator of adult liver repair. *The Journal of clinical investigation* **123,** 2380-2394.

Min, L., Ji, Y., Bakiri, L., Qiu, Z., Cen, J., Chen, X., *et al.* (2012). Liver cancer initiation is controlled by AP-1 through SIRT6-dependent inhibition of survivin. *Nature cell biology* **14,** 1203-1211.

Morio, L.A., Chiu, H., Sprowles, K.A., Zhou, P., Heck, D.E., Gordon, M.K. and Laskin, D.L. (2001). Distinct roles of tumor necrosis factor-alpha and nitric oxide in acute liver injury induced by carbon tetrachloride in mice. *Toxicology and applied pharmacology* **172,** 44-51.

Morton, S., Davis, R.J., McLaren, A. and Cohen, P. (2003). A reinvestigation of the multisite phosphorylation of the transcription factor c-Jun. *The EMBO journal* **22,** 3876-3886.

Moser, A.R., Mattes, E.M., Dove, W.F., Lindstrom, M.J., Haag, J.D. and Gould, M.N. (1993). ApcMin, a mutation in the murine Apc gene, predisposes to mammary carcinomas and focal alveolar hyperplasias. *Proceedings of the National Academy of Sciences of the United States of America* **90,** 8977-8981.

Musti, A.M., Treier, M. and Bohmann, D. (1997). Reduced ubiquitin-dependent degradation of c-Jun after phosphorylation by MAP kinases. *Science* **275,** 400-402.

Nateri, A.S., Riera-Sans, L., Da Costa, C. and Behrens, A. (2004). The ubiquitin ligase SCFFbw7 antagonizes apoptotic JNK signaling. *Science* **303,** 1374-1378.

Nateri, A.S., Spencer-Dene, B. and Behrens, A. (2005). Interaction of phosphorylated c-Jun with TCF4 regulates intestinal cancer development. *Nature* **437,** 281-285.

Nayak, A., Pednekar, L., Reid, K.B. and Kishore, U. (2012). Complement and non-complement activating functions of C1q: a prototypical innate immune molecule. *Innate immunity* **18,** 350-363.

Nilsson, M., Unden, A.B., Krause, D., Malmqwist, U., Raza, K., Zaphiropoulos, P.G. and Toftgard, R. (2000). Induction of basal cell

carcinomas and trichoepitheliomas in mice overexpressing GLI-1. *Proceedings of the National Academy of Sciences of the United States of America* **97,** 3438-3443.

Nordenstedt, H., White, D.L. and El-Serag, H.B. (2010). The changing pattern of epidemiology in hepatocellular carcinoma. *Digestive and liver disease : official journal of the Italian Society of Gastroenterology and the Italian Association for the Study of the Liver* **42 Suppl 3,** S206-214.

Omenetti, A., Choi, S., Michelotti, G. and Diehl, A.M. (2011). Hedgehog signaling in the liver. *Journal of hepatology* **54,** 366-373.

Omenetti, A. and Diehl, A.M. (2008). The adventures of sonic hedgehog in development and repair. II. Sonic hedgehog and liver development, inflammation, and cancer. *American journal of physiology. Gastrointestinal and liver physiology* **294,** G595-598.

Orban, P.C., Chui, D. and Marth, J.D. (1992). Tissue- and site-specific DNA recombination in transgenic mice. *Proceedings of the National Academy of Sciences of the United States of America* **89,** 6861-6865.

Palmada, M., Kanwal, S., Rutkoski, N.J., Gustafson-Brown, C., Johnson, R.S., Wisdom, R. and Carter, B.D. (2002). c-jun is essential for sympathetic neuronal death induced by NGF withdrawal but not by p75 activation. *The Journal of cell biology* **158,** 453-461.

Papachristou, D.J., Batistatou, A., Sykiotis, G.P., Varakis, I. and Papavassiliou, A.G. (2003). Activation of the JNK-AP-1 signal transduction pathway is associated with pathogenesis and progression of human osteosarcomas. *Bone* **32,** 364-371.

Paredes-Turrubiarte, G., Gonzalez-Chavez, A., Perez-Tamayo, R., Salazar-Vazquez, B.Y., Hernandez, V.S., Garibay-Nieto, N., *et al*. (2015). Severity of non-alcoholic fatty liver disease is associated with high systemic levels of tumor necrosis factor alpha and low serum interleukin 10 in morbidly obese patients. *Clinical and experimental medicine*.

Raha, D., Wang, Z., Moqtaderi, Z., Wu, L., Zhong, G., Gerstein, M., *et al*. (2010). Close association of RNA polymerase II and many transcription factors with Pol III genes. *Proceedings of the National Academy of Sciences of the United States of America* **107,** 3639-3644.

Rauscher, F.J., 3rd, Cohen, D.R., Curran, T., Bos, T.J., Vogt, P.K., Bohmann, D., *et al*. (1988). Fos-associated protein p39 is the product of the jun proto-oncogene. *Science* **240,** 1010-1016.

Reddy, C.E., Albanito, L., De Marco, P., Aiello, D., Maggiolini, M., Napoli, A. and Musti, A.M. (2013). Multisite phosphorylation of c-Jun at threonine 91/93/95 triggers the onset of c-Jun pro-apoptotic activity in cerebellar granule neurons. *Cell death & disease* **4,** e852.

Sancho, R., Nateri, A.S., de Vinuesa, A.G., Aguilera, C., Nye, E., Spencer-Dene, B. and Behrens, A. (2009). JNK signalling modulates intestinal homeostasis and tumourigenesis in mice. *The EMBO journal* **28,** 1843-1854.

Saraiva, M. and O'Garra, A. (2010). The regulation of IL-10 production by immune cells. *Nature reviews*. *Immunology* **10,** 170-181.

Sassone-Corsi, P., Lamph, W.W., Kamps, M. and Verma, I.M. (1988). fos-associated cellular p39 is related to nuclear transcription factor AP-1. *Cell* **54,** 553-560.

Schnidar, H., Eberl, M., Klingler, S., Mangelberger, D., Kasper, M., Hauser-Kronberger, C., *et al*. (2009). Epidermal growth factor receptor signaling synergizes with Hedgehog/GLI in oncogenic transformation via activation of the MEK/ERK/JUN pathway. *Cancer research* **69,** 1284-1292.

Schreiber, M., Kolbus, A., Piu, F., Szabowski, A., Mohle-Steinlein, U., Tian, J., *et al*. (1999). Control of cell cycle progression by c-Jun is p53 dependent. *Genes & development* **13,** 607-619.

Schuppan, D. and Kim, Y.O. (2013). Evolving therapies for liver fibrosis. *The Journal of clinical investigation* **123,** 1887-1901.

Schutte, J., Minna, J.D. and Birrer, M.J. (1989). Deregulated expression of human c-jun transforms primary rat embryo cells in cooperation with an activated c-Ha-ras gene and transforms rat-1a cells as a single gene. *Proceedings of the National Academy of Sciences of the United States of America* **86,** 2257-2261.

Seki, E., Brenner, D.A. and Karin, M. (2012). A liver full of JNK: signaling in regulation of cell function and disease pathogenesis, and clinical approaches. *Gastroenterology* **143,** 307-320.

Seki, E. and Schwabe, R.F. (2015). Hepatic inflammation and fibrosis: functional links and key pathways. *Hepatology* **61,** 1066-1079.

Shaulian, E. and Karin, M. (2001). AP-1 in cell proliferation and survival. *Oncogene* **20,** 2390-2400.

Shaulian, E. and Karin, M. (2002). AP-1 as a regulator of cell life and death. *Nature cell biology* **4,** E131-136.

Shaulian, E., Schreiber, M., Piu, F., Beeche, M., Wagner, E.F. and Karin, M. (2000). The mammalian UV response: c-Jun induction is required for exit from p53-imposed growth arrest. *Cell* **103,** 897-907.

Sibilia, M., Fleischmann, A., Behrens, A., Stingl, L., Carroll, J., Watt, F.M., *et al*. (2000). The EGF receptor provides an essential survival signal for SOS-dependent skin tumor development. *Cell* **102,** 211-220.

Sicklick, J.K., Li, Y.X., Choi, S.S., Qi, Y., Chen, W., Bustamante, M., *et al*. (2005). Role for hedgehog signaling in hepatic stellate cell activation and viability. *Laboratory investigation; a journal of technical methods and pathology* **85,** 1368-1380.

Smart, D.E., Green, K., Oakley, F., Weitzman, J.B., Yaniv, M., Reynolds, G., *et al*. (2006). JunD is a profibrogenic transcription factor regulated by Jun N-terminal kinase-independent phosphorylation. *Hepatology* **44,** 1432-1440.

Smith, M.J. and Prochownik, E.V. (1992). Inhibition of c-jun causes reversible proliferative arrest and withdrawal from the cell cycle. *Blood* **79,** 2107-2115.

Stepniak, E., Ricci, R., Eferl, R., Sumara, G., Sumara, I., Rath, M., *et al*. (2006). c-Jun/AP-1 controls liver regeneration by repressing p53/p21 and p38 MAPK activity. *Genes & development* **20,** 2306-2314.

Subramanian, D., Bunjobpol, W. and Sabapathy, K. (2015). Interplay between TAp73 and selected Activator Protein-1 family members promotes AP-

1 target gene activation and cellular growth. *The Journal of biological chemistry*.

Suzuki, T., Okuno, H., Yoshida, T., Endo, T., Nishina, H. and Iba, H. (1991). Difference in transcriptional regulatory function between c-Fos and Fra-2. *Nucleic acids research* **19,** 5537-5542.

Swiderska-Syn, M., Syn, W.K., Xie, G., Kruger, L., Machado, M.V., Karaca, G., *et al*. (2014). Myofibroblastic cells function as progenitors to regenerate murine livers after partial hepatectomy. *Gut* **63,** 1333-1344.

Syn, W.K., Teaberry, V., Choi, S.S. and Diehl, A.M. (2009). Similarities and differences in the pathogenesis of alcoholic and nonalcoholic steatohepatitis. *Seminars in liver disease* **29,** 200-210.

Treier, M., Staszewski, L.M. and Bohmann, D. (1994). Ubiquitin-dependent c-Jun degradation in vivo is mediated by the delta domain. *Cell* **78,** 787-798.

Trouw, L.A., Blom, A.M. and Gasque, P. (2008). Role of complement and complement regulators in the removal of apoptotic cells. *Molecular immunology* **45,** 1199-1207.

Tsukada, S., Parsons, C.J. and Rippe, R.A. (2006). Mechanisms of liver fibrosis. *Clinica chimica acta; international journal of clinical chemistry* **364,** 33-60.

Tsurumi, C., Ishida, N., Tamura, T., Kakizuka, A., Nishida, E., Okumura, E., *et al*. (1995). Degradation of c-Fos by the 26S proteasome is accelerated by c-Jun and multiple protein kinases. *Molecular and cellular biology* **15,** 5682-5687.

van Dam, H. and Castellazzi, M. (2001). Distinct roles of Jun : Fos and Jun : ATF dimers in oncogenesis. *Oncogene* **20,** 2453-2464.

Vandel, L., Montreau, N., Vial, E., Pfarr, C.M., Binetruy, B. and Castellazzi, M. (1996). Stepwise transformation of rat embryo fibroblasts: c-Jun, JunB, or JunD can cooperate with Ras for focus formation, but a c-Jun-containing heterodimer is required for immortalization. *Molecular and cellular biology* **16,** 1881-1888.

Verheij, M., Bose, R., Lin, X.H., Yao, B., Jarvis, W.D., Grant, S., *et al*. (1996). Requirement for ceramide-initiated SAPK/JNK signalling in stress-induced apoptosis. *Nature* **380,** 75-79.

Vikhanskaya, F., Toh, W.H., Dulloo, I., Wu, Q., Boominathan, L., Ng, H.H., *et al*. (2007). p73 supports cellular growth through c-Jun-dependent AP-1 transactivation. *Nature cell biology* **9,** 698-705.

Vinciguerra, M., Esposito, I., Salzano, S., Madeo, A., Nagel, G., Maggiolini, M., *et al*. (2008). Negative charged threonine 95 of c-Jun is essential for c-Jun N-terminal kinase-dependent phosphorylation of threonine 91/93 and stress-induced c-Jun biological activity. *The international journal of biochemistry & cell biology* **40,** 307-316.

Vogt, P.K. (2001). Jun, the oncoprotein. *Oncogene* **20,** 2365-2377.

Vogt, P.K., Bos, T.J. and Doolittle, R.F. (1987). Homology between the DNA-binding domain of the GCN4 regulatory protein of yeast and the carboxyl-terminal region of a protein coded for by the oncogene jun. *Proceedings of the National Academy of Sciences of the United States of America* **84,** 3316-3319.

Walters, R.D., McSwiggen, D.T., Goodrich, J.A. and Kugel, J.F. (2014). Selection and characterization of a DNA aptamer that can discriminate between cJun/cJun and cJun/cFos. *PloS one* **9,** e101015.

Wang, H., Birkenbach, M. and Hart, J. (2000). Expression of Jun family members in human colorectal adenocarcinoma. *Carcinogenesis* **21,** 1313-1317.

Wang, Z.Q., Liang, J., Schellander, K., Wagner, E.F. and Grigoriadis, A.E. (1995). c-fos-induced osteosarcoma formation in transgenic mice: cooperativity with c-jun and the role of endogenous c-fos. *Cancer research* **55,** 6244-6251.

Wang, Z.Y., Sato, H., Kusam, S., Sehra, S., Toney, L.M. and Dent, A.L. (2005). Regulation of IL-10 gene expression in Th2 cells by Jun proteins. *Journal of immunology* **174,** 2098-2105.

Watson, A., Eilers, A., Lallemand, D., Kyriakis, J., Rubin, L.L. and Ham, J. (1998). Phosphorylation of c-Jun is necessary for apoptosis induced by survival signal withdrawal in cerebellar granule neurons. *The Journal of neuroscience : the official journal of the Society for Neuroscience* **18,** 751-762.

Wertz, I.E., O'Rourke, K.M., Zhang, Z., Dornan, D., Arnott, D., Deshaies, R.J. and Dixit, V.M. (2004). Human De-etiolated-1 regulates c-Jun by assembling a CUL4A ubiquitin ligase. *Science* **303,** 1371-1374.

Whitmarsh, A.J. and Davis, R.J. (1996). Transcription factor AP-1 regulation by mitogen-activated protein kinase signal transduction pathways. *Journal of molecular medicine* **74,** 589-607.

Wisdom, R. (1999). AP-1: one switch for many signals. *Experimental cell research* **253,** 180-185.

Wisniewska, M.B., Ameyar-Zazoua, M., Bakiri, L., Kaminska, B., Yaniv, M. and Weitzman, J.B. (2007). Dimer composition and promoter context contribute to functional cooperation between AP-1 and NFAT. *Journal of molecular biology* **371,** 569-576.

Xia, Z., Dickens, M., Raingeaud, J., Davis, R.J. and Greenberg, M.E. (1995). Opposing effects of ERK and JNK-p38 MAP kinases on apoptosis. *Science* **270,** 1326-1331.

Xie, J., Murone, M., Luoh, S.M., Ryan, A., Gu, Q., Zhang, C., *et al.* (1998). Activating Smoothened mutations in sporadic basal-cell carcinoma. *Nature* **391,** 90-92.

Xie, M. and Sabapathy, K. (2010). Tyrosine 170 is dispensable for c-Jun turnover. *Cellular signalling* **22,** 330-337.

Yang, L., Wang, Y., Mao, H., Fleig, S., Omenetti, A., Brown, K.D., *et al.* (2008). Sonic hedgehog is an autocrine viability factor for myofibroblastic hepatic stellate cells. *Journal of hepatology* **48,** 98-106.

Zahran, W.E., Salah El-Dien, K.A., Kamel, P.G. and El-Sawaby, A.S. (2013). Efficacy of Tumor Necrosis Factor and Interleukin-10 Analysis in the Follow-up of Nonalcoholic Fatty Liver Disease Progression. *Indian journal of clinical biochemistry : IJCB* **28,** 141-146.

Zanke, B.W., Boudreau, K., Rubie, E., Winnett, E., Tibbles, L.A., Zon, L., *et al.* (1996). The stress-activated protein kinase pathway mediates cell death following injury induced by cis-platinum, UV irradiation or heat. *Current biology : CB* **6,** 606-613.

Zenz, R., Scheuch, H., Martin, P., Frank, C., Eferl, R., Kenner, L., *et al*. (2003). c-Jun regulates eyelid closure and skin tumor development through EGFR signaling. *Developmental cell* **4,** 879-889.

Zenz, R. and Wagner, E.F. (2006). Jun signalling in the epidermis: From developmental defects to psoriasis and skin tumors. *The international journal of biochemistry & cell biology* **38,** 1043-1049.

Zhao, G., Hatting, M., Nevzorova, Y.A., Peng, J., Hu, W., Boekschoten, M.V., *et al*. (2014). Jnk1 in murine hepatic stellate cells is a crucial mediator of liver fibrogenesis. *Gut* **63,** 1159-1172.

Zheng, B., Zhang, Z., Black, C.M., de Crombrugghe, B. and Denton, C.P. (2002). Ligand-dependent genetic recombination in fibroblasts : a potentially powerful technique for investigating gene function in fibrosis. *The American journal of pathology* **160,** 1609-1617.

Zhu, F., Choi, B.Y., Ma, W.Y., Zhao, Z., Zhang, Y., Cho, Y.Y., *et al*. (2006). COOH-terminal Src kinase-mediated c-Jun phosphorylation promotes c-Jun degradation and inhibits cell transformation. *Cancer research* **66,** 5729-5736.

Zuckerman, V., Wolyniec, K., Sionov, R.V., Haupt, S. and Haupt, Y. (2009). Tumour suppression by p53: the importance of apoptosis and cellular senescence. *The Journal of pathology* **219,** 3-15.

List of Publications

Teoh WW, **Xie M**, Vijayaraghavan A, Yaligar J, Tong WM, Goh LK, Sabapathy K (2015) Molecular characterization of hepatocarcinogenesis using mouse models. *Disease models & mechanisms* (In press)

Xie M, Sabapathy K (2010) Tyrosine 170 is dispensable for c-JUN turnover. *Cellular signalling* **22:** 330-337 **(Paper attached)**

Lin CY, Vega VB, Thomsen JS, Zhang T, Kong SL, **Xie M**, Chiu KP, Lipovich L, Barnett DH, Stossi F, Yeo A, George J, Kuznetsov VA, Lee YK, Charn TH, Palanisamy N, Miller LD, Cheung E, Katzenellenbogen BS, Ruan Y, Bourque G, Wei CL, Liu ET (2007) Whole-genome cartography of estrogen receptor alpha binding sites. *PLoS genetics* **3:** e87

Vega VB, Lin CY, Lai KS, Kong SL, **Xie M**, Su X, Teh HF, Thomsen JS, Yeo AL, Sung WK, Bourque G, Liu ET (2006) Multiplatform genome-wide identification and modeling of functional human estrogen receptor binding sites. *Genome biology* **7:** R82

Melamed P, Zhu Y, Tan SH, **Xie M**, Koh M (2006) Gonadotropin-releasing hormone activation of c-jun, but not early growth response factor-1, stimulates transcription of a luteinizing hormone beta-subunit gene. *Endocrinology* **147:** 3598-3605